The Thesis Committee for Argenis Jesus Pelayo Nava
Certifies that this is the approved version of the following Thesis:

Impact of Subsurface Setting on CO_2 Storage Leakage Risk: Implications for Financial Responsibility and the Insurance Industry

APPROVED BY
SUPERVISING COMMITTEE:

Susan Hovorka, Supervisor

Sahar Bakhshian, Co-Supervisor

Seyyed Hosseini, Reader

Impact of Subsurface Setting on CO_2 Storage Leakage Risk: Implications for Financial Responsibility and the Insurance Industry

by

Argenis Jesus Pelayo Nava

Thesis

Presented to the Faculty of the Graduate School of

The University of Texas at Austin

in Partial Fulfillment

of the Requirements

for the Degree of

Master of Science in Energy and Earth Resources

The University of Texas at Austin

August 2025

Dedication

I dedicate this thesis to my family, my friends, and the friends who became family. A special thanks goes to my mother, Yuraima, for instilling in me the belief that education is one of life's most valuable assets; to my angel and father, Tomás; to my partner, Sawsan; and to everyone who supported me in achieving this life goal.

I am also deeply grateful to The University of Texas at Austin, the Bureau of Economic Geology, and the Gulf Coast Carbon Center for providing the environment that allowed me to carry this work forward.

Acknowledgements

I would like to thank the Gulf Coast Carbon Center (GCCC) team, GCCC industrial associates, and SECARB USA for supporting this research and providing me with the tools and skills to see it through to completion. I am deeply grateful to my advisor, Susan Hovorka, for her guidance and invaluable advice during the times when I felt stuck and nothing seemed to work. My sincere thanks also go to Sahar Bakhshian for her mentorship, advice, and for providing the foundational framework that shaped this project, and to Seyyed Hosseini for her support in the reservoir modeling.

I also want to thank William Wang, Romal Ramadhan, Germán Chávez, Sawsan Almalki, Alex Bump, and the CMG team for their help in various aspects of the research. My gratitude extends to the many people whose contributions to the field allowed me to build upon their knowledge and push it a little further.

Finally, I would like to thank Dr. Fred Beach for his support, advice, and mentorship throughout my master's program, and to everyone—whether directly or indirectly—who helped me through this journey of graduate studies and research.

This material is based upon work supported by the Department of Energy under Award Number DE-FE0031830.

This report was prepared as an account of work sponsored by an agency of the United States Government. Neither the United States Government nor any agency thereof, nor any of their employees, makes any warranty, express or implied, or assumes any legal liability or responsibility for the accuracy, completeness, or usefulness of any information, apparatus, product, or process

disclosed, or represents that its use would not infringe privately owned rights. Reference herein to any specific commercial product, process, or service by trade name, trademark, manufacturer, or otherwise does not necessarily constitute or imply its endorsement, recommendation, or favoring by the United States Government or any agency thereof. The views and opinions of authors expressed herein do not necessarily state or reflect those of the United States Government or any agency thereof.

Abstract

Impact of Subsurface Setting on CO_2 Storage Leakage Risk: Implications for Financial Responsibility and the Insurance Industry

Argenis Jesus Pelayo Nava, M.S. Energy and Earth Resources

The University of Texas at Austin, 2025

Supervisor: Susan Hovorka, Sahar Bakhshian, Seyyed Hosseini

Geologic carbon sequestration (GCS) is pivotal for reducing greenhouse gas emissions, yet CO_2 and brine leakage, and their environmental and financial impacts, remain critical concerns. This research links technical leakage simulations with financial risk assessments to evaluate how subsurface conditions and reservoir geometries influence leakage behavior and associated costs. Central to the study is the premise that wellbores—particularly unidentified plug and abandoned wells—serve as the most likely conduits for leakage, representing a worst-case scenario when these open pathways connect the reservoir to the surface. An integrated modeling framework was developed using static geological models and dynamic multiphase flow simulations to analyze various aspects of leakage behavior. We examined the variation of CO_2 and brine leakage with distance from the injection well; the percentage of CO_2 leaked and the financial impact with and without detection and remediation; sensitivity to different subsurface settings; the effects of well density; and the influence of reservoir geometry, specifically comparing anticline and dipping structures. Results indicate that rapid pressure propagation drives early leakage, with most incurred costs occurring within the first five years of the project. In scenarios without monitoring and remediation, significant cumulative leakage is observed; however, effective detection and repair strategies reduce cumulative CO_2 leakage to less than 1% of the injected volume—even under

extreme high well density conditions. Cost analysis reveals that the contractual penalty is the primary expense driver, followed by environmental remediation capital costs. Among all parameters studied, well density emerged as the most significant driver of financial impact, with higher densities substantially increasing both leakage volume and total financial impact. Furthermore, probabilistic assessments incorporating various well failure probabilities show that, although higher failure rates can increase normalized costs over the project's lifespan, the overall leakage remains minimal, thus reducing financial risk when remediation is applied during injection and post-injection periods. Although different reservoir geometries and subsurface settings affect cumulative leakage, their financial impacts converge to negligible differences when monitoring and remediation measures are implemented. This study provides critical insights into the interplay between reservoir conditions, leakage dynamics, and financial outcomes in GCS projects, offering practical guidance for optimizing monitoring strategies, risk management, and site selection to ensure both environmental safety and economic viability.

Table of Contents

List of Tables

List of Figures

CHAPTER I: INTRODUCTION

1.1. INTRODUCTION

Climate Change and the Role of Carbon Capture and Storage

According to the IPCC (2023), human activities, principally through emissions of greenhouse gases, have unequivocally caused global warming. Global surface temperature reached 1.1°C above 1850-1900 in 2011-2020, affecting many weather and climate extremes in every region across the globe, but there is more yet to come, so deep, rapid, and sustained reduction in greenhouse gas emissions is needed.

The Paris Agreement, adopted by 196 Parties at the UN Climate Change Conference (COP21) in Paris, France, is a legally binding international treaty on climate change. Its overarching goal is to hold "the increase in the global average temperature to well below 2°C above pre-industrial levels" and pursue efforts "to limit the temperature increase to 1.5°C above pre-industrial levels." (UNFCCC, 2023). Nonetheless, the IPCC indicates that crossing the 1.5°C threshold risks unleashing far more severe climate change impacts, including more frequent and severe droughts, heatwaves and rainfalls (IPCC, 2018).

Projected CO_2 emissions from existing and planned fossil fuel infrastructure without additional abatement would exceed the remaining carbon budget for 1.5°C, and would equal to the carbon budget for limiting warming to 2°C. Being said that, sustained net negative global CO_2 emissions are required, so additional deployment of carbon dioxide removal (CDR) technologies is imperative (IPCC 2023).

Carbon dioxide capture and storage (CCS) represents an option in the portfolio of mitigation actions for stabilizing atmospheric greenhouse gas concentrations, as it has the potential to reduce overall emissions costs and increase flexibility in achieving climate goals (IEA, 2020;

IPCC, 2018). Furthermore, CCS serves as a critical mechanism for deep, rapid, and sustained reduction in greenhouse gas emissions in line with 1.5°C pathways and to sustain net negative global CO_2 levels to reduce adverse and irreversible impacts of overshoot – exceeding 1.5°C, as well as additional risks for human and natural systems (IPCC, 2023; UNFCCC, 2023).

Although several CCS technologies have been proposed, geologic carbon storage (GCS) has been identified as the most technically viable approach (IPCC, 2023; U.S. EPA, 2008). GCS has the potential to reduce emissions from large-scale fossil-based energy and industry sources, as well as serve as the storage component of CDR methods, such as direct air capture (DACCS) and biomass with CCS (BECCS) (IPCC, 2023).

Risks from Geologic Carbon Storage

GCS technology is not without risks. The major risk and concern associated with GCS projects is the leakage of CO_2 from storage sites (Deel & Mahajan, n.d.). If CO_2 leaks out of the injection formation and escapes back to the atmosphere, the benefits gained in regard to mitigation of atmospheric CO_2 are evidently diminished. Nonetheless, if the GCS site is appropriately selected and managed, it is estimated that the CO_2 can be permanently isolated from the atmosphere (IPCC, 2023). In fact, appropriately selected and managed geological reservoirs are very likely to exceed 99% containment over 100 years and are likely to exceed 99% containment over 1000 years (IPCC, 2005).

This non-zero probability has driven numerous studies to investigate the physical causes and consequences of this leakage, including the outcomes of leakage into overlying formations, groundwater, and the surface, as well as remediation approaches by natural or engineering methods (Carroll et al., 2014; Celia et al., 2011; Esposito & Benson, 2011; Jenkins et al., 2015; Jones et al., 2015; Little & Jackson, 2010; Nordbotten et al., 2009; Zhang & Bachu, 2011).

The potential consequences of CO_2 and brine leakage depend heavily on the nature of the impacted environment—particularly underground sources of drinking water (USDWs) and the atmosphere. Existing studies suggest that CO_2 leakage alone is unlikely to significantly alter groundwater chemistry. For instance, laboratory and field tests show no obvious degradation in water quality following CO_2 intrusion (C. Yang et al., 2015). However, when CO_2 interacts with brine or mobilizes fluids from deeper formations, it may lead to groundwater salinization or the release of trace metals into aquifers due to pH reduction (Carroll et al., 2014; Keating et al., 2014). Even so, many studies have found that the extent of these changes is limited. Contaminated plumes tend to be spatially small, and rarely do water quality parameters exceed primary maximum contaminant levels (Carroll et al., 2014; Xiao et al., 2020). Broader reviews have confirmed that observed increases in key parameters such as electrical conductivity, alkalinity, major ions, and trace metals are generally minor and often remain close to detection limits (Gupta & Yadav, 2020; Zheng et al., 2021).

Regarding atmospheric release, CO_2 emissions from leakage events tend to disperse quickly once released into the aquifer, seawater, or the air. Surface seeps are typically localized, covering areas on the order of meters to tens of meters (Jones et al., 2015). Mixing, dispersion, and geochemical buffering also help reduce environmental impact and promote relatively rapid recovery following leakage events. Overall, the scientific literature indicates that CO_2-brine leakage is more likely to cause transient, localized effects rather than widespread or long-term damage. This background informs the need for differentiated treatment of CO_2 and brine leakage when assessing environmental risks and designing potential remediation strategies.

Leakage Pathways from Geologic Carbon Storage

CO_2 and brine can leak from geological storage sites through various pathways, including faults, fractures, caprock breaches, seismic events, and spill points (See Fig. 1) (Damen et al., 2006; IPCC, 2005). However, leakage through distributed legacy active or abandoned wells is widely recognized as the most significant risk pathway for geologic carbon storage (Gasda et al., 2004; IPCC, 2005; Lewicki et al., 2007). Every legacy well that penetrates the confining zone of a storage formation represents a potential leakage conduit until reservoir pressure dissipates or the driving force for CO_2 and brine migration is removed (U.S. EPA, 2013a).

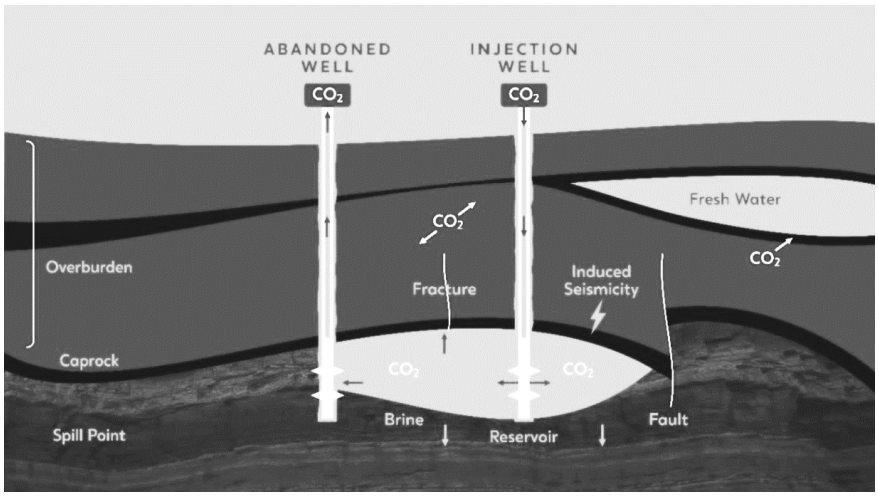

Figure 1. Leakage pathways and environmental risks in geologic carbon storage projects (modified after Damen et al., (2006))

Leakage along wells—especially legacy or improperly abandoned wells—can occur through several mechanisms. These include missing long-string casing, uncemented open-hole sections, degraded or absent mechanical plugs, chemically or mechanically compromised cement in the annulus, poor bonding between cement, casing, and formation, and micro-annuli or channeling along the cement sheath (Celia & Bachu, 2003). These features can form direct conduits for CO_2 or displaced brine to migrate upward, posing both environmental and regulatory challenges.

To address these risks, the U.S. Environmental Protection Agency (EPA) established the Class VI rule, which requires a risk-based framework for site characterization, corrective action, and monitoring. As part of the Underground Injection Control (UIC) program, operators must delineate an Area of Review (AoR)—defined as the region where pressure buildup could mobilize fluids from the injection zone to protected underground sources of drinking water (USDWs). This delineation must be based on computational modeling of the projected CO_2 plume and pressure front. Within the AoR, all wells that penetrate the injection or confining zones must be identified. Wells lacking adequate construction, documentation, or zonal isolation must undergo corrective action before injection operations can proceed. Additionally, site-specific monitoring plans must be developed and approved during the permitting process to ensure that CO_2 and displaced fluids remain contained (U.S. EPA, 2010b, 2013b).

Despite these regulatory safeguards, challenges remain in accurately assessing long-term leakage risk. To date, there have been no confirmed cases of CO_2 leakage reaching USDWs or the surface from Class VI operations. Hence, empirical data on CO_2 and brine leakage over the long-term injection lifecycle remains limited. In the absence of comprehensive datasets, current risk assessments often rely on analogs from blowouts or leakage events associated with other well types, such as oil and gas wells, wastewater disposal wells, or enhanced oil recovery (EOR) operations. These analogs, however, are often problematic. For instance, many documented blowouts are linked to operational activities such as tripping or circulation and typically fail to distinguish between CO_2 and hydrocarbon sources (Porse et al., 2014; Skalle & Podia, 1998)

Also, the regulatory framework governing each well type significantly affects the associated risk profile, further complicating comparisons. As an example, leakage events due to Class II injection wells—used primarily for disposing co-produced brine from hydrocarbon production and for EOR—have been documented in the Permian Basin of Texas and New Mexico. These events are frequently attributed to elevated and extensive pressure zones resulting from the

dense clustering of shallow injection projects (Hovorka et al., 2024). But, as expected, unlike Class VI wells, Class II wells are subject to less stringent requirements: their AoR is defined by a fixed radius (typically ¼ mile) rather than pressure-front modeling, and they are not constrained by regulations that limit injection well bottom-hole pressure to below the reservoir fracture pressure. These differences increase the risk of pressure buildup and leakage events, and make the Class II well experience a poor proxy for CO_2 storage operations. Therefore, using these datasets to estimate CO_2-specific failure frequencies can be misleading and may not reflect current best practices in carbon capture and storage (CCS).

Despite the early success of Class VI wells, concerns persist about how Class VI wells will perform at commercial scale over the long term, particularly in geologically complex areas with a long history of oil and gas development. Legacy wells in the AoR—including "wildcat" wells—may lack construction records or may not have been completed to modern standards. Some may have been designed to isolate deeper zones, leaving shallower storage targets inadequately protected. Even wells listed as properly plugged and abandoned (P&A) may not have been sealed as reported. Plus, undocumented wells may still exist, especially in cases where surface structures are absent or historical records are incomplete.

These uncertainties hinder accurate site-specific risk assessments and complicate the development of financial models used for insurance underwriting, liability allocation, and regulatory compliance. Therefore, a reliable site-specific risk assessment framework is essential for ensuring CO_2 storage containment and permanence, meeting EPA Class VI permit requirements, justifying financial preparedness for emergency events, and supporting long-term liability planning. In response, various efforts have attempted to correlate well construction parameters with risk profiles by assigning permeability values to wells based on design and completion features parameters to then calculate CO_2 and brine leakage rates to the USDW and the surface (Nogues et al., 2012; Watson & Bachu, 2008). While these approaches offer a starting

point for quantifying risk, they have not been broadly validated at the field scale and remain subject to considerable uncertainty.

Despite this, several frameworks for geologic CO_2 storage risk assessment (Bielicki et al., 2013a; Humphries Choptiany & Pelot, 2014; Meyer et al., 2009; Oldenburg et al., 2009; Pawar et al., 2015; Trabucchi et al., 2014), and assessing financial responsibility of leakage events (Bielicki et al., 2014a, 2016; Deng et al., 2014; Trabucchi et al., 2010) have been developed, but they still fail to account for the previously mentioned uncertainties, as well as the specific characteristics that make a project more or less risky in terms of CO_2 and brine leakage impacts and their associated financial consequences.

Without better data and validated frameworks, stakeholders—including insurers, regulators, and operators—face uncertainty in quantifying the financial consequences of CO_2 leakage. This impedes the creation of equitable and site-appropriate financial assurance and long-term liability mechanisms that are both protective and economically viable.

All in all, no studies have developed a site-specific framework that accounts for the uncertainties associated with well characteristics and project location to determine maximum potential leakage rates and financial impacts. This limitation has left a gap in the ability to inform insurance providers, regulators, and operators about the upper bounds of environmental and financial risks. The uniqueness of this study lies in addressing this gap by simulating a range of geologic conditions and estimating the resulting CO_2 and brine leakage behavior and associated financial consequences. Given the scarcity of empirical data on the probability and consequences of leakage through legacy wells, this study adopts a conservative, worst-case scenario by modeling open wellbores as fully connected conduits to the surface. This framework enables the quantification of upper-bound impacts, offering a practical tool to define risk thresholds, support

site-specific evaluations, and guide decisions related to insurance pricing, permitting, and long-term liability management.

1.2. PROBLEM STATEMENT

Currently, there is a significant gap in our understanding of the potential risks associated with CO_2 leakage and the resulting material and financial damages. This gap exists in both the compliance carbon market (e.g., EPA Class VI Permits) and voluntary carbon market.

EPA Class VI Permit Framework

EPA Class VI applicants are required to demonstrate financial responsibility under 40 CFR 146.85 for their permit approval. This financial responsibility encompasses various activities, including corrective actions, plugging injection wells, and post-injection site care and closure and emergency and remedial response (ERR) which would deal with failure of any legacy wells in the project area to isolate the injection zone from USDW. While the costs associated with the first three activities can be estimated based on industry experience, emergency and remedial response activities involve addressing the movement of injection or formation fluids, which may endanger Underground Sources of Drinking Water (USDWs) during construction, operation, and post-injection site care periods (U.S. EPA, 2010a). These events are uncertain in occurrence and timing but can potentially occur throughout the entire lifecycle of the GCS project. It is crucial not to underestimate their potential impact and to ensure adequate resources are available to address such contingencies (U.S. EPA, 2011).

Some insurance companies, such as Allianz, Aon, Kita, Howden, CarbonPool, Marsh, Aspen, Ascot, Enviant, Hamilton, and Markel, currently offer insurance for CO_2 storage projects, such as policies related to reversal, non-delivery, casualty, and environmental liability, covering

emergency and remedial response activities as per the Class VI Permits requirements (*Application of Red Trail Energy, LLC Requesting Consideration for the Geologic Storage of Carbon Dioxide in the Broom Creek Formation from the Red Trail, LLC Ethanol Facility*, 2021; *The Application of Blue Flint Sequester Company, LLC Requesting Consideration for the Geologic Storage of Carbon Dioxide in the Broom Creek Formation from the Blue Flint Ethanol Facility*, 2023; *The Application of Dakota Gasification Company Requesting Consideration for the Geologic Storage of Carbon Dioxide from the Great Plains Synfuels Plant*, 2023; *The Application of DCC West Project LLC Requesting Consideration for the Geologic Storage of Carbon Dioxide in the Broom Creek Formation from the Milton R. Young Station*, 2023; *The Application of Minnkota Power Cooperative, INC. Requesting Consideration for the Geologic Storage of Carbon Dioxide in the Deadwood Formation from the Milton R. Young Station*, 2022; *Wabash Carbon Services, LLC. "Underground Injection Control Permit: Class VI.,"* 2024; Frontier Carbon Solutions, Inc. & Schlumberger Technology Corporation, 2022; IEAGHG, 2024; Tallgrass High Plains Storage, LLC & Numeric Solutions, LLC, 2023). However, due to the inherent uncertainty associated with the geologic and fluid characteristics of storage formations and potential environmental and financial damages from leakage events, insurance carriers in charge of quantifying financial risks often overestimate potential damages by imagining hypothetical worst-case scenarios. Consequently, the premiums offered by insurers reflect this uncertainty as well as their limited coverage time- ranging from one to two years.

After reviewing 22 publicly Class VI permits where emergency and remedial response plans and costs were provided, it can be observed that the assumptions currently incorporated into their cost models are hypothetical, non-standard, and sometimes over-conservatives. These hypothetical assumptions go from assuming every well in the Area of Review (AoR) serves as a leakage pathway, all injected CO_2 leaks to the USDW and/or atmosphere, several monitoring wells are required to determine the extent of the contaminated plume, operators must treat contaminated

aquifers using expensive remediation methods, and every plugged and abandoned well should be investigated.

Carbon Credit Framework

Carbon credits are tradable certificates that represent the reduction or removal of one metric ton of carbon dioxide equivalent (CO_2e) from the atmosphere. They serve as a market-based tool to incentivize climate mitigation. Credits are used either in compliance markets, where emissions are regulated through mechanisms such as cap-and-trade, or in the voluntary carbon market (VCM), where companies and individuals purchase credits to meet internal climate targets (Arbonics, 2023). Independent certification bodies—such as Verra, Gold Standard, American Carbon Registry (ACR), and Puro.earth—oversee the issuance of these credits. They rely on established methodologies to ensure that credited projects are real, additional, measurable, and permanent.

In the case of geologic carbon storage, verification systems assess the project's permanence, risk of leakage, monitoring protocols, and additionality. Projects must demonstrate safe storage conditions, including impermeable cap rocks, minimal leakage pathways, and geological features that promote long-term CO_2 trapping. Compliance with national regulatory frameworks, such as the U.S. EPA's Class VI well permitting, is typically required (IPCC, 2005). To manage the risk of reversal, standards like Verra use a non-permanence risk assessment tool and require a percentage of credits—typically 1–5%—to be withheld in a buffer pool. Others, like ACR, avoid buffer contributions and instead use legal instruments, such as Risk Mitigation Covenants, which assign long-term liability for any future leakage to the project developer.

However, several limitations remain. Current methodologies often lack robust and standardized approaches to quantify long-term geological uncertainty—such as identifying key

site-specific risk drivers and understanding the sensitivity of outcomes to various subsurface conditions. Verifiers commonly rely on deterministic or semi-quantitative scoring tools, which depend on expert judgment and documentation review. These approaches may oversimplify complex geological behavior and fail to incorporate probabilistic risk modeling grounded in reservoir simulation or stochastic analysis. Moreover, the fragmentation across certification bodies—each using different approaches to assess permanence and manage liability—leads to inconsistent credit quality. Some standards require buffer contributions, while others rely solely on regulatory compliance or legal contracts. This lack of harmonization undermines market credibility, confuses credit buyers, and increases transaction and compliance costs for project developers. It also facilitates "standard shopping," where developers opt for the least stringent certification, further weakening trust in the integrity of carbon credits and slowing the global scaling of geologic carbon storage as a high-quality climate solution.

Therefore, a more standard and justified method is required to assess financial leakage impacts that allow stakeholders to evaluate different GCS projects under the same rules.

1.3. RESEARCH GOALS

The primary goal of this research is to develop a robust, site-specific methodology for quantifying the financial risks associated with containment loss in geologic carbon storage (GCS) projects to help inform insurers, carbon markets, operators, and regulators focusing on legacy well containment risks. By directly linking technical leakage simulations to financial impact assessments, this study enables more informed decision-making around risk management, site selection, and financial assurance requirements. The approach explicitly considers variations in subsurface properties, reservoir geometry, open wellbore locations, and monitoring and remediation strategies.

This research seeks to answer the following key questions:

1. What are the main physical mechanisms and reservoir conditions that drive CO_2 and brine leakage through open wellbores?
2. What site-specific variables most strongly influence the environmental and financial consequences of CO_2 and brine leakage in GCS projects?
3. How do environmental and financial risks evolve throughout the project lifecycle—from injection through post-injection site care and closure?
4. How can monitoring investments be optimized based on site-specific leakage risks and their financial implications?

1.4. RESEARCH BENEFICIARIES

The following entities can benefit from the outcome of this study:

- Insurance sector: This research provides necessary information to insurance companies to quantify, in dollar values, the site-specific financial impact of leakage.
- Project developers: It offers operators a simplified and more efficient methodology to evaluate and compare different project or site risks and justify financial assurance demonstrations for class VI permit applications based on the financial impacts of the worst-case scenario of leakage events. Furthermore, it offers operators a way to quantify the material and financial impacts of CO_2 and brine leakage to offer the foundations for economically efficient risk management decisions, such as improving monitoring or remediation strategy or select a suitable injection location.
- Regulatory sector: It offers regulators a more quantifiable way to evaluate financial assurance demonstration from Class VI permits applicants in a way that is suitable with the site-specific conditions.
- Credit buyers: It gives carbon credit buyers greater confidence in the quality and durability of the credits they purchase. It makes it easier to compare projects, reduce the chance of buying

low-integrity offsets, and support more credible climate claims. This helps buyers make more informed and impactful decisions, while reducing reputational and financial risk.

1.5. RESEARCH METHODOLOGY

The research combines geological modeling, reservoir simulation, and financial risk analysis to capture how subsurface conditions, failure mechanisms, and mitigation strategies influence both environmental and economic outcomes (See Figure 2).

Static Modeling

A portfolio of simplified static geological models was developed to represent a range of plausible subsurface configurations. These included various reservoir geometries—flat-lying, dipping, and anticlinal structures—to assess how different trapping mechanisms, such as simple structural, migration-assisted trapping or CO_2 trapping on an anticline, influence leakage risk (see Lyu et al. (2024) for more information about migration-assisted structural trapping). These models were built using Petrel software and incorporate variations in petrophysical properties (e.g., permeability, salinity, capillary entry pressure, critical water saturation, and critical gas saturation), reservoir thickness, depth, and reservoir size. These parameters were systematically varied to evaluate their influence on CO_2 and brine migration, leakage potential, and overall environmental and financial impact.

Dynamic Modeling

Dynamic reservoir simulations were conducted using Computer Modelling Group (CMG) software to model the injection, migration, and potential leakage of CO_2 and brine over time. The dynamic model simulates the full lifecycle of a GCS project, including CO_2 injection, post-injection, brine displacement, pressure front evolution, and upward fluid migration through

compromised wellbores. A fixed CO_2 injection rate was used during the injection period but the bottom-hole pressure was limited by the 90% of the fracture pressure as established by the EPA for CO_2 injection operations.

To eliminate uncertainty and capture the full range of potential environmental and financial impacts, the simulation framework adopts a conservative worst-case scenario in which no pre-injection remediation is performed on the wellbores within the project area. This scenario assumes that all legacy plugged-and-abandoned wells intersecting the storage formation are fully open, cased, unplugged, and lack surface wellheads—allowing them to act as direct vertical conduits for CO_2 and brine to reach the surface. By modeling this extreme case, the framework is designed to quantify the upper bounds of risk, ensuring that any real-world consequences would fall within the envelope of outcomes derived from this analysis. This approach also reflects the inherent uncertainty surrounding the location and condition of legacy wells, particularly in areas where historical records are incomplete or unreliable.

No thief zones or impacts to USDWs were considered in the simulation in order to represent a worst-case scenario in which leaked CO_2 and brine migrate directly to the surface. In a realistic setting, CO_2 and brine would follow preferential flow paths and the path of least resistance. Therefore, in the presence of legacy wellbores without plugs, fluids would be expected to migrate upward directly to the surface.

Also, wellbore density was varied across simulations to evaluate how the number of possible leakage pathways affects cumulative leakage volumes, environmental and financial impacts.

Environmental Impact Assessment

The mass of CO_2 and brine leaking to the surface through the open conduits was recorded for each simulation. Leakage results were expressed in absolute terms and as a percentage of the total CO_2 injected at reservoir conditions. Temporal profiles were also analyzed to examine how environmental impacts vary across the project lifecycle, from active injection to post-closure period.

Financial Impact Assessment

A simplified version of the Leakage Impact Valuation (LIV) framework (Pollak et al., 2013). was used to monetize leakage outcomes. The LIV method considers features, events, and processes (FEPs) that may lead to undesirable surface impacts during the operational lifetime of a CO_2 storage project. This methodology has been applied in previous policy and basin-scale analyses (Bielicki et al., 2013b, 2014b, 2016; Deng et al., 2014).

The financial analysis in this study is tailored to reflect the economic perspective of the injection operator. Stakeholders considered include the injector and CO_2 producer, under a take-or-pay agreement. Under this contract, the injector is obligated to accept the CO_2 in exchange for receiving the associated tax credits (e.g., 45Q) upon its permanent storage. If the injector is unable to accept and inject the CO_2, they incur a penalty for each ton not sequestered. Financial cost drivers considered include:

- Cost of environmental remediation due to brine leakage
- Cost of repairing the leaky wellbore
- Detection threshold defined by monitoring system
- Contractual penalties due to injection interruption
- Loss of 45Q tax credits due to CO_2 leakage

- Time required to fix the well

Note that environmental remediation due to CO_2 leakage is not included, as discussed earlier, because evidence shows that CO_2 leakage does not significantly harm water quality and disperses quickly when released to the atmosphere.

Monte Carlo simulation framework was used to vary the financial cost drivers and run thousands of iterations based on a smaller number of simulations, producing statistically robust estimates of financial outcomes under varying scenarios.

In addition, an annual probability of well failure was assigned to enable more realistic estimation of the financial and environmental impacts associated with CO_2 and brine leakage. Plus, to capture the temporal evolution of these impacts, Bayesian inference was applied, allowing for dynamic updates to risk estimates as new information (e.g., absence or presence of leakage) becomes available over time.

By assigning a range of annual failure probabilities, the model captures how financial consequences evolve as wells fail at different points across the injection and post-injection periods. This introduces temporal variability into the financial risk profile—reflecting the fact that leakage events are not simultaneous but distributed over decades.

This approach differs from others in the literature that rely on assumed effective wellbore permeability values (e.g., Watson and Bachu (2008)). Instead, it removes permeability as a source of uncertainty and uses failure probability as a proxy for well integrity. This allows for a more direct and probabilistically grounded evaluation of long-term containment risk.

Monitoring and Mitigation Analysis

To assess the value of early leak detection and effective remediation, scenarios with varying detection thresholds were analyzed. The results show how investment in more sensitive monitoring strategies can affect cumulative CO_2 leakage and overall financial impact.

This methodology provides a general (not site-specific) framework for integrating reservoir behavior, failure probabilities, and financial consequences, offering valuable insights for risk management, regulatory compliance, and investment decision-making in GCS projects.

Research Mechanisms

Figure 2 presents the research methodology flow diagram used in this study. The process begins with the development of a base model, constructed using data representative of geologic formations in the U.S. Gulf Coast. Key input parameters—such as permeability, reservoir size, salinity, and well density—were selected based on literature sources and industry data.

To evaluate the influence of these parameters on leakage risk, a sensitivity analysis was performed. For the probability of well failure, five discrete probability values were evaluated to capture a range of possible risk scenarios. For each property, high and low values were analyzed in addition to the base case, resulting in a total of 23 dynamic simulation models.

Also, the effect of reservoir geometry on leakage behavior was also assessed. Three different structural settings—flat-lying, dipping, and anticlinal—were modeled using the same base input values. For each geometry, a model was built featuring one injection well and one open (leaky) wellbore. Within each geometry, three distinct reservoir facies were created to represent different petrophysical properties, resulting in a total of nine additional simulations.

In all simulations, a fixed amount of CO_2 was injected, limited by 90% of the formation's fracture pressure to avoid mechanical failure. Using the dynamic reservoir simulator CMG-GEM, both CO_2 and brine leakage rates were calculated for each scenario.

These leakage rates were then used to quantify both environmental impacts—including well repair time and detection thresholds—and financial consequences, such as the cost of environmental remediation, the cost of repairing leaky wellbores, contractual penalties due to injection interruption, and lost 45Q tax credits associated with CO_2 leakage. All environmental and financial impacts were normalized by the total volume of CO_2 injected to allow for comparison across scenarios and support scalable, per-ton impact estimates.

This modeling framework allows for a comprehensive understanding of how different subsurface settings, failure probabilities, and monitoring conditions influence leakage behavior and associated risk profiles. It ultimately supports site-specific evaluations and decision-making for insurance pricing, permitting, and long-term liability planning.

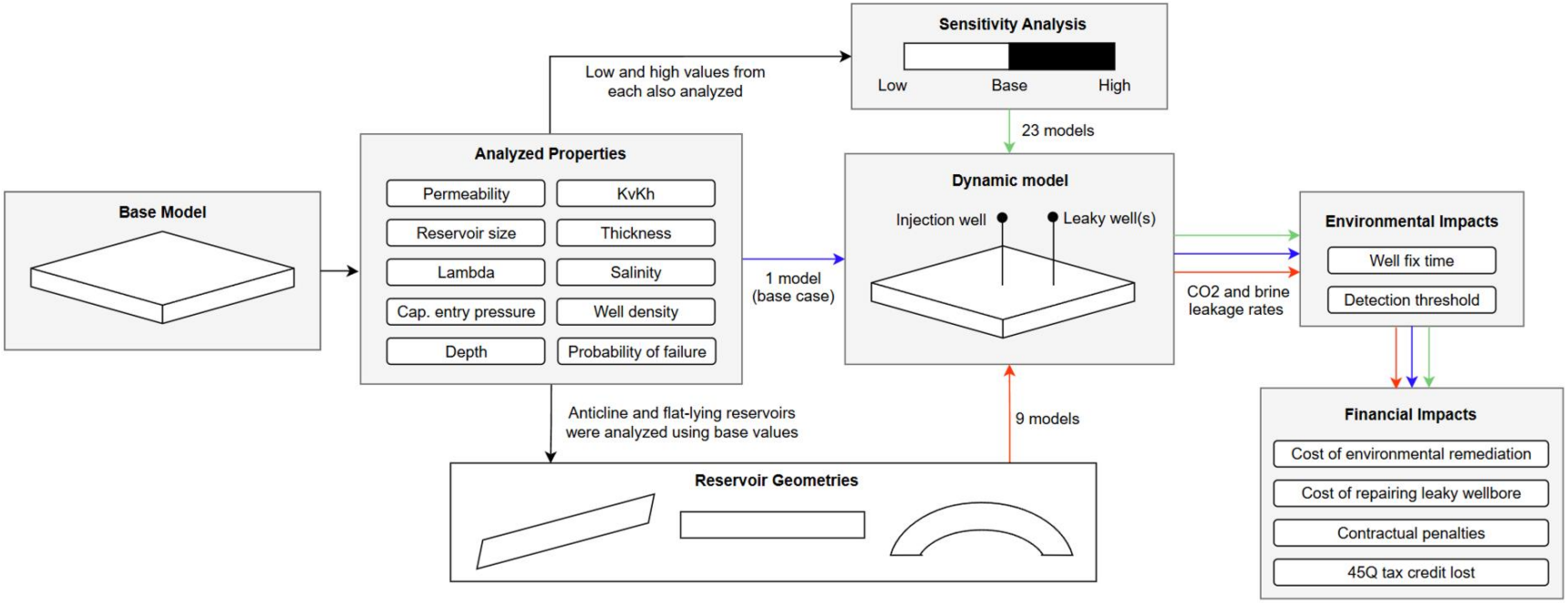

Figure 2. Research Methodology Flow Diagram.

CHAPTER II: METHODOLOGY

2.1. INTRODUCTION

This chapter outlines the methodological framework used to evaluate CO_2 and brine leakage risks in geologic carbon storage (GCS) and their corresponding financial impacts under a worst-case leakage scenario. The approach integrates geological characterization, dynamic multiphase flow simulations, open wellbore leakage modeling, and financial risk estimation. The analysis begins with the development of a static geologic model based on U.S. Gulf Coast reservoir properties, followed by dynamic simulation of CO_2 injection and migration using CMG-GEM. Leakage behavior through open wellbores is evaluated using CMG-GEM to simulate direct leakage from the reservoir to the surface. Finally, a financial modeling framework is applied to assess the economic consequences of leakage events under varying monitoring conditions, subsurface settings, well failure probabilities, and leakage durations.

2.2. STATIC MODELLING

Geological Settings

Values from statistical analysis were used to calculate the primary parameters for the geological setting, such as thickness, porosity, permeability, and depth. For the statistical analysis, some selection criteria were implemented, such as the sand body should have a thickness higher than 10 meters, should have a porosity higher than 10%, permeability higher than 10 millidarcies. The selection of these criteria allows the sand body to be feasible for being an injection zone for CO_2 storage from an economic and risk assessment perspective (Callas et al. 2022; Geological Survey 2008; Raza et al. 2016; Ramírez et al. 2010).

The “storage window” for CO_2 (Bump et al., 2021) is defined vertically between the base of the lowest Underground Source of Drinking Water (USDW)—classified as water with less than

10,000 ppm total dissolved solids (UIC Class VI, 2010)—and the shallower of either the geologic overpressure limit or basement rock. At a minimum, injection must occur below the lowest USDW. To maximize storage efficiency, injected CO_2 is typically kept in a supercritical state, which requires a depth of roughly 800 m or more below the top of the water column. In the U.S. Gulf Coast, this storage window generally spans from about 800 to 3,000 m depth. All reservoir property data for this study were therefore extracted from within this depth range.

To determine the range of injection zone thicknesses and depths, 344 wells from the US Gulf Coast, Lower, Middle, and Upper Miocene were used. The dataset used is from the Southwest Louisiana and Mississippi River Chemical Corridor. In the Figure 3 and Figure 4 are shown the histogram and cumulative distribution of thickness values and depth values, respectively. The P10, P50, and P90 were used as low, base, and high case values for the sensitivity analysis.

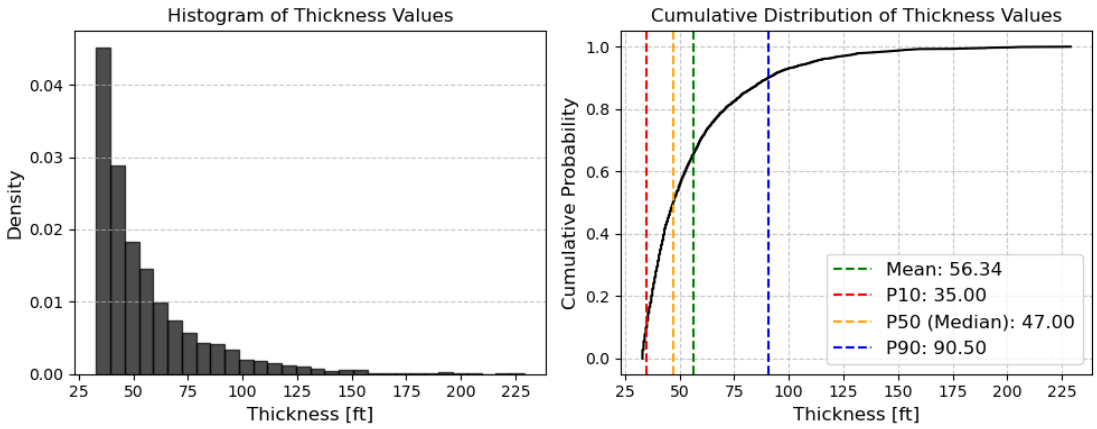

Figure 3. Thickness Distribution of Lower, Middle, and Upper Miocene Formations from 344 Wells in the U.S. Gulf Coast (Southwest Louisiana and Mississippi River Chemical Corridor): P10 = 35 ft, P50 = 47 ft, P90 = 90.5 ft

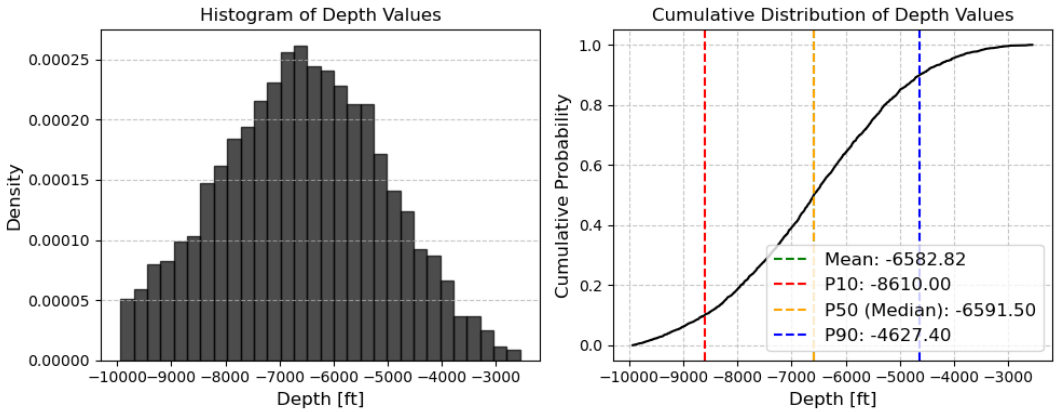

Figure 4. Depth Distribution of Lower, Middle, and Upper Miocene Formations from 344 Wells in the U.S. Gulf Coast (Southwest Louisiana and Mississippi River Chemical Corridor): P10 = -8610 ft, P50 = -6591.5 ft, P90 = -4627.4 ft

For porosity and permeability, the Atlas of Northern Gulf of Mexico Gas and Oil Reservoirs, Volume 1 – Miocene and Older Reservoirs by Seni et al. (1997) was used. This dataset surveys 4325 Miocene and older reservoir in the Federal Outer Continental Shelf (OCS) and offshore waters of Alabama, Louisiana, and Texas. After applying the selection criteria, porosity and permeability values were calculated from 2347 and 59 observations, respectively (Figure 5 and Figure 6). The P10, P50, and P90 were used as low, base, and high case values for the sensitivity analysis.

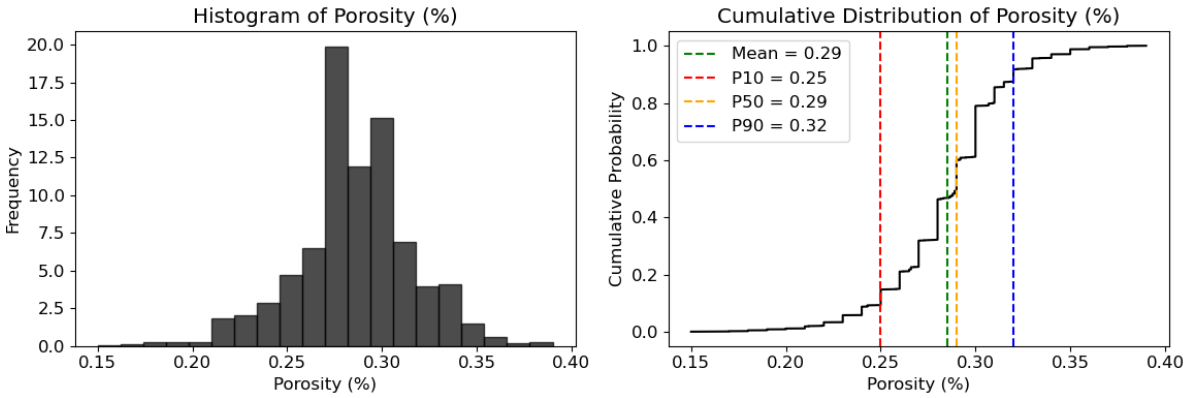

Figure 5. Porosity Distribution of 2,347 Miocene and Older Reservoirs in the Federal OCS and Offshore Waters of Alabama, Louisiana, and Texas (Seni et al., 1997). P10 = 0.25, P50 = 0.29, P90 = 0.32

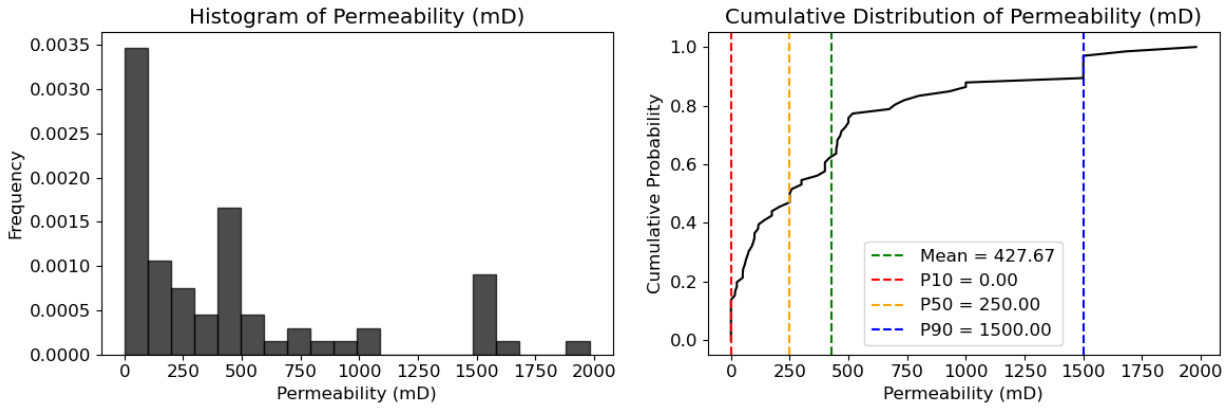

Figure 6. Permeability Distribution of 59 Miocene and Older Reservoirs in the Federal OCS and Offshore Waters of Alabama, Louisiana, and Texas (Seni et al., 1997). P10 = 51.6 mD, P50 = 367 mD, P90 = 1500 mD

Vertical to horizontal permeability ratio (kv/kh) is another important parameter in geologic CO_2 storage, as it affects the migration and distribution of CO_2 within saline aquifers. In many sedimentary formations, including those in the Gulf Coast, kv/kh ratios often range from 0.01 to 0.1 (Kumar et al., 2005; Thibeau & Mucha, 2011).

Saline Aquifer Geometry

Three simplified aquifers structures were created to analyze how different geological structures and trapping mechanisms (e.g., migration assisted trapping or structural trapping) can affect CO_2 and brine leakage behavior. The geological structures used are: flat, dipping, and anticline. The slope from the base to the top of the anticline is 5°. This slope matches to values reported by Ulfah et al. (2021) for an anticline formed by a salt dome in the Gulf Coast, and the average slope of the Cranfield field, Mississippi. As for the dipping reservoir, a slope of 5° was also assigned to be comparable with the anticline structure (Figure 7). The model size is 10 by 10 km, and hydrologic model boundaries were assumed to be an uncertainty, hence different boundary conditions were analyzed as a part of the sensitivity analysis study (shown in section 2.3).

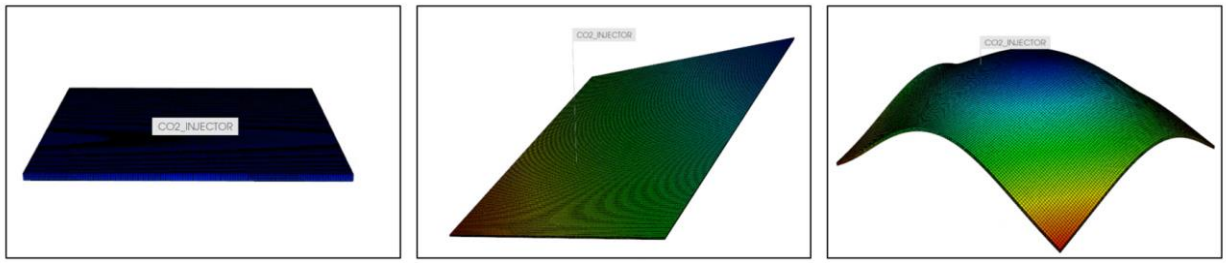

(a) Flat Reservoir (b) Dipping Reservoir (c) Anticline Reservoir

Figure 7. Geometries used for the research project.

Rock Fluid Properties

Relative Permeability Curves

The relative permeability curves for gas and water were derived using two established models. The relative permeability of gas was modeled using Corey's Model (Corey, 1954), which is defined as:

$$k_{gr} = \left(1 - \hat{S}^2\right)\left(1 - \hat{S}\right)^2,$$

where:

$$\hat{S} = \frac{(S_w - S_{wr})}{\left(1 - S_{gr} - S_{wr}\right)}$$

Here, S_w is water saturation, S_{wr} is the critical water saturation, and S_{gr} is the critical gas saturation.

The relative permeability of water was calculated using the Van Genuchten-Mualen Model (Van Genuchten, 1980), given by:

$$k_w = \sqrt{S^*}\left(1 - \left(1 - [S^*]^{\frac{1}{\lambda}}\right)^{\lambda}\right)^2$$

where

$$S^* = \frac{(S_l - S_{wr})}{(1 - S_{wr})}$$

S_l is the water saturation and λ is the fitting parameters characterizing the pore structure, also called Pore Size Distribution index. For the λ value, a value ranging from 0.1 to 0.5 is recommended when no real data is available (Baker et al., 2015).

As for the critical water saturation and critical gas saturation, the empirical correlations proposed by Holtz (2022) were used. These correlations were developed using real-world datasets compiled from a wide range of oil and gas reservoirs in U.S Gulf Coast.

$$S_{gr} = 0.5473 \ - 0.969\emptyset$$

$$S_{wr} = 5.6709[\log(k)/\emptyset]^{-1.6349}$$

Where κ is the permeability in millidarcies and φ is the porosity. For this study, critical water saturation and critical gas saturation values were derived from porosity and permeability values.

For the hysteresis model, the trapping model proposed by Land (1968) was used. In this model, the trapped gas saturation S_{gt} is computed as:

$$S_{gt} = \frac{S_{gi}}{1 + CS_{gi}}$$

Where S_{gi} is the initial gas saturation (actual gas saturation at flow reversal) and C is the Land trapping coefficient. A C value equal to 1 was used to calculate the trapped gas saturation. A C value equal to 1 was determined by Juanes et al. (2006) from the relative permeabilities of water and gas taken from Oak, Baker, and Thomas (1990) for water wet Berea sandstone and a

gas-water system, which aligns with the lowest range from what (Hosseini et al., 2024) recommends when no data is available.

Capillary Pressure Curves

For the capillary pressure curves, the van Genuchten (1980) model was used.

$$P_c = -P_o \left([S^*]^{-\frac{1}{\lambda}} - 1 \right)^{1-\lambda}$$

Where Pc is the capillary pressure (pressure difference between gas and water phases) and Po is the capillary entry pressure (the minimum pressure required for the non-wetting phase to enter the porous medium).

For gas-water systems in sandstone reservoirs, typical P_o values range from 0.1 psi to 10 psi, as noted by several studies (e.g., Zhou, Hatzignatiou, and Helland (2017); Borazjani et al. (2021); Ni et al. (2019)).

In the following figure is shown the gas relative permeability, water relative permeability, and capillary pressure curves used for the base case for the sensitivity analysis.

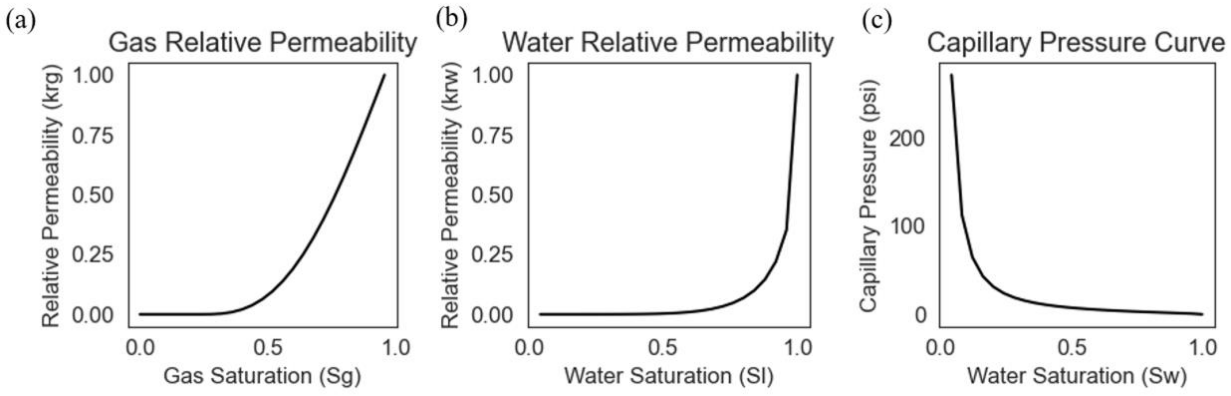

Figure 8. (a) Gas and (b) water relative permeability and (c) capillary pressure curves for the base case.

In the following figure is shown the gas relative permeability, water relative permeability, and capillary pressure curves used for the different geometries case. It is important to mention that for the different geometry cases, three representative facies were developed to simulate poorly-sorted (Facies 1), moderately-sorted (Facies 2), and well-sorted (Facies 3) sand formations. These facies were constructed to reflect more geologically realistic conditions by incorporating natural correlations among reservoir properties, such as porosity, permeability, capillary entry pressure, and saturation parameters. Values used for building these facies are shown in table 2.

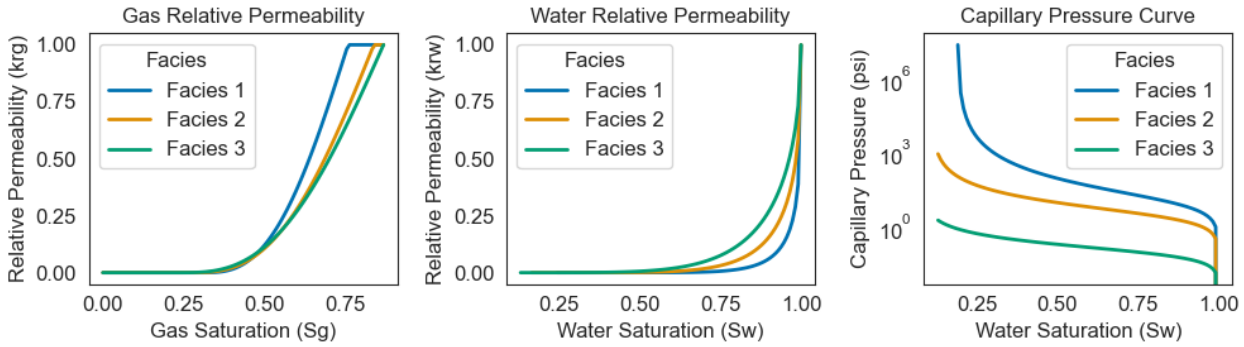

Figure 9. Gas and water relative permeability and capillary pressure curves for the different geometries case.

Salinity

The diffusion and dispersion of CO_2 within an aquifer have a direct impact on solubility trapping. Such trapping mechanism is highly sensitive to temperature, pressure, salinity and the composition of the brine (Hosseini et al., 2024). Most waters in the Gulf Coast aquifers have salinities in the range of 10,000 to 80,000 mg/L (Ghomian et al., 2024; Kreitler & Richter, 1986). Nonetheless, highest concentrations (in excess of 150,000 mg/L) were measured in Frio, Vicksburg and Wilcox units (Kreitler & Richter, 1986). These salinity ranges were used for the multi-phase flow simulation and posterior sensitivity analysis.

Sensitivity Analysis

In the following table is shown the low and high bound for each of the variables used on the sensitivity analysis. For the values calculated statistically – porosity, permeability, thickness, and depth-, the low, base and high values correspond to the P10, P50, P90 respectively.

Variable	Low	Base	High
Porosity	0.25	0.29	0.32
Permeability	51.6 mD	367 mD	1500 mD
KvKh	0.01	0.1	1
Thickness	35 ft (10.67 m)	47 ft (14.33 m)	90.5 ft (27.58 m)
Depth	4627.4 ft (1410.4 m)	6591.5 ft (2009.1 m)	8610.0 ft (2324.3 m)
Salinity	10,000 mg/l	30,000 mg/l	100,000 mg/l
Capillary Entry Pressure	0.1 psi	3 psi	10 psi
Pore Size Distribution (λ)	0.3	0.4	0.5
Critical Water Saturation	0.023	0.043	0.094
Critical Gas Saturation	0.237	0.257	0.305
Saline Aquifer Size	25200x25200 km	770000x770000 km	7610000x7610000 km
Saline Aquifer Geometry	Flat, Dipping, and Anticline Structures		

Table 1: Sensitivity Analysis for the leakage model.

In the base case, default values were used along with a flat-lying reservoir geometry. For the sensitivity analysis, each variable was tested individually by assigning its low and high values while keeping all other parameters at their base values. For example, to assess the impact of porosity, the low porosity value was applied while all other variables remained unchanged. The same was done for the high porosity value. This approach was used to isolate and evaluate the influence of each variable on CO_2 and brine leakage rates.

To assess how injection zone geometry affects leakage risk, three representative facies were defined to simulate poorly sorted (Facies 1), moderately sorted (Facies 2), and well-sorted (Facies 3) sand formations. Homogeneous models containing only one facies type were simulated for each case, allowing direct comparison of CO_2 and brine migration patterns under varying facies properties and geometries. This approach helps ensure that the modeled CO_2 plume migration and leakage behavior more closely reflect the subsurface heterogeneity typically observed in real-world formations. The following table summarizes the reservoir properties associated with each facies used in the sensitivity analysis.

Variable	Facies 1	Facies 2	Facies 3
Permeability	51.6 mD	367 mD	1500 mD
Porosity	0.25	0.29	0.32
Critical Gas Saturation	0.305	0.266	0.237
Critical Water Saturation	0.244	0.161	0.133
Pore Size Distribution (λ)	0.3	0.4	0.5
Capillary Entry Pressure	10 psi	3 psi	0.1 psi

Table 2. Sensitivity Analysis for the different geometries.

Due to time constraints, an initial screening assessment was conducted using NRAP-OPEN-IAM (see Appendix A.2) to identify the key parameters influencing CO_2 and brine leakage from the injection zone. A total of 24 simulations were performed to evaluate the sensitivity of leakage volumes to various subsurface variables. The analysis revealed that the most influential parameters are permeability, pore size distribution (λ), vertical-to-horizontal permeability ratio (kv/kh), reservoir depth, capillary entry pressure, aquifer size, salinity, and thickness. Based on these findings, a more detailed and physically realistic simulation was subsequently conducted

using the CMG-GEM multiphase flow simulator to capture dynamic leakage behavior under varying geological and operational conditions.

2.3. DYNAMIC MODELLING

Numerical injection simulations were conducted using Computer Modeling Group-Generalized Equation of State (CMG-GEM) (https://www.cmgl.ca/gem), a multiphase numerical reservoir flow simulator widely used for simulating CO_2 injection and behavior in deep saline reservoirs (Foroozesh et al., 2018; Gianni et al., 2025; Khan et al., 2015; Kumar et al., 2005).

Model Configuration & Sizing

The model domain spans 10 × 10 km with a uniform grid spacing of 250 ft (76 m), resulting in 132 cells along both the x- and y-axes. The vertical grid resolution varies based on reservoir thickness, with a maximum cell thickness of less than 3 m across all scenarios. The location of the CO_2 injection well is at the coordinate (3772, 3772) meters.

Because multiple wells were evaluated in this study, the simulation grid was not locally refined around individual injection wells or open wellbores. However, it is important to note that local grid refinement around open wellbores typically reduces simulated CO_2 and brine leakage rates by capturing near-well flow dynamics more accurately (see Section A.3 for further discussion of this effect).

Additionally, the open wellbores themselves function as boundary conditions at the top of the model domain, creating vertical pathways for pressure relief. This has a direct impact on the spatial distribution of pressure and CO_2 saturation. Specifically, increasing the number of open wellbores enhances pressure dissipation, reducing pressure buildup in the reservoir and accelerating pressure decline over time. As a result, simulations with a higher density of open wells

exhibit altered plume behavior, including reduced lateral migration and potentially lower leakage volumes.

For the sensitivity analysis on the lateral extent of the saline aquifer—which represents variations in aquifer size—the lateral boundary condition was modeled using the approach proposed by Ghomian et al. (2024). For this analysis, the geometric progression-based attenuation method was utilized, where the pore volume and transmissibility are gradually changed over the last boundary cells in the model using a geometric progression function. For this study, unlike the approach used by Ghomian et al. (2024), transmissibility multipliers were applied one cell inward toward the model center. In Ghomian's method, the outermost cells have no transmissibility multiplier because they are assumed to represent a no-flow boundary. Here, the outermost cells were instead assigned transmissibility values calculated using a geometric progression function. This adjustment was intended to account for uncertainty by imposing a "closer" effective boundary condition—meaning each cell has a slightly lower transmissibility multiplier than in Ghomian's setup. As a result, the model predicts a slightly higher short-term pressure increase, while maintaining similar long-term behavior.

For the base and high boundary condition cases, a six-step attenuation with a common ratio of 3 was applied, using pore volume modifiers of 10,000 and 100,000, respectively. For the low boundary case, a four-step attenuation with a common ratio of 1.2 was used, with a pore volume modifier of 100.

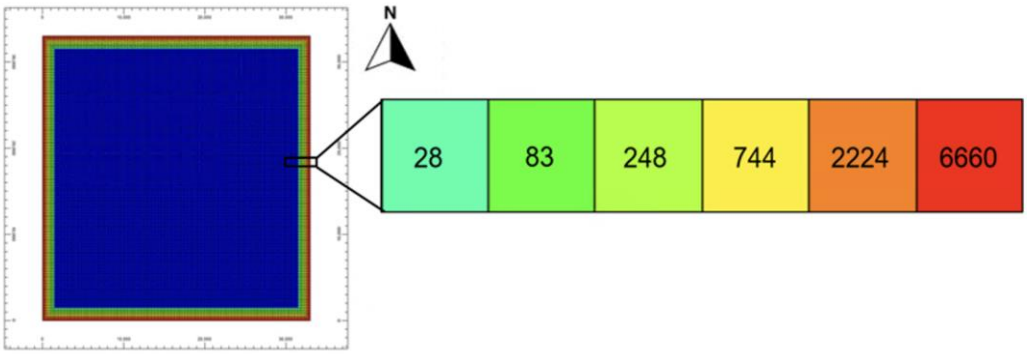

Figure 10. Pore volume modifiers on the cells at the boundaries of the reservoir model for the base boundary condition case.

Initial Simulation Conditions

For the simulation workflow, the hydrostatic pressure gradient, fracture pressure gradient, and temperature gradient used were 0.465 psi/ft, 0.7 psi/ft, and (15°C + 25°C/ft) respectively. The initial pressure in the reservoir was assumed to be hydrostatic and the reservoir was initially saturated with water.

CMG-Winprop was used to estimate the phase behavior and the properties of reservoir fluids. CO_2 solubility is modelled using Henry's law (Nghiem & Li, 1986) for different brine salinities. The brine phase density and viscosity were estimated by using Rowe and Chou (1970) correlation and Kestin, Khalifa, and Correia (1981) correlation, respectively. For the CO_2 properties, the Peng-Robinson Equation of State (PR-EOS), widely accepted for nonpolar gases like CO_2 was used to predict phase-equilibrium compositions and to derive EOS parameters (Peng & Robinson, 1976).

Regarding the operating conditions of the injection well, 0.2 million tonnes (MT) of CO_2 per year were injected over a 20-year period for all cases. However, the bottom-hole pressure was constrained to 90% of the fracture pressure. This means that if the 90% threshold was reached, the

injection rate was reduced to avoid exceeding this operational limit, making the injection rate dependent on the bottom-hole pressure.

As a result, environmental and financial impacts were normalized based on the cumulative amount of CO_2 injected in each case. The 20-year injection period was followed by a 100-year post-injection monitoring phase, which was analyzed in all scenarios.

2.4. Open Wellbore Simulation

Open Wellbore Distributions

For the Open Wellbore Simulation, CMG-GEM was used, specifically the module Cap Rock Leakage Using Wells. This module assumes that reservoirs are initially bounded by competent cap rock that is sealing, and as pressures chance in the reservoir and becomes sufficiently large, the seal provided by the cap rock may be breached and flow across the breach might occur. To implement this, a rock type is first defined using the keyword CROCKTYPE along with its assigned rock type number. Production wells are then designated as caprock leakage wells by specifying them with the CRL_WELLS keyword. The simulation was set so that the cap rock breaches once the pressure is higher than the hydrostatic pressure, hence CO_2 or brine is produced from the designated production wells. Namely, once there is a pressure change, fluids are going to flow through the wellbore.

Note that these simulations represent a worst-case scenario, in which no pre-injection remediation of open wellbores is performed. All wells are assumed to be unplugged, cased, and lacking a wellhead, providing a direct pathway to the surface. Additionally, it is assumed that there are no thief zones or intermediate permeable layers that could intercept migrating CO_2 or brine—meaning that any leakage would migrate directly to the surface without attenuation.

These wellbores are modeled as open conduits from the top of the injection zone to the surface. Operational constraints specify a minimum wellhead pressure of 1 atm (14.65 psi) and a minimum bottomhole pressure equal to the hydrostatic pressure. This means that any increase in bottomhole pressure above hydrostatic will cause fluids to flow through the well. The wellbores have a radius of 0.164 feet, or 0.05 meters.

Two well distributions were used along the analysis: a linear well distribution and a random well distribution.

- **Linear well distribution:** This was used to understand how CO_2 and brine leakage vary depending on the distance. 4 open wellbores were located at distances of 100 meters, 500 meters, 1000 meters, and 2000 meters from the injection well. Different was the case when analyzing how different geometries affect the leakage risk. In this case, an open wellbore was located on the location on top of the anticline (center of the model) to understand how the different structures and potential accumulation of CO_2 on the anticline affects leakage risks and financial impacts versus having a dipping structure with no evident accumulation of CO_2.
- **Random well distribution:** This was used to understand how the financial damages vary depending on the well density and subsurface settings. For the location of the open wellbores, the well density of the Texas Gulf Coast was used as an analog. The State of Texas has more than 1 million wells related to oil and gas activities and many more, generally shallower, water wells. The average surface density of the Texas Gulf Coast is ~ 2.4 wells/km^2, concentrated in areas containing traps and hydrocarbons. Nonetheless, the average well penetration density drops to 0.27 well/km^2 below a depth of 2440 meters (Nicot, 2009). To understand how sensitive is the financial damages depending on the well density and to calculate financial impact of geologic CO_2 storage, three cases were created, a low-density, a base-density, and high-density case of 0.27 wells/km^2, 2.4 wells/km^2, and 4.8 wells/km^2 respectively. The wells locations were assigned randomly around the model

domain using a random location generator code generated using Python. The high-density case, even though it is double the average well density of the Texas Gulf Coast, it was created to evaluate a worst-case scenario (Figure 11).

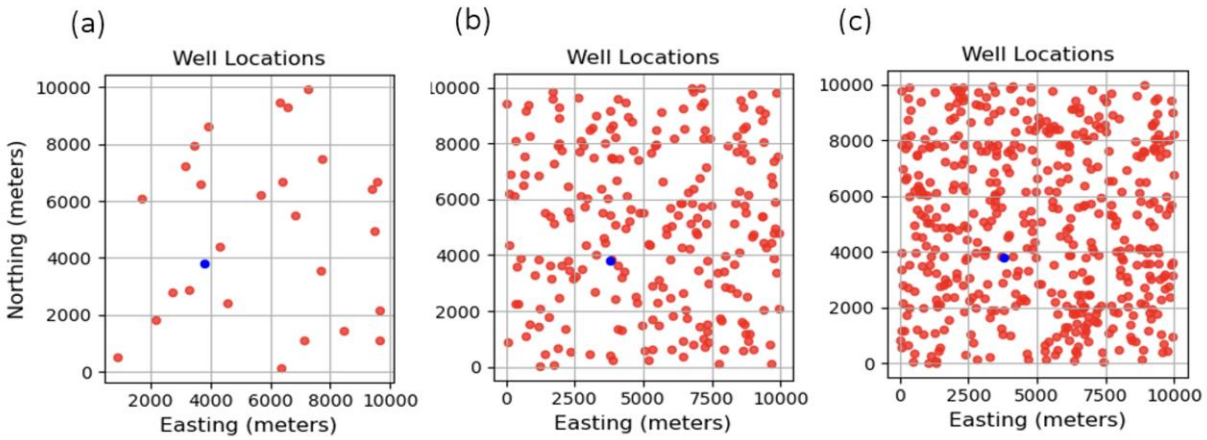

Figure 11. Open Wellbore densities for the leaky well simulation. (a) well density of 0.27 wells/km2, (b) well density of 2.4 wells/km2, and (c) well density of 4.8 wells/km2. The blue dots are the injection well, and the red dots are the leaky wells.

Geometry Sensitivity Analysis

The shapes of the CO_2 and pressure plumes for Facies 2 and 3 are illustrated in Figure 11. Simulation results for Facies 2 and 1 indicate that the CO_2 plume does not reach the open wellbore in any of the geometries. However, for Facies 3, the CO_2 plume reaches the open wellbore in both the anticline and dipping scenarios (See Figure 12). The flat scenario and the Facies 1 and 2 have been excluded from further analysis because the CO_2 plume does not reach the open wellbore, and the primary objective is to assess whether the anticline geometry presents a higher risk due to CO_2 accumulation on the top and how the risk profile over time changes due to it. For these reasons, just Facies 3 was analyzed for posterior studies.

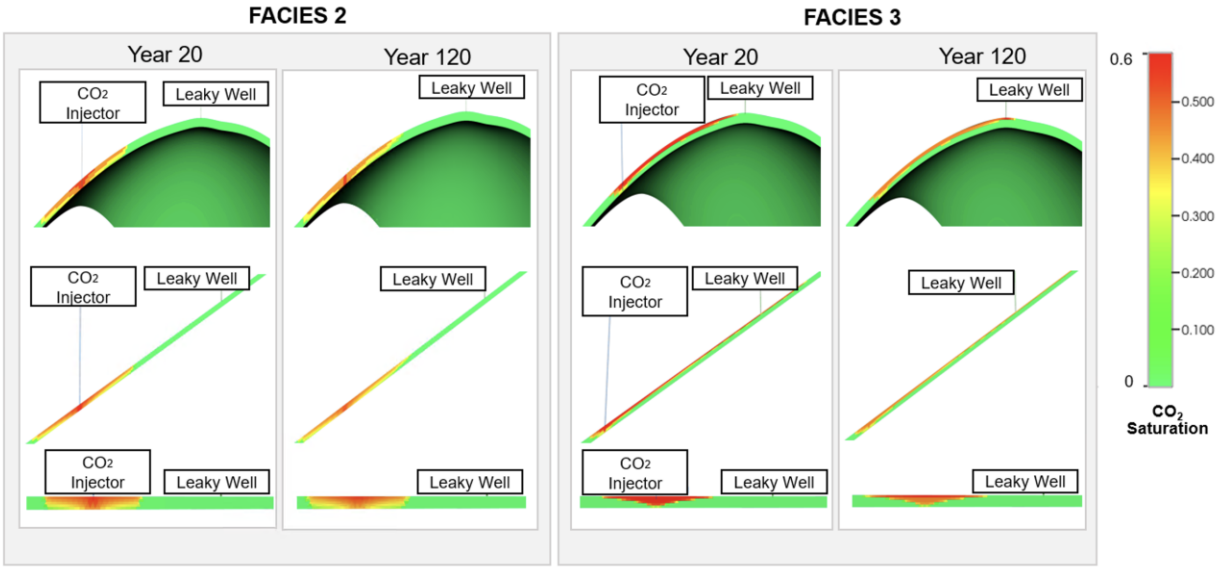

Figure 12. CO_2 plume distribution at years 20 and 120 for different reservoir geometries: anticline, dipping, and flat. The left panels illustrate plume behavior using Facies 2 properties, while the right panels depict plume behavior using Facies 3 properties.

2.5. Financial Impact Evaluation

Financial Model Assumptions

The financial model developed in this study estimates the potential economic consequences of CO_2 and brine leakage in geologic carbon storage (GCS) projects. Financial and environmental damages are calculated based on leakage rates to the surface. Impacts to underground sources of drinking water (USDWs) are not explicitly considered, due to limited empirical data and to maintain focus on a conservative, worst-case scenario: direct leakage to the surface through open wellbores.

Scientific literature shows that brine leakage can negatively impact surface water quality, so the model includes environmental remediation costs for brine reaching the surface. In contrast, CO_2 leakage is unlikely to significantly harm water quality or human health, as it disperses rapidly

once released. Therefore, the model excludes CO_2 remediation costs and instead accounts for financial penalties and tax credit losses resulting from leakage.

The model incorporates several key assumptions:

- Cost of environmental remediation due to brine leakage
- Cost of repairing the leaky wellbore
- Detection threshold defined by the monitoring system, which determines the minimum detectable leakage rate
- Time required to fix the well, based on literature estimates
- Contractual penalties due to injection interruption
- Loss of 45Q tax credits due to CO_2 leakage

These assumptions reflect realistic commercial operations and assume the injection operator is fully responsible for remediation and compliance. A take-or-pay agreement is assumed between the operator and the CO_2 emitter, whereby:

- The operator must inject a contracted CO_2 volume or pay a penalty for unmet delivery.
- In return, the operator receives the full value of the 45Q tax credit per tonne of CO_2 successfully sequestered.

If leakage occurs, injection is suspended under regulatory requirements, triggering:

- Take-or-pay penalties for the CO_2 not injected
- Loss of 45Q tax credits for the leaked CO_2

This structure incentivizes early detection and fast remediation to reduce economic and environmental exposure.

For the purposes of this study, financial impacts are assessed solely from the perspective of the injection operator. This approach reflects both the low likelihood and high uncertainty associated with quantifying costs to other stakeholders. Hence, the model assumes that CO_2 and brine leak directly to the surface and do not affect third parties such as water users, oil and gas producers, or waste injection operators. Accordingly, no third-party damages or liabilities are considered, and no labor or remediation burdens are attributed to external entities. Additionally, the model does not incorporate lost revenue or opportunity costs for the injector operator.

Financial damages are calculated using a simplified version of the Leakage Impact Valuation (LIV) framework developed by Pollak et al. (2013). Inspired by the LIV approach, this study adapts its structure to emphasize the key cost drivers listed above while capturing the timing and magnitude of leakage events. The framework connects leakage features, events, and processes (FEPs) to quantifiable outcomes like leakage volumes, detection timing, and remediation costs. By simplifying these elements, the model supports transparent evaluation of leakage impacts under both worst-case and mitigated scenarios, tailored to site-specific conditions.

Financial Model Components

Contractual Penalty

The contractual penalty represents a contractual fee paid to the emitter as compensation if the project operator fails to receive and permanently store the contracted amount of CO_2. For first-of-a-kind (FOAK) projects, this penalty is typically higher due to higher uncertainty and risk, estimated at $20 per ton of CO_2. For nth-of-a-kind (NOAK) projects, reflecting more mature and lower-risk scenarios, the penalty is around $5 per ton. To capture this uncertainty, a uniform distribution ranging from $5 to $20 per ton was utilized, based on values from Bielicki et al. (2014b).

Inflation Rate

An annual inflation rate of 2.9% was used, based on data from the U.S. Bureau of Labor Statistics (BLS) for the year 2024. This rate is employed to adjust historical and current costs into future dollars, ensuring the accuracy of future cost projections.

45Q Tax Credits Lost

The model applies a carbon price of $85 per tonne of CO_2, as established by the Inflation Reduction Act (2022). In the event of a leakage, the model assumes that the financial value of the leaked CO_2 must be repaid through the forfeiture of 45Q tax credits. Specifically, if any portion of the stored CO_2 escapes into the atmosphere within a designated time frame, the operator is required to return the tax credits received for that volume (IRS, Department of the Treasury, 2023). This effectively treats CO_2 leakage as a reversal of the financial incentive provided by the 45Q program.

Discount Rate

The discount rate was set equal to the inflation rate (2.9%) to achieve a real discount rate of zero. Given the long-term nature of CCS projects (typically spanning 100 years or more), employing a real discount rate of zero ensures that future financial impacts have equivalent weighting to present-day impacts.

Detection Threshold

Different approaches to monitoring sites to detect leakage are available such as down-hole geophysical methods (e.g., time lapse seismic methods or pulsed neutron logs) or surface fluid samples for geochemical analysis (e.g., air or soil detection, dissolved inorganic carbon alkalinity, and pH) (U.S. DOE, 2017) to satellite-based InSAR. But due to the limited empirical data and potentially site-specific nature of the detection threshold across various monitoring technologies, for this study a detection threshold was defined as the minimum leakage rate (both CO_2 and brine) required for a leak to be identified and reported by the collective monitoring systems. Hence, a

triangular distribution was applied, ranging from 0.33 tons per day (minimum sensitivity) to 30 tons per day (maximum reasonable detection threshold). Meaning, that when the CO_2 and brine leakage from a well is equal or higher than such detection threshold, the leakage will be detected and posteriorly remediated. The selected values reflect findings from Trabucchi et al. (2012). Nonetheless, choosing an appropriate detection threshold remains critical for operators and regulators, impacting response times and total leakage volume.

Well Fix Time

Well fix time represents the interval between leak detection and successful remediation. To establish this parameter, empirical data from the Texas Railroad Commission (TRRC) was analyzed. Operators in Texas are required to submit Mechanical Integrity Tests (MIT) annually, resulting in a robust dataset of 471,033 registered events since February 2020. Analysis identified 3,157 events transitioning from failure to approval status, and 1,120 events transitioning from approval status to failure to approval. The latter dataset was used to derive a normal distribution for the well fix time, reflecting industry practices and regulatory timelines (Figure 13). For this study, it is assumed that the time required to repair a leaking well in a storage project would be similar to that observed in various production cases. While carbon storage projects may respond more quickly due to higher financial risks, the repair timelines used in this analysis are intended to represent a conservative, worst-case scenario to bound the financial model.

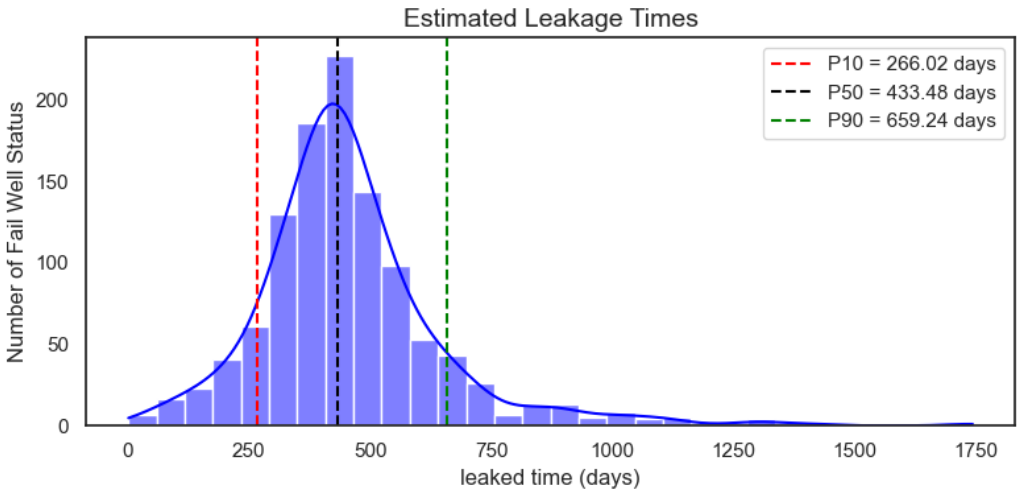

Figure 13. Normal distribution of estimated well fix times calculated based on MITs. Data provided by the Texas Railroad Commission. Well fix time serves as a proxy in this study for time over which leakage continued

Environmental Remediation Costs

Environmental remediation costs associated with brine leakage in this study are based on a pump-and-treat strategy, where contaminated groundwater leaking to the surface is extracted, treated, and reinjected into the aquifer. Cost data were obtained from the U.S EPA Remediation Technology Cost Compendium (U.S. EPA, 2001), which reports both capital and operating costs for various remediation technologies. Specifically, the unit capital cost is defined as the cost per 1,000 gallons of groundwater treated annually, and the unit average annual operating cost reflects the ongoing expenses per 1,000 gallons of groundwater treated each year.

To capture the uncertainty and skewed distribution often observed in environmental remediation costs, driven by variability in system throughput, treatment intensity, and operational efficiency, a lognormal distribution was fitted separately for capital and operating costs using the reported median**,** 25th percentile (P25)**,** and 75th percentile (P75) values. This probabilistic approach ensures that rare, high-impact events are appropriately reflected in the financial model.

Leaky Well Remediation Costs

Leaky well remediation costs refer to the total expenses incurred to restore the integrity of a leaking well once a leakage is detected. Based on U.S. EPA (2010) estimates, these costs consist of three main components: a clean-out cost of $31,200 per well to remove debris, scale, and contaminants; a replug cost of $13,500 per well to seal the well properly; and a log cost of $11,400 per well for well logging services to assess the remediation.

Finally, all financial values were adjusted for inflation and subsequently discounted to the base year (2025) to calculate the net present value (NPV), facilitating a consistent comparative basis across scenarios.

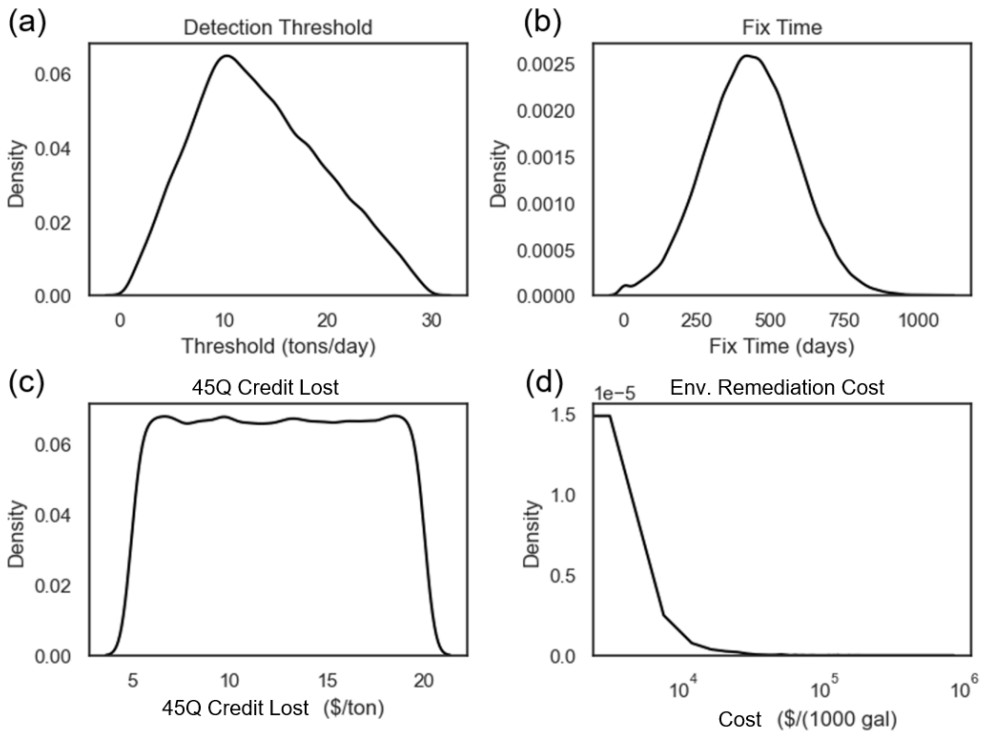

Figure 14. Figure: Input Distributions Used in Monte Carlo Simulation. (a) Detection threshold (tons/day), modeled as a triangular distribution; (b) Fix time (days), modeled as a truncated normal distribution (truncated at 0); (c) 45Q credit lost ($/ton), modeled as a uniform distribution with a minimum of 5 and maximum of 20; (d) Environmental remediation costs, including capital expenditure (P25 = $23, median = $78, P75 = $350) and operating expenditure (P25 = $5, median = $16, P75 = $41), based on 1999 USD. Each distribution was generated using 100,000 samples.

2.6 FINANCIAL MODEL FRAMEWORK

Three financial models were developed to explore how detection and remediation, well failure probability, and project timing influence the financial consequences of CO_2 leakage. All three models use Monte Carlo simulation to capture uncertainty in key input parameter (e.g., time to fix the well, detection threshold, 45Q tax credit lost, environmental remediation cost, leaky well remediation costs) and produce distributions of normalized cost and percentage of CO_2 leaked. Each model reflects a different assumption set to test how financial risks evolve under various operational scenarios.

Detection and Remediation Adjustment

This model was developed to evaluate the effectiveness of active monitoring and remediation strategies in limiting both environmental and financial impacts from CO_2 and brine leakage in geologic carbon sequestration (GCS) projects (see Appendix A.7 for more information about the algorithm). It represents a conservative worst-case scenario, where it is assumed that all leaky wells fail from year 0—that is, a 100% probability of failure is applied to all wells in the simulation. This setup ensures that every well has the potential to leak, enabling the model to stress-test the system under the most pessimistic assumptions. This adjustment serves as the basis for the base case analysis and was also applied in the sensitivity analysis of key variables such as permeability, reservoir thickness, salinity, and depth.

The objective is to isolate the role of detection and remediation in mitigating leakage consequences. Using Monte Carlo simulation, this model incorporates uncertainty in key operational and economic variables—such as detection threshold, remediation delay, water treatment cost, and injection penalty. Leaks are monetized only when detected, and it is assumed that once a well is remediated, it ceases to leak. By aggregating thousands of simulation iterations,

this model quantifies the expected cost and leakage performance under a proactive site management strategy.

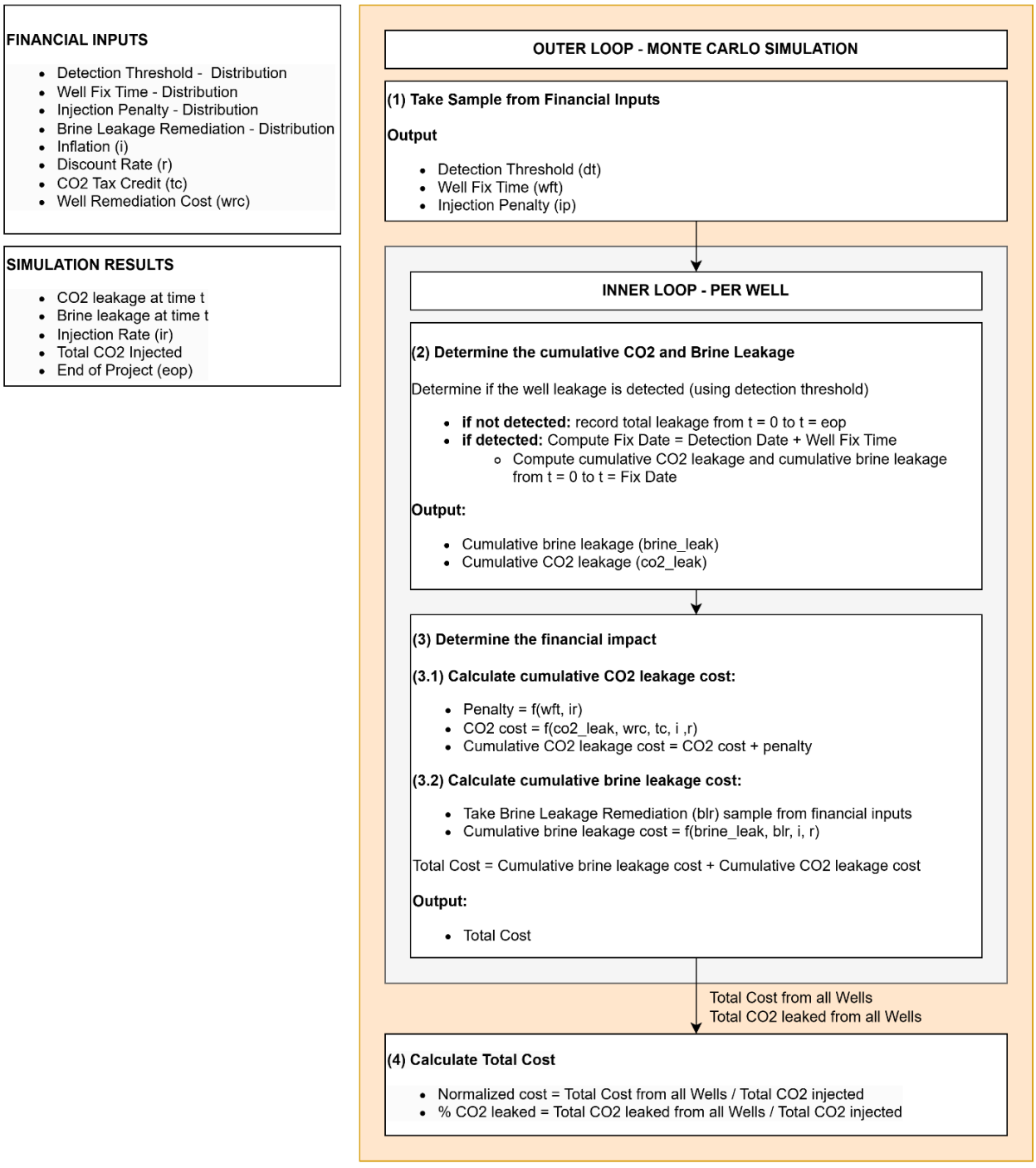

Figure 15. High-Level Monte Carlo Flow for CCS Well Cost & Leakage with Detection & Remediation.

Annual Probabilities of Well Failure Adjustment

This model was developed to assess how financial and environmental outcomes vary depending on the assumed annual probability of well failure (see Appendix A.8 for more information about the algorithm). Although certain well attributes found in regulatory databases or industry records can be used to estimate leakage risk (Watson & Bachu, 2008), such datasets are often incomplete, inconsistent, or nonexistent for older or undocumented wells. This data gap increases uncertainty and concern among project developers, insurers, and regulators regarding the actual risk of CO_2 and brine leakage from storage sites.

Therefore, historical information from well failures associated to oil and gas operations were used as a basis for estimating plausible failure probabilities. These probabilities are influenced by multiple factors, including well integrity, construction quality, age, material type, bottom-hole pressure and CO_2 saturation, and regional regulatory oversight.

To address this uncertainty, the model applies a range of fixed annual failure probabilities to wells in the simulation and uses Monte Carlo Simulation to estimate the range of uncertainty for the financial and environmental impact calculations. Once a well fails and it's remediated, it remains fixed for the rest of the project life. This assumption represents a conservative yet practical scenario for financial risk planning. Failure probabilities in this model span both historically derived values (Jordan & Benson, 2009; Porse et al., 2014; Trabucchi et al., 2012)—0.0001%, 0.01%, and 0.1%—and more aggressive or hypothetical cases, including 1% and 10%. These scenarios serve as analogs for varying well conditions mentioned previously and enable a comprehensive evaluation of risk across a spectrum of realistic to worst-case assumptions.

By simulating a range of failure probabilities, this model demonstrates how financial assurance requirements and environmental impacts varies with the level of expected well failure risk. The overall logic for this financial model is shown in Figure 16.

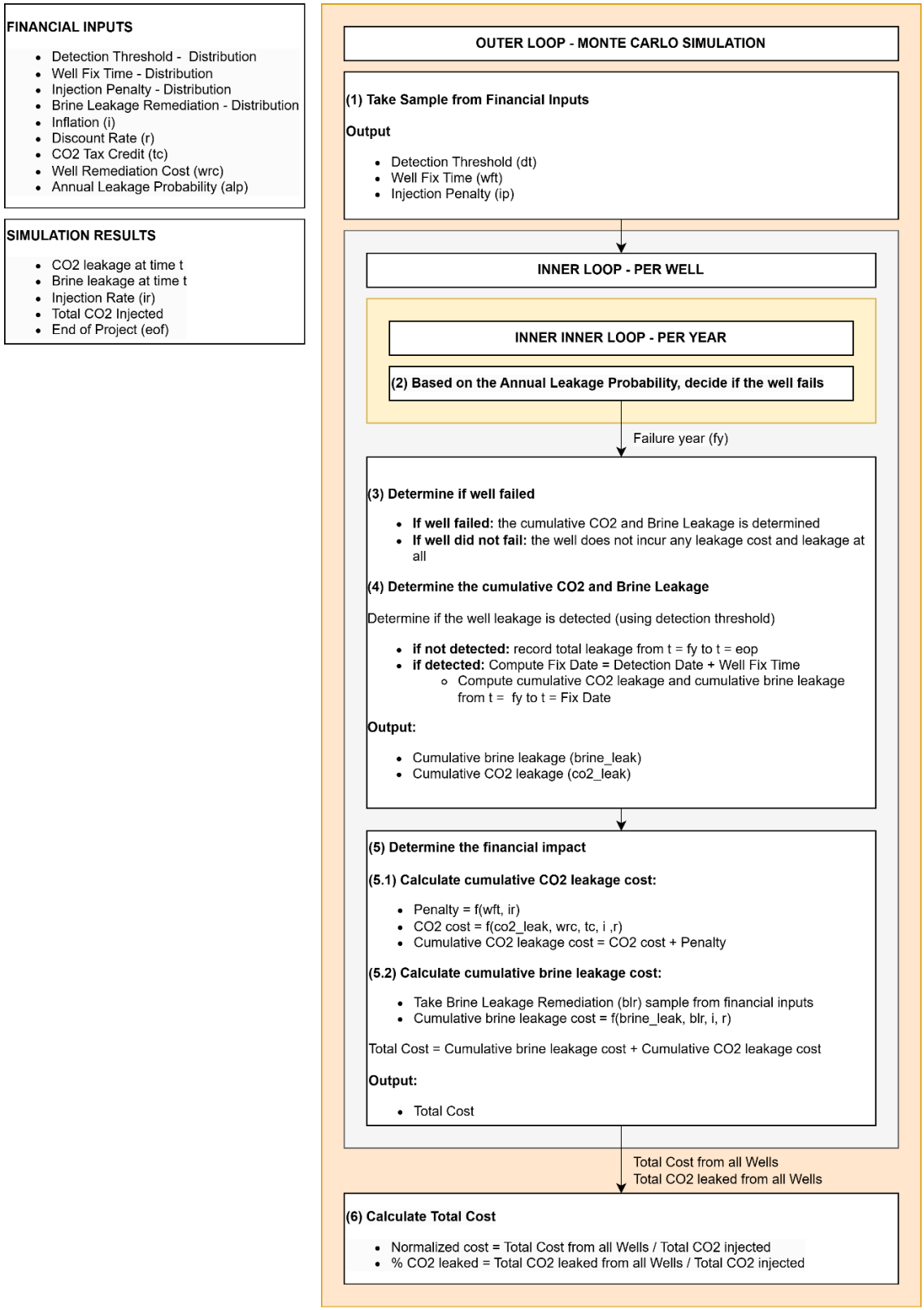

Figure 16. Monte Carlo Simulation with Multiple Annual Failure Probability.

Bayesian Updating Adjustment

This model was developed to explore how the financial risk profile of a GCS project evolves over time as more information becomes available (see Appendix A.9 for more information about the algorithm). Previous studies on GCS have applied Bayesian frameworks to improve leakage detection (e.g., Yang et al. (2012) used a Bayesian belief network to combine evidence from multiple CO_2 monitoring technologies; Wang and Small (2014) applied Bayesian methods to detect leakage using pressure anomalies; and Wang et al. (2021) modeled containment effectiveness using a Bayesian decision network). These efforts focused on improving monitoring system design and detection accuracy during site operations.

In contrast, this research's approach uses Bayesian updating not to detect a leak, but to simulate how the probability of leakage—and therefore the expected financial impact—changes over time in response to observed outcomes, such as continued non-leakage. The model incorporates this dynamic probability into the financial risk profile of the project. This novel application helps quantify how effective monitoring and a strong operational track record can gradually lower perceived risk and inform decisions related to insurance premiums, credit buffers, or long-term liability across the project lifecycle.

The probability of failure, P(F), is treated as an input uncertainty and explored across a broad range (0.0001% to 10%). Initially, the probability of leakage given failure, P(Leak | F), is conservatively assumed to be 100%, but it is updated using Bayesian inference each year based on new data. If no leaks are observed among failed wells, P(Leak | F) is revised downward, reducing the marginal leakage probability over time.

To represent initial uncertainty in P(Leak|F), a Beta distribution is used. The model is initialized with a Beta(100, 0) prior, corresponding to a conservative assumption (mean of 1) and

an equivalent of 100 pseudo-observations (0 leaks, 100 non-leaks). Given this, the initial marginal probability of leakage is computed as:

$$P(Leak) = P(F) \times P(Leak \mid F) = P(F) \times \frac{100}{100 + 0} = 1 \times P(F)$$

In each subsequent year of the simulation, it is assumed that well failures occur, but no leaks are observed. This lack of observed leakage is used to update the Beta distribution. If n wells fail in a given year and none leak, the posterior becomes:

$$P(Leak \mid F) \sim Beta(\alpha + x, \beta + n - x)$$

where x= 0 is the number of observed leaks, and n is the number of new failed wells. For example, if 10 new failures are observed with zero leaks, the posterior becomes Beta(100,10), reducing the expected value of P(Leak|F) from 1 to 0.9.

This process is repeated annually, progressively refining the expected leakage probability based on observed outcomes. If no leaks are observed following well failures, the conditional leakage probability decreases, leading to lower projected financial risk. The result is a dynamic, time-resolved simulation of leakage risk and associated costs across the full project timeline—from the injection phase through post-injection care. This time-dependent approach enables both operators and insurers to better estimate and manage expected financial damages across the project lifecycle, accounting for evolving reservoir conditions such as pressure dissipation and CO_2 saturation dynamics.

All in all, this temporal evolution supports strategic decision-making regarding monitoring intensity and financial risk mitigation instruments. It provides critical insight into how the need

for safeguards—such as CO_2 credit buffers or insurance premiums—may diminish or shift over time, aligning protection strategies with actual risk exposure as the project matures (See Figure 17).

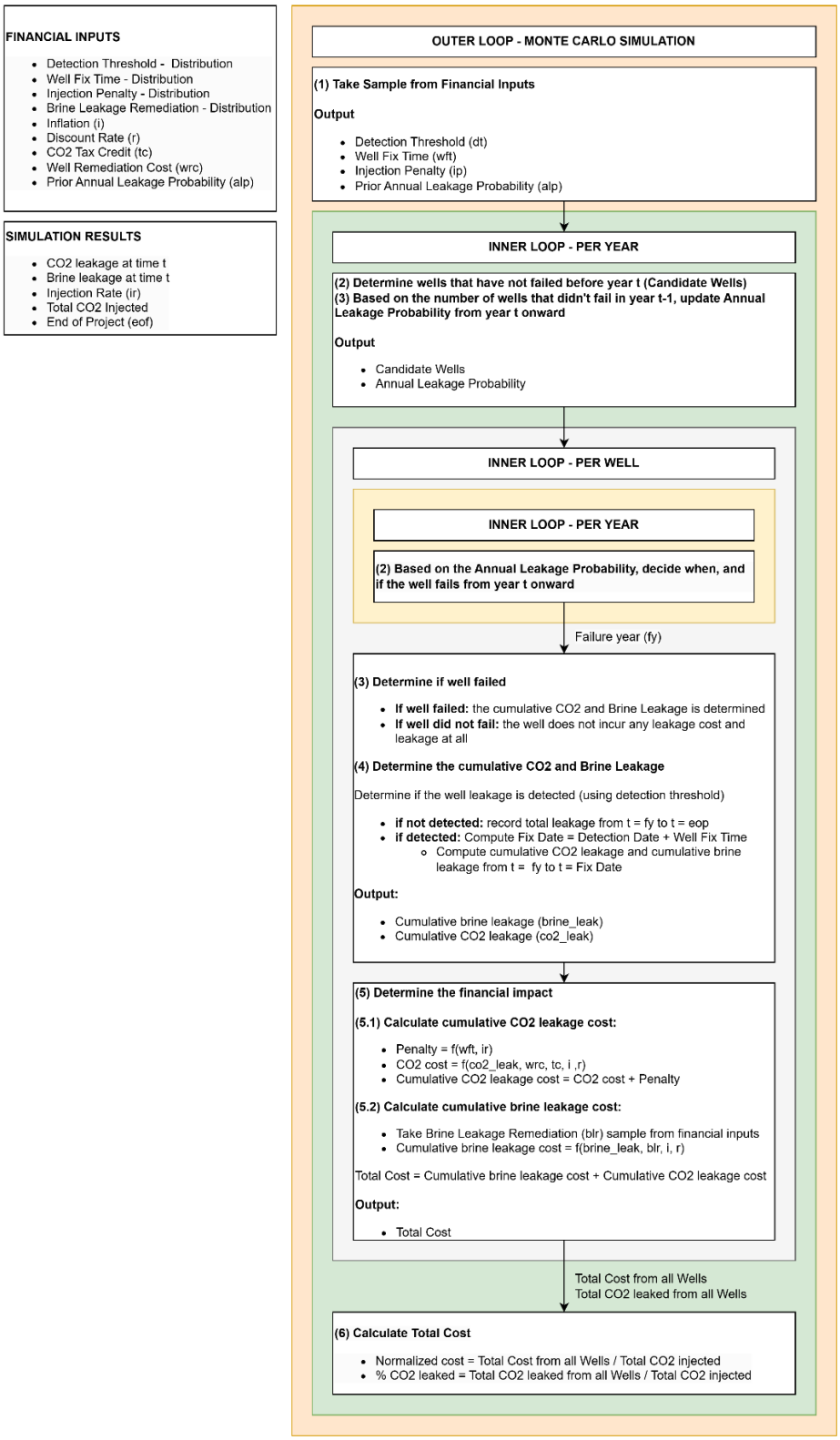

Figure 17. Year-by-Year Monte Carlo Approach for CCS Well Failures and Costs using Bayesian Update Over Time.

CHAPTER III: RESULTS AND ANALYSIS

3.1. INTRODUCTION

This chapter presents the results of a set of dynamic multiphase flow simulations and financial risk assessments conducted to evaluate the environmental and economic impacts of CO_2 and brine leakage in geologic carbon storage (GCS) projects. Each case study in this chapter corresponds to a specific scenario or sensitivity analysis, designed to isolate the effect of key geological, operational, or risk-related variables.

The simulations are structured into several categories, each representing a different real-world uncertainty or design decision. These include:

- Distance Sensitivity: How pressure, CO_2 saturation, and leakage vary spatially and over time as a function of distance from the injection well.
- Financial Impact: Decomposition of total cost to determine the relative weight of cost components and estimate the overall financial risk profile across time.
- Well Density Sensitivity: How increasing the number of potential leakage pathways influences outcomes.
- Subsurface Parameter Sensitivity: How properties like porosity, permeability, salinity, and capillary pressure affect outcomes.
- Geologic Setting Sensitivity: How different reservoir geometries (flat, dipping, anticline) affect plume migration and leakage risk.
- Probability Sensitivity: How varying assumptions on well failure probabilities impact leakage and cost.
- Bayesian Updating Model: How financial risk projections evolve over time when incorporating new (non-leakage) evidence.

- Monitoring and Remediation Analysis: How detection thresholds, time to remediation, and mitigation costs affect the total risk, and how the financial value of monitoring can be quantified.

To help the reader navigate the different cases, Table 3 summarizes the key simulation cases, what each represents, and the purpose of their inclusion in the analysis.

Case	Variable(s) Studied	Description	Purpose
Distance Sensitivity	Distance from injection well	Open wellbores at fixed distances (100–2000m) from injection point; spatial and temporal variation of pressure, CO_2 saturation, and leakage are tracked	Assess how flow dynamics and leakage behavior evolve in space and time
Financial Impact	Disaggregated cost components	Cost breakdown using leakage simulation under base assumptions	Understand cost drivers and estimate the time-dependent risk profile
Well Density Sensitivity	Open well density (0.27, 2.4, 4.8 wells/km^2)	Randomly placed wells at low, medium, and high densities	Identify how increasing leak pathway density affects leakage and cost
Subsurface Settings Sensitivity	Permeability, thickness, salinity, depth, etc.	High vs. low bounds for geologic and petrophysical parameters	Determine most influential variables on leakage risk and financial impact
Subsurface Geometry Sensitivity	Flat, Dipping, Anticline (Facies 3)	Simulates plume migration and leakage in different structural trapping settings	Understand risk implications of different subsurface geometries
Probability Sensitivity	Annual well failure probability (0.0001% to 10%)	Fixed failure probability applied to all wells	Estimate risk exposure under varying leak likelihood scenarios
Bayesian Updating	Time-evolving leak probability	Adjusts leak probability annually based on non-leakage observations	Estimate how risk exposure varies over time
Monitoring & Remediation Analysis	Detection threshold, fix delay, cost distributions	Models reduction in impact from early detection and response actions	Evaluate how monitoring strategy influences financial risk; quantify its value

Table 3. Summary of Simulation Cases

3.2. DISTANCE SENSITIVITY

Leakage Rate vs. Distance

Base case reservoir properties were used for this scenario, featuring a flat-lying reservoir. Four open wellbores connected from the injection zone to the surface are positioned at varying distances from the injection well—100 m, 500 m, 1,000 m, and 5,000 m—to evaluate the effect of proximity on leakage behavior. This case represents a worst-case scenario, in which no detection or remediation measures are implemented—allowing CO_2 and brine to leak indefinitely without intervention. As for how the AoR was estimated, see appendix A.1 and A.5.

Figure 18 shows the CO_2 and pressure fronts at Year 20, immediately after injection stops. The CO_2 plume reaches the open wellbore located 500 meters from the injection well, and significant pressure changes are observed around the plume boundary.

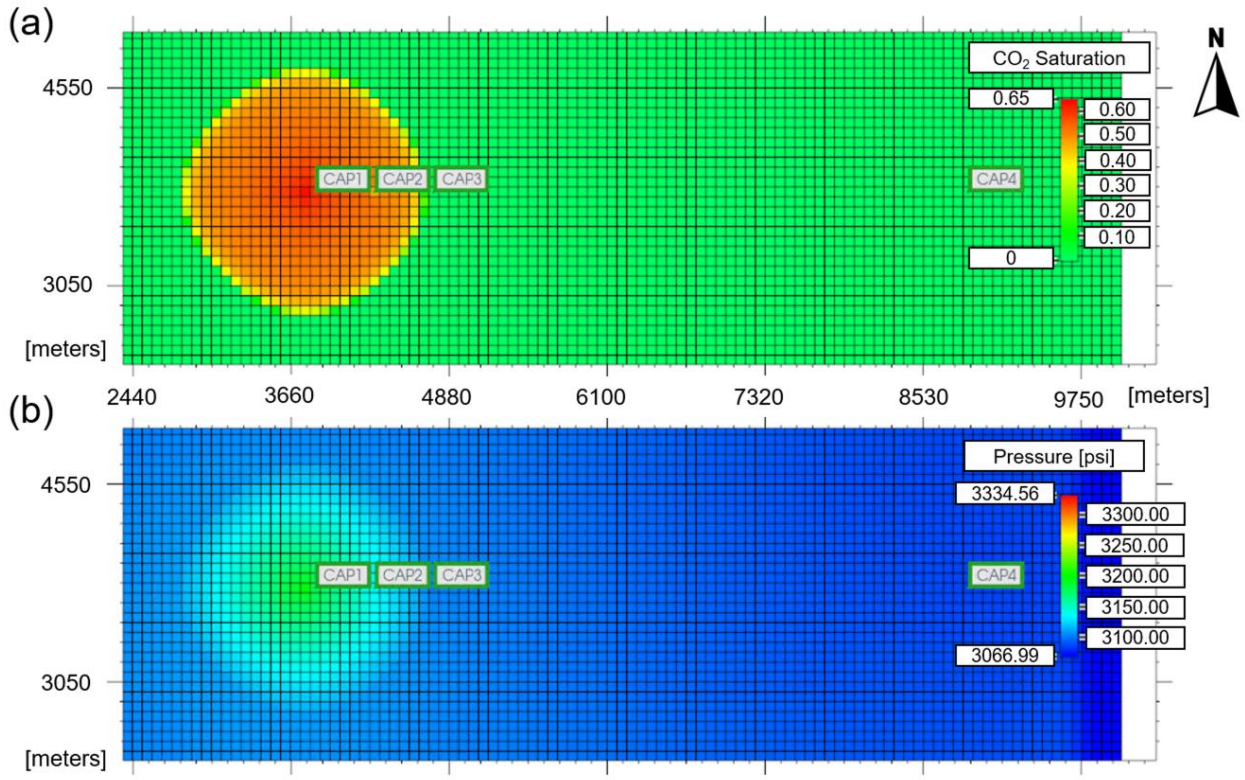

Figure 18. Top-down view of (a) CO_2 saturation and (b) reservoir pressure (psi) at Year 20, immediately following the end of injection. The figure shows a portion of the full 10×10 km model. Open wellbores CAP1, CAP2, CAP3, and CAP4 are positioned at distances of 100 m, 500 m, 1,000 m, and 5,000 m from the injection well, respectively.

Figure 19 illustrates how CO_2 and brine leakage rates, reservoir pressure and CO_2 saturation at each well location evolve over time at various distances from an injection well. The vertical dashed line at year 20 marks the end of CO_2 injection.

Notably, when CO_2 reaches a particular well, the buoyant force of CO_2 can prevent bottom-hole pressure from returning to hydrostatic conditions. This phenomenon influences the duration and magnitude of leakage, as well as pressure evolution in the system.

Main Observations:

- Injection Period:

- Under the modeled conditions, an almost immediate increase in reservoir pressure causes almost immediate brine leakage along the model domain.
- The spatial footprint of the pressure front is significantly larger than that of the CO_2 plume, resulting in brine leakage through more wells than those directly contacted by the injected CO_2.
- Peak CO_2 and brine leakage rates reached 140 tons/day and 70 tons/day at 100 meters from the injection well, respectively. At 500 meters, peak CO_2 leakage dropped to 20 tons/day, while brine leakage was 50 tons/day. These peaks occurred just before injection ceased, when both pressure and CO_2 saturation reached their highest levels.
- At the 500 m well, a distinct pressure spike is observed upon CO_2 arrival, indicating the role of CO_2 buoyancy in maintaining elevated reservoir pressures.
- Once the CO_2 plume reaches the open wellbore, brine leakage dramatically decreases, and as pressure and saturation build, a CO_2 flow to surface occurs. This leads to a phase of co-produced CO_2 and brine, with CO_2 being the primary leaking fluid. The timing of CO_2 flow to surface appears more closely related to CO_2 saturation than to pressure: in both the 100 m and 500 m wells, breakthrough occurs when saturation exceeds 30%, regardless of pressure conditions.
- At the 100 m well, CO_2 surface flow occurs approximately 2 months after plume arrival; at the 500 m well, breakthrough takes about 1 year. Following breakthrough, CO_2 leakage is primarily driven by increasing CO_2 saturation rather than pressure changes, but pressure dictates CO_2 leakage intensity.

- Post-Injection Period:
  - Due to the sustained buoyancy pressure from a column of mobile CO_2, slow leakage persists well after injection ends. At the 100 m well, CO_2 leakage continues for 100 years, whereas at the 500 m well, leakage ceases after 15 years.

- At the wells located 100 and 500 meters from the injection point, pressure drops significantly once injection ceases but then model-wide equilibration of pressure causes a slight increase (less than 4 psi) over the following 100 years.
- Post-injection behavior shows that reservoir pressure does not return to hydrostatic levels (3,067 psi) within the 120-year simulation period. This is due to the gradual nature of pressure dissipation, as outer boundary cells remain fixed at hydrostatic pressure while adjacent cells continue to decline. Consequently, over a longer timeframe, pressure is expected to equilibrate. This pressure behavior also influences brine leakage: wells with CO_2 breakthrough show no brine leakage after injection stops, while those without CO_2 flow experience reduced but ongoing brine leakage, driven by residual overpressure. Over time, as pressure normalizes, this leakage is expected to cease (see Appendix A.4 for more on boundary condition effects).
- For wells with CO_2 breakthrough, the cessation of brine leakage after injection is likely due to sustained high CO_2 saturation. Preferential mobility of low viscosity non-wetting phase CO_2 dominates the flow system which prevents further brine migration to the surface. Complex geysering and gas lift type processes could occur but are not modeled in this wellbore by the software used.

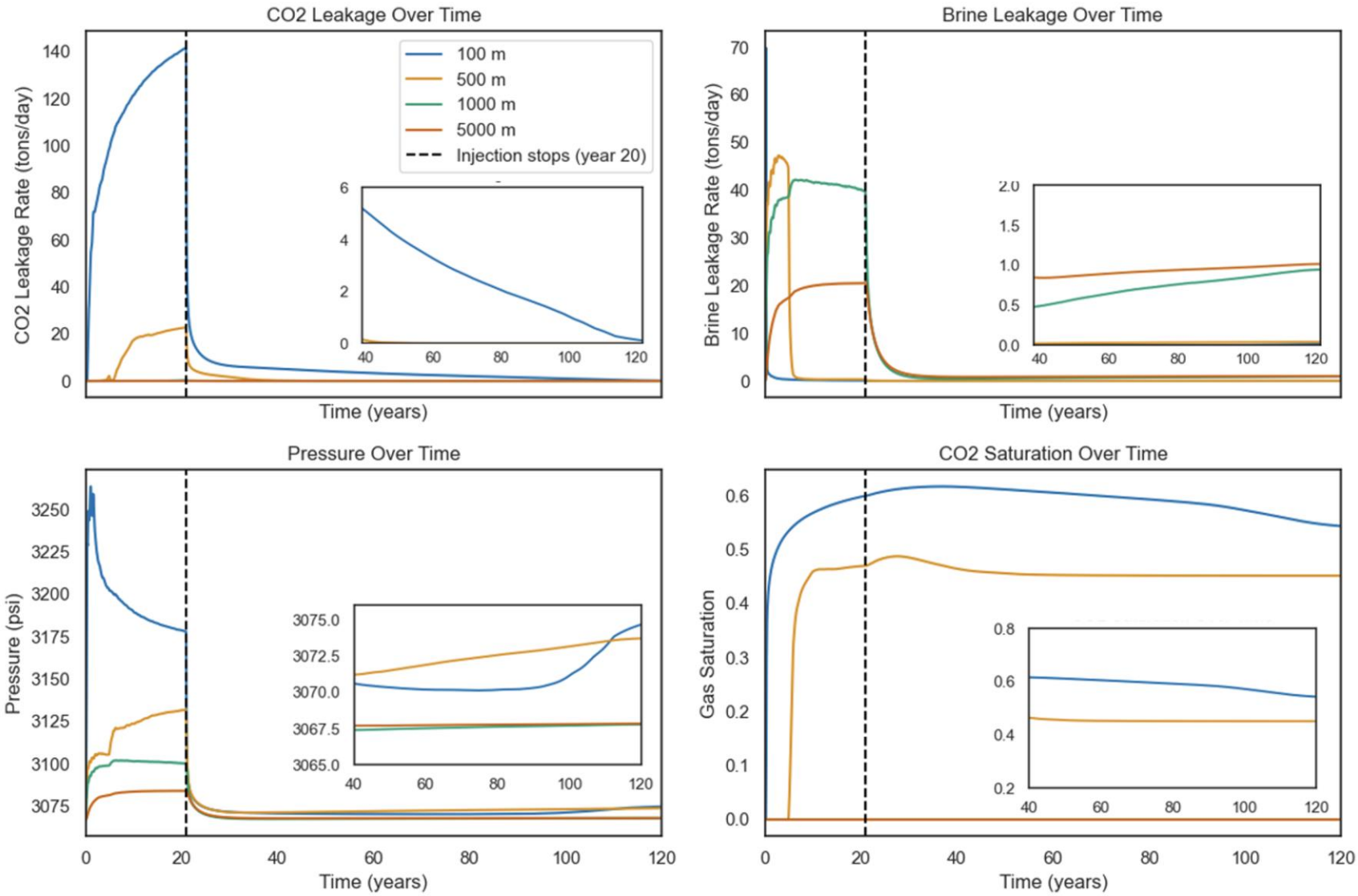

Figure 19. Dynamics of Reservoir Pressure, CO_2 Saturation, and Leakage during Injection and Post-Injection Phases.

Cumulative Leakage Rate vs. Distance

Base case reservoir properties were used for this scenario, featuring a flat-lying reservoir. Ten open wellbores connected from the injection zone to the surface are positioned at varying distances to the east and west from the injection well—100 m, 500 m, 1,000 m, 2,000 m, and 3,000 m—to evaluate the effect of proximity on leakage behavior.

Figure 20 compares cumulative CO_2 and brine leakage alongside peak reservoir conditions across varying distances from the injection well, covering a 120-year timeframe.

Main Observations:

- Peak bottom-hole pressure decreases with distance from the injection well, indicating a rapid decline in the driving force for fluid migration at greater distances.
- Wells located closer to the injection point exhibit higher cumulative CO_2 leakage but lower brine leakage. In contrast, wells farther away experience delayed CO_2 breakthrough due to lower CO_2 saturation, leading to greater brine leakage relative to CO_2.
- There is a strong inverse correlation between cumulative brine leakage and peak CO_2 saturation, highlighting that higher CO_2 saturation limits brine migration.
- Cumulative CO_2 leakage strongly correlates with peak reservoir pressure. While CO_2 saturation influences the timing of breakthrough, it is pressure that primarily controls the intensity of leakage—higher pressures result in higher CO_2 leakage rates.
- Brine leakage is observed up to 3,000 meters from the injection well. This occurs because, as shown in the figure, peak pressure at that distance still exceeds hydrostatic pressure. The reservoir is over-pressurized relative to the surface due to the size and boundary conditions of the model, allowing brine to leak even at wells located far from the injection point.

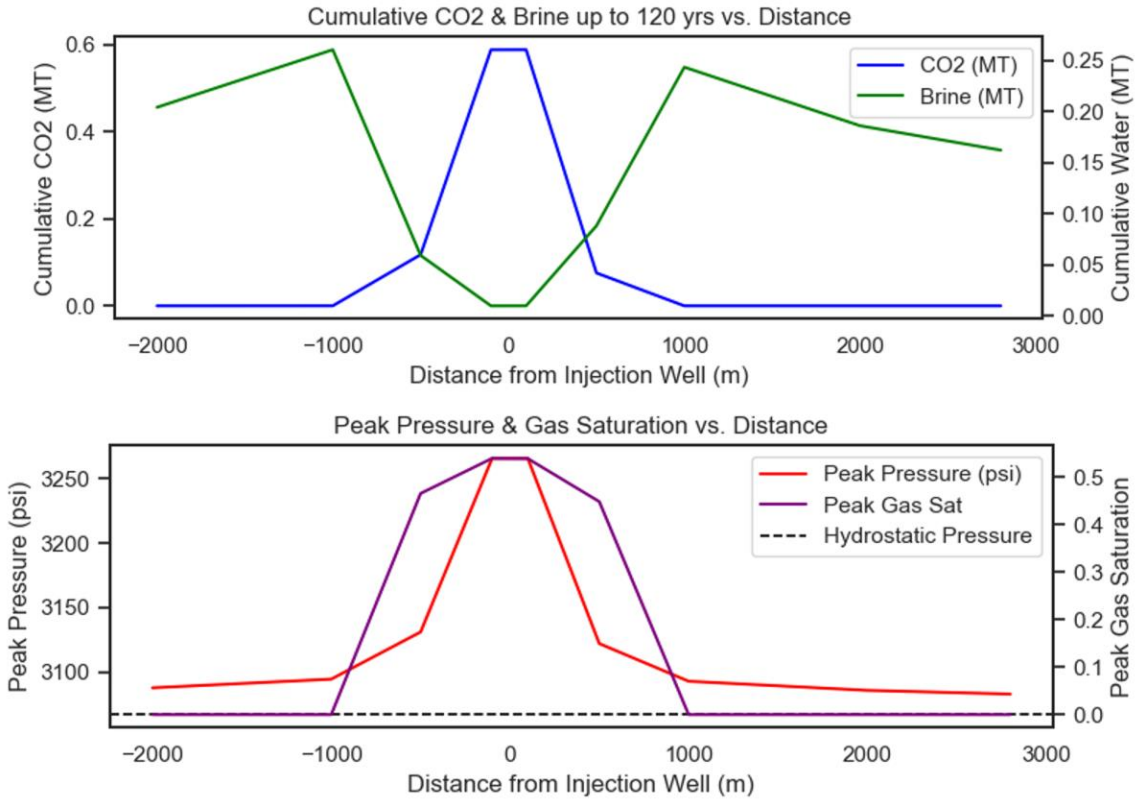

Figure 20. Distance-Dependent Trends in Cumulative Leakage and Reservoir Conditions over 120 Years

3.3. FINANCIAL IMPACT

Financial Impact Results

Base case reservoir properties were used for this scenario, assuming a flat-lying reservoir and 240 open wellbores randomly distributed across the project area. The wells are modeled as direct conduits from the injection zone to the surface, and both leakage rates and financial impacts are calculated based on their effects at the surface. Unlike a worst-case scenario where leaks persist indefinitely as in the previous section, this scenario assumes wells are detected and remediated once leakage occurs, preventing further losses. For this scenario, different cost components were included, such as environmental remediation, leaky wellbore remediation, and regulatory and contractual penalties. This scenario also assumes that all wells fail (100% annual probability of

failure), meaning that any change in pressure and/or CO_2 saturation sufficient to drive upward fluid migration results in leakage through the wells.

The next figure displays cumulative distribution functions (CDFs) for both the normalized remediation cost (left) and the final percentage of CO_2 leaked (right) for the financial model adjusted by detection and remediation. Over 2,000 Monte Carlo simulations were conducted, varying parameters such as well repair time, detection threshold, remediation costs, and penalty costs to generate the cumulative distribution functions (CDFs).

Main Observations:

- The median (p50) financial impact normalized by the total injected CO_2 is around $15 per ton of injected CO_2, indicating that for half of the scenarios, the cost is at or below this value.
- The median (p50) final leakage rate is about 0.08%, demonstrating that timely detection and remediation keep total leakage relatively low, even if all wells fail.
- The spread between p10 and p90 underscores the inherent uncertainty, with some scenarios resulting in minimal leakage and hence financial impacts, while others approach higher leak percentages and higher costs.
- The majority of the costs are associated with remediating wells due to brine leakage. Because the pressure front rapidly propagates throughout the reservoir in this model, brine leakage occurs at nearly all leaky wells, triggering detection, injection interruption, and remediation efforts.

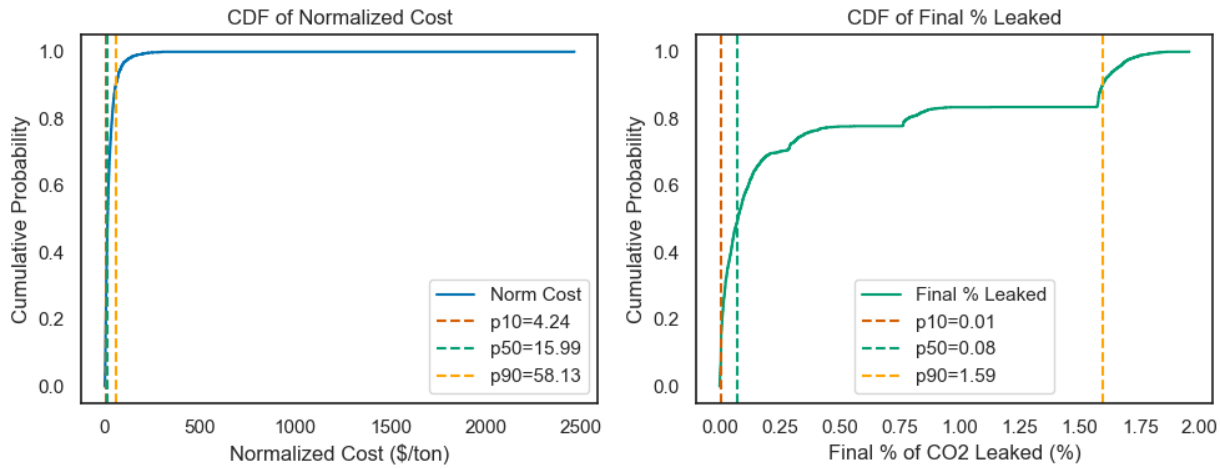

Figure 21. CDFs of Remediation Costs and Final CO_2 Leakage under Detection and Repair Scenarios

Figure 22 presents the breakdown of cost contributions from each component included in the financial model. The results show that the contractual penalty (64.7%) and environmental remediation capital costs (30.5%) together account for approximately 95% of the total expenses. These costs are largely influenced by the volume of brine leaked and the time required to detect and repair the leakage.

In contrast, well remediation and loss of 45Q Tax Credits represent relatively minor portions of the total cost. This highlights the critical importance of rapid leak detection and remediation, especially for first-of-a-kind (FOAK) projects, where we have assumed that higher injection penalties place a greater financial burden on early adopters.

It is also important to note that environmental costs—comprising water leakage remediation and well remediation—make up only 35% of total costs, while contractual costs—including loss of 45Q Tax Credits and contractual penalties—account for the remaining 65%. This distinction emphasizes how project agreements and policy design can significantly influence financial outcomes.

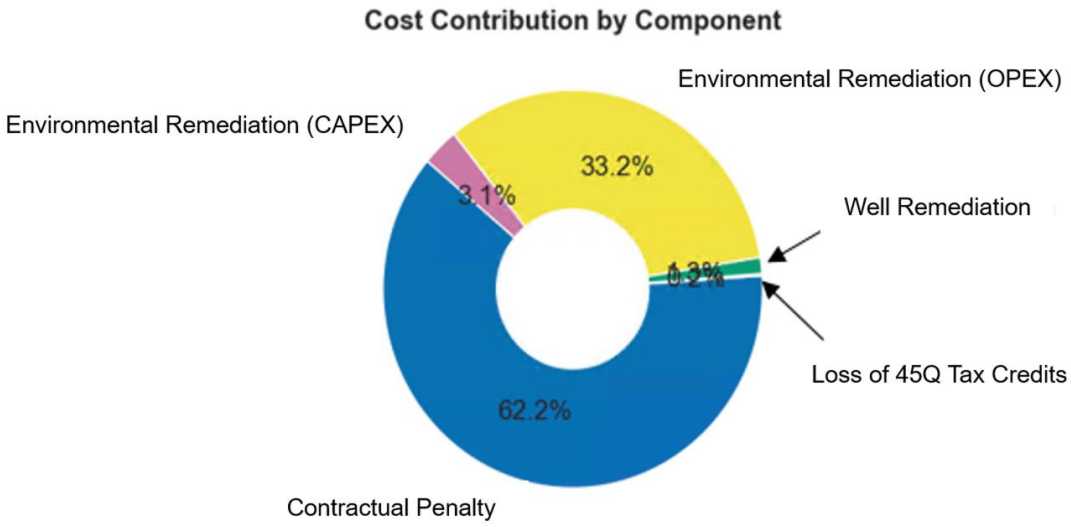

Figure 22. Average cost contribution by component.

Figure 23 shows the normalized cost per ton of CO_2 injected (top) and the discounted incurred cost per year (bottom). Most expenses arise in the first five years because of the rapid pressure front propagation, reflecting a scenario in which wells fail early, are quickly detected, and then remediated. Once leaks are addressed, subsequent CO_2 injections occur without additional costs, causing the normalized cost to peak in year one and then diminish as more CO_2 is injected. The bottom plot highlights how the discounted costs are heavily front-loaded, tapering off substantially after early remediation efforts.

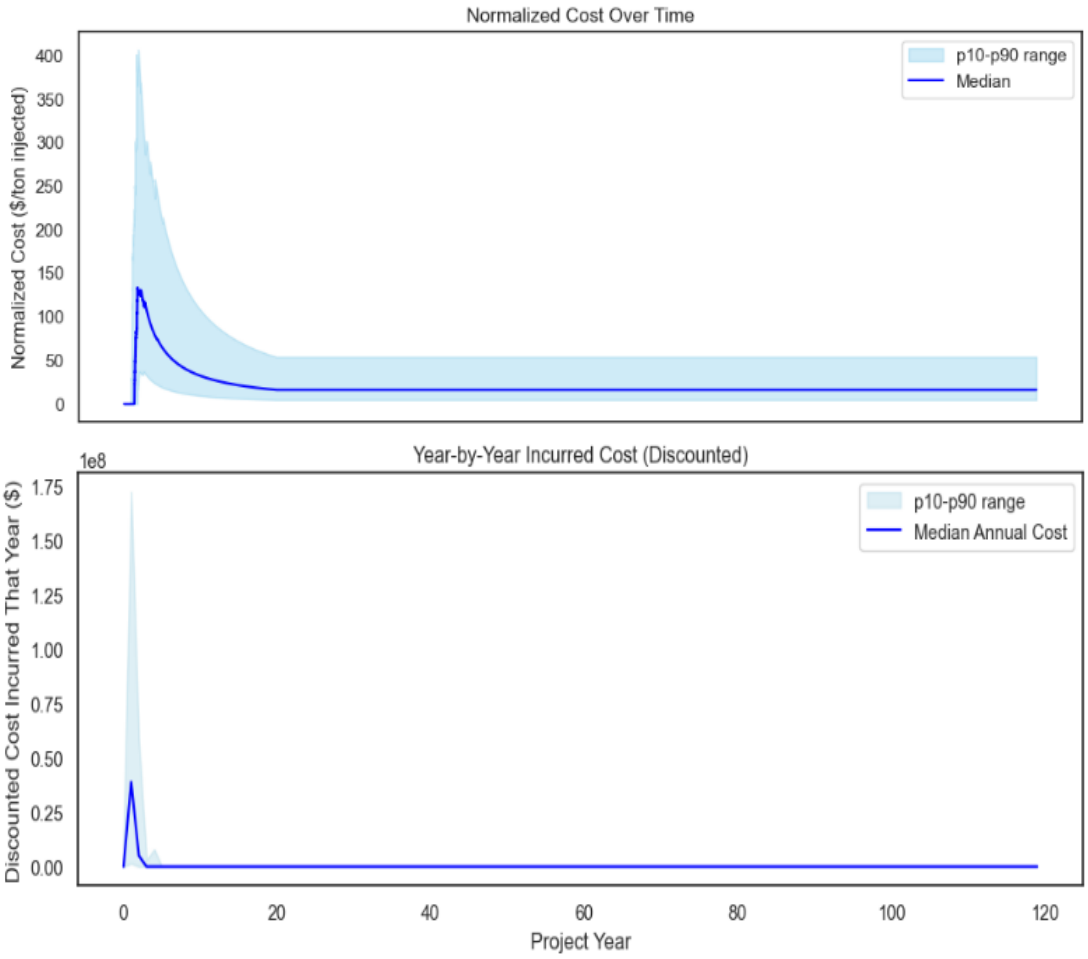

Figure 23. Time-Resolved CO_2 Leakage Costs: Normalized and Discounted Annual Expenses

3.4. Well Density Sensitivity

As in the previous section, base reservoir properties were used for this scenario, which assumes a flat-lying reservoir. A varying number of open wellbores were randomly distributed across the project area. The wells are modeled as direct conduits from the injection zone to the surface, and both leakage rates and financial impacts are calculated based on their effects at the surface. Also, for this scenario, different cost components were included, such as environmental remediation, open wellbore remediation, loss of 45Q Tax Credits, and contractual penalty. This

scenario also assumes that all wells fail, meaning that any change in pressure and/or CO_2 saturation sufficient to drive upward fluid migration results in leakage through the wells.

These plots compare the cumulative distribution functions (CDFs) of normalized cost (left) and final CO_2 leakage (right) under two different well densities: (a) 0.27 wells per km² (top) and (b) 4.8 wells per km² (bottom). These results correspond to the financial model adjusted by detection and remediation. The lower density represents deeper Gulf Coast wells below 2,440 m, while the higher density is twice the average surface density of 2.4 wells per km², serving as a worst-case scenario. By examining these extremes, we see how injection depth and the number of potential leakage pathways affect overall cost and leakage outcomes.

Low-Density Scenario (0.27 wells/km²) – Figure 24.a:

- The median (p50) normalized cost is $31.07 per ton of CO_2 injected, with a relatively wide distribution extending beyond $60/ton at p90.
- The final CO_2 leakage remains extremely low, with p50, p10, and p90 values all approximately at 0%, with P90 being less than 0.0005% of the total CO_2 injected. This indicates that although CO_2 leakage is virtually nonexistent, the cost per ton is relatively high due to environmental remediation and contractual and regulatory penalties due to injection interruption.
- The higher cost in comparison to the high-density scenario is attributed to limited pressure dissipation due to fewer leaky wells. As a result, brine leakage is concentrated in fewer wells, increasing the per-well environmental remediation burden and overall cost.

High-Density Scenario (4.8 wells/km²) – Figure 24.b:

- The median (p50) normalized cost is significantly lower at $16.16/ton, with a narrower distribution.

- The cumulative CO_2 leakage increases with well density, reaching a p50 value of 0.29% and a p90 value of 8.05% of total CO_2 injected.
- Despite the higher leakage risk in this scenario, the costs remain lower because pressure is more evenly distributed across a greater number of wells, reducing the burden on individual wells and the associated water remediation cost per well.

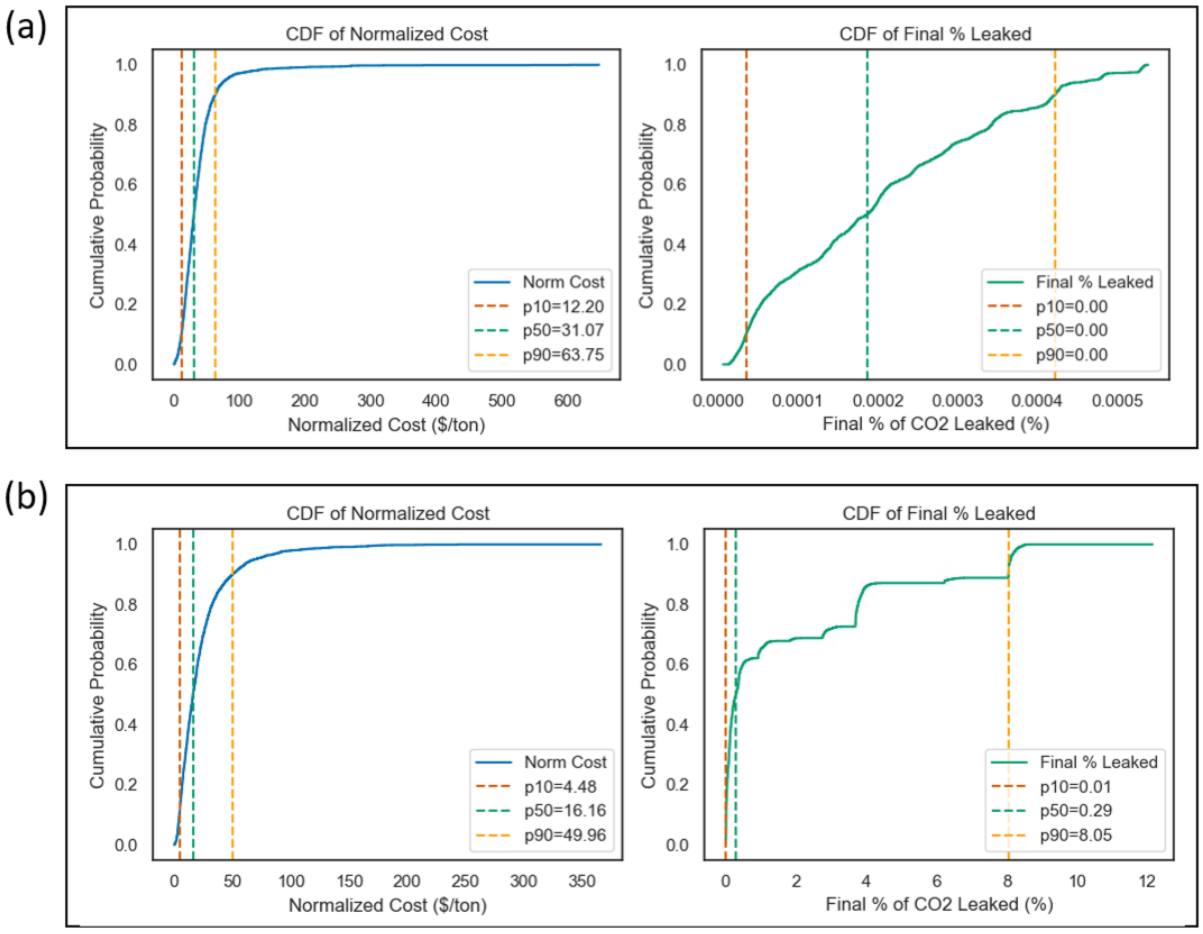

Figure 24. Comparative CDF of CO_2 Leakage and Cost under Varying Well Densities. (a) corresponds to a density of 0.27 wells/km^2, and (b) of 4.8 wells/km^2

3.5. SUBSURFACE SETTINGS SENSITIVITY

Cumulative Leakage Rates

Figures 25 and 26 illustrate how subsurface parameters influence both the amount of CO_2 and brine that leak from a storage reservoir and the resulting financial and environmental impacts. The analysis considers scenarios with and without detection and remediation measures in place. By examining variables such as permeability, kv/kh, reservoir depth, and capillary entry pressure, we identify which factors most strongly affect leakage rates—and assess whether these differences lead to significant changes in normalized costs and final percentages of CO_2 leaked under each scenario.

The Figure 25 corresponds to the flat-lying reservoir scenario, where the open wellbores are open conduits connected from the injection zone to the surface. For this case, no detection and remediation are considered. In the Table 4 is shown the cumulative volume of CO_2 leakage, brine leakage, and CO_2 injected at reservoir conditions per case.

Environmental Impacts (Figure 25):

- Permeability, λ (Pore Size Distribution index), and kv/kh ratios have the greatest positive correlation with CO_2 leakage, as they facilitate easier migration of the plume through the reservoir and therefore encounter more leaky wells.
- In contrast, higher permeability and kv/kh can lower brine leakage by reducing overall reservoir pressure buildup.
- Deeper reservoirs exhibit lower CO_2 and brine leakage, likely because the higher CO_2 density at greater depths results in less brine displacement and reduced pressure buildup (see Table 4 for more information about cumulative CO_2 injected at reservoir conditions per case).
- Greater reservoir thickness reduces pressure buildup by providing more pore volume for CO_2 injection, which in turn limits lateral plume migration. This smaller plume footprint decreases

the number of open wellbores contacted by the CO_2 plume, thereby reducing cumulative CO_2 and brine leakage rates.

- Higher brine salinity increases the brine's density and viscosity, making it more resistant to displacement. As a result, greater injection pressures are required to mobilize the brine, which can lead to increased pressure buildup in the reservoir and elevate the overall rates of CO_2 and brine leakage through the open wellbores.
- Saline aquifer size (lateral extension) has minimal impact on CO_2 and brine leakage during the injection phase. All three scenarios—low, base, and high-capacity aquifers—show similar leakage rates, with only slightly higher brine leakage in the low-capacity case due to faster pressure buildup. However, each aquifer accommodates the full 4 MT of injected CO_2 without reaching injection well's pressure operating constraints. Post-injection behavior highlights clearer differences. In all cases, pressure drops below hydrostatic due to continued CO_2 leakage, but recovers by year 120 in the base and high-capacity aquifers thanks to boundary-driven pressure dissipation. In contrast, the low-capacity aquifer maintains a slight pressure deficit, reflecting its limited ability to offset fluid loss over time (See Appendix A.4 for more information about how different saline aquifer sizes affects pressure buildup).

Variables	Cumulative CO_2 Leakage [MT]			Cumulative Brine Leakage [MT]			Volume of CO_2 Injected [MMCF]		
	Low	Base	High	Low	Base	High	Low	Base	High
Depth	0.91	0.86	0.81	4.47	4.40	4.26	202.94	198.26	195.08
Permeability	0.14	0.86	1.06	1.91	4.40	4.16	72.66	198.26	202.70
Kv/Kh	0.69	0.86	0.90	4.56	4.40	4.23	196.78	198.26	198.29
Capillary Entry Pressure	0.89	0.86	0.84	4.28	4.40	4.44	199.41	198.26	196.96
λ	0.71	0.86	1.07	4.41	4.40	4.26	190.07	198.26	200.69
Salinity	0.84	0.86	0.90	4.34	4.40	4.63	198.34	198.26	197.78
Thickness	1.02	0.86	0.52	4.21	4.40	3.77	197.06	198.26	200.00
Saline Aquifer Size	0.84	0.86	0.86	4.53	4.40	4.41	198.26	198.26	198.26

Table 4. Cumulative volume of CO_2 leakage, brine leakage, and CO_2 injected at reservoir conditions per case.

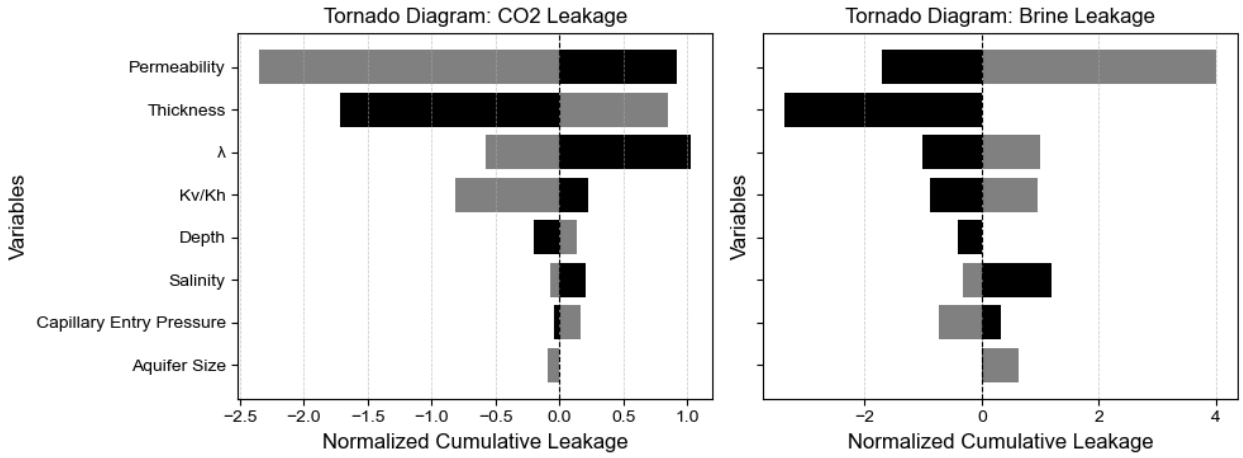

Figure 25. Sensitivity of CO_2 and Brine Leakage to Subsurface Parameters: Tornado Diagrams. Black and gray bars represent the high and low case, respectively.

Financial Impact Results

Financial Impacts (Figure 26):

- Despite the variations in leakage rates shown in the tornado diagrams, once detection and remediation strategies are factored in, the financial cost (per ton of CO_2 injected) and final leaked percentage do not vary dramatically across different subsurface settings.
- The ability to quickly identify and fix leaks dampens the influence of reservoir parameters on overall financial and environmental outcomes. In other words, a highly permeable reservoir or a shallower depth does not necessarily translate into a proportionally higher cost if leaks are detected and remediated effectively.
- While certain reservoir conditions can lead to higher CO_2 or brine leakage in a worst-case scenario, robust monitoring and mitigation measures minimize the ultimate difference in both cost and final leaked fraction across varying subsurface settings.
- Higher CO_2 leakage percentages are observed in the low-permeability scenario because the bottom-hole pressure reaches the operating limit—set at 90% of the fracture pressure—sooner. As a result, less CO_2 is injected overall, and the leaked volume represents a larger proportion of the total injected mass.

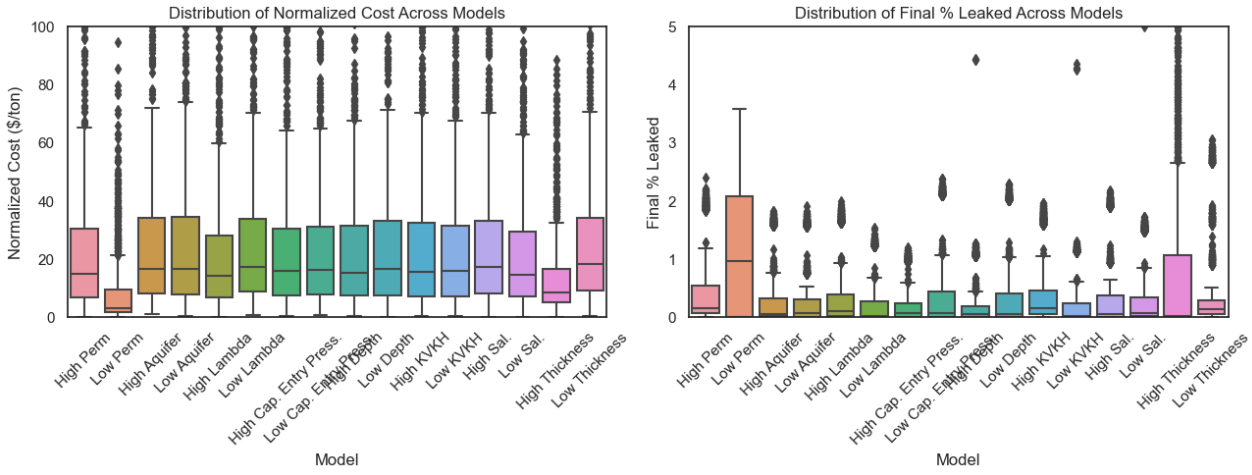

Figure 26. Normalized Cost and CO_2 Leakage Across Different Subsurface Parameters: Impact of Detection and Remediation

3.6. SUBSURFACE GEOMETRY SENSITIVITY

CO_2 and Brine Leakage Rates vs. Distance

These figures compare CO_2 leakage behavior and associated financial impacts for two different reservoir geometries: an anticline and a dipping reservoir. The injection well is located downdip whereas one open wellbore is placed in the up-dip part of each model to observe how CO_2 accumulates and migrates, particularly focusing on whether CO_2 collects at the crest of the anticline, what trapping mechanisms are more efficient, and how that affects leakage patterns, costs, and overall risk.

- In the dipping reservoir, CO_2 arrives at the open wellbore more quickly, causing a short-lived but intense leakage rate that rapidly drops to near zero after injection stops. This occurs because, as CO_2 continues to migrate updip, it becomes immobile at the open wellbore location due to the dominance of residual CO_2 saturation.
- In the anticline scenario, CO_2 takes longer to reach the well, and the peak leakage rate is approximately half that of the dipping case. However, the anticline acts as a structural trap, allowing CO_2 to accumulate at its crest. This leads to a prolonged, low-rate leakage phase that continues well after injection ends.
- Consequently, total (cumulative) CO_2 leakage in the anticline is approximately 25% higher, driven by this extended leakage tail over time.

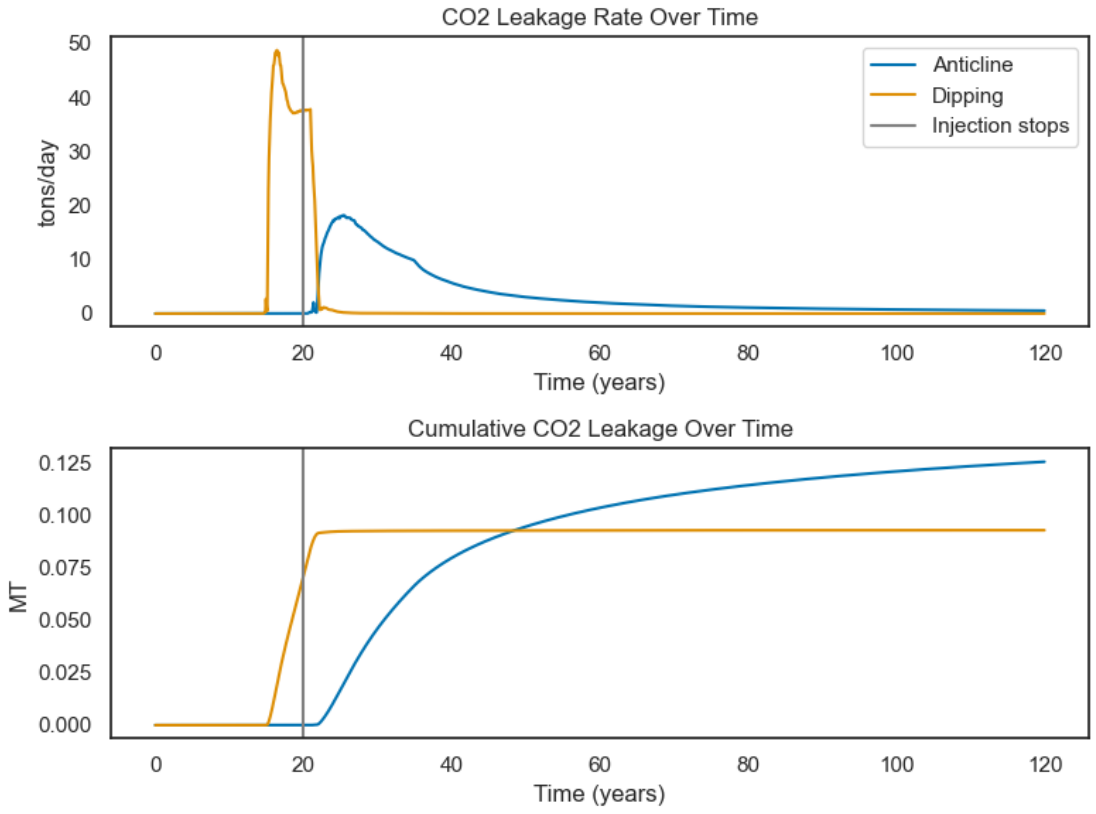

Figure 27. CO_2 Leakage Rate and Cumulative Leakage over Time for Anticline vs. Dipping Reservoir

Financial Impact Results

Financial Impacts (Figure 28):

- Box plots show that, when accounting for detection and remediation, both anticline and dipping reservoirs yield near-zero normalized costs and similarly negligible final percentages of CO_2 leaked (around 0.000002%).
- The geometry-specific differences in leakage timing and volume have no impact on financial outcomes under detection and remediation protocols.

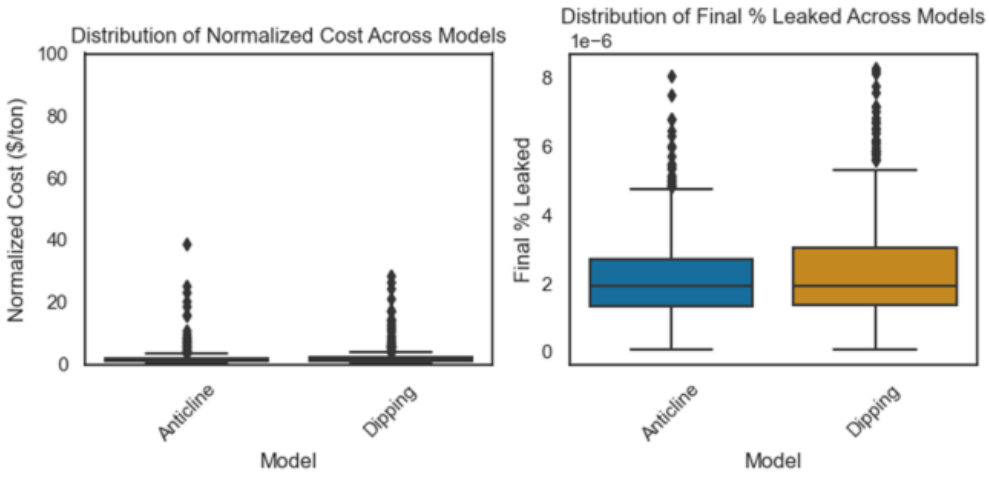

Figure 28. Comparison of Normalized Cost, Percentage of CO_2 Leaked, and Their Cumulative Distributions under Detection and Remediation

3.7. PROBABILITY SENSITIVITY

Annual Well Failure Probability Results

The Intergovernmental Panel on Climate Change (IPCC) emphasizes the importance of minimizing CO_2 leakage from storage sites to less than 1% over a 100-year period to maintain the integrity of climate mitigation efforts (IPCC, 2005). Similarly, the California Low Carbon Fuel Standard (LCFS) has established a CCS Protocol that mandates rigorous permanence requirements. This protocol requires that geologic carbon sequestration projects demonstrate a high likelihood—specifically, a probability exceeding 90%—that less than 1% of the injected CO_2 will leak over a 100-year post-injection period (CARB, 2018).

Achieving Permanence Certification is essential for CCS projects to qualify for greenhouse gas reduction credits under California's climate programs. However, there remains a notable discrepancy between certification criteria and regulatory expectations. For example, under the Emergency and Remedial Response Plan required during the EPA's Class VI permitting process,

any verified leakage event requires an immediate shutdown of injection operations until the issue is fully resolved.

Despite this operational constraint, using Permanence Certification standards as part of project selection and design is still valuable. It enables developers to assess whether a site is likely to meet long-term containment thresholds and to tailor monitoring and remediation strategies according to the project's specific risk profile.

Figure 29 presents both box plots and cumulative distribution functions (CDFs) illustrating how different annual well failure probabilities (ranging from 0.0001% to 10%) affect normalized costs (in $ per ton of CO_2 injected) and the final percentage of CO_2 leaked. These scenarios correspond to the base case, flat-lying reservoir, where 240 open wellbores are located around the project area. These scenarios were analyzed with respect to the permanence criteria mentioned before. Each scenario underwent 1,000 Monte Carlo iterations, varying parameters such as well repair time, detection threshold, environmental remediation costs, and contractual and regulatory penalties to account for variability in cost and leakage outcomes.

These results show the need to reduce the well leakage failure probably via screening for and repairing high risk wells and bounds the financial value of screening and remediation.

Main Observations

- Even at the 0.1% annual failure probability, which is the highest probability according to historical data, the 90th-percentile leakage remains comfortably below 1% (0.4%). Costs are also modest ($1.4), indicating that rare well failures (<0.1%) carry negligible risk of violating permanence criteria.
- In the 1% annual failure scenario, the mean CO_2 leakage remains below 1%, with an average cost of $3.60 per ton, thus meeting the IPCC permanence criteria on average. However, the

90th-percentile leakage reaches 1.87%, with a corresponding cost of $8.90 per ton, which fails to meet the LCFS requirement of "greater than 90% probability of less than 1% leakage." As a result, the project either fails or marginally passes the more stringent LCFS permanence standard.

- At 10% annual failure, 90th-percentile leakage can exceed 3%, and average costs climb above $18 /ton. This scenario clearly falls outside LCFS criteria and underscores the high financial and environmental risk of frequent well failures.

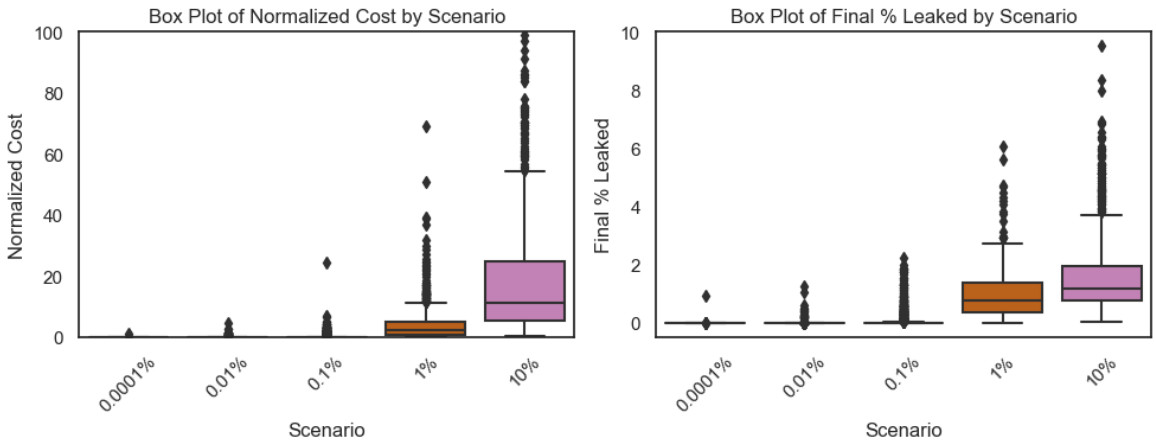

Figure 29. Probabilistic Assessment of Well Failure: Effects on CO_2 Leakage and Normalized Cost

3.8. BAYESIAN UPDATING

These three plots illustrate the results of a Bayesian updating financial model that simulates the evolution of leakage risk and financial impact over the lifetime of a geologic carbon storage (GCS) project. The model begins with an assumed probability of failure and an initial belief that every failure results in leakage. However, as the simulation progresses, if no leakage is observed from failed wells, the conditional probability of leakage given failure is updated using Bayesian inference, leading to reduced expectations of leakage in future years. Results assuming no updating of leakage probability—meaning that the probability of leakage remains fixed regardless of new

observations—, and that wells may fail with replacement are presented in Figure A7 and Figure A8. The following observations summarize the trends across the two figures.

Average Normalized Leakage Cost (Figure 30):

This figure presents the projected net present value (NPV) of financial impacts over time, broken down by year. For example, under a 0.1% annual well failure probability, which is the highest annual probability of failure according to historical data, the projected NPV of financial impacts from year 10 to year 120 is approximately $2 per ton of CO_2 injected, while from year 20 to year 120, the value drops to effectively $0 per ton. This time-resolved financial projection reflects the declining risk profile of the project and provides a basis for estimating the appropriate insurance premium at each stage of the storage lifecycle. Here some observations:

- For all scenarios, the average normalized leakage cost ($/ton CO_2) declines rapidly and approaches zero by approximately year 20, which corresponds to the end of the injection period.
- During the injection period, the primary cost driver is the contractual penalty, which is triggered when CO_2 leakage interrupts injection operations. After year 20, when injection ceases, no detectable CO_2 leakage occurs, and thus no additional contractual penalties are incurred.
- Additionally, because reservoir pressure dissipates quickly after injection ceases and no significant/detectable brine leakage occurs during the post-injection phase, environmental remediation costs are minimal or nonexistent.
- Consequently, during the post-injection period, financial impacts from leakage become negligible, indicating that the bulk of the economic burden is front-loaded during active CO_2 injection.

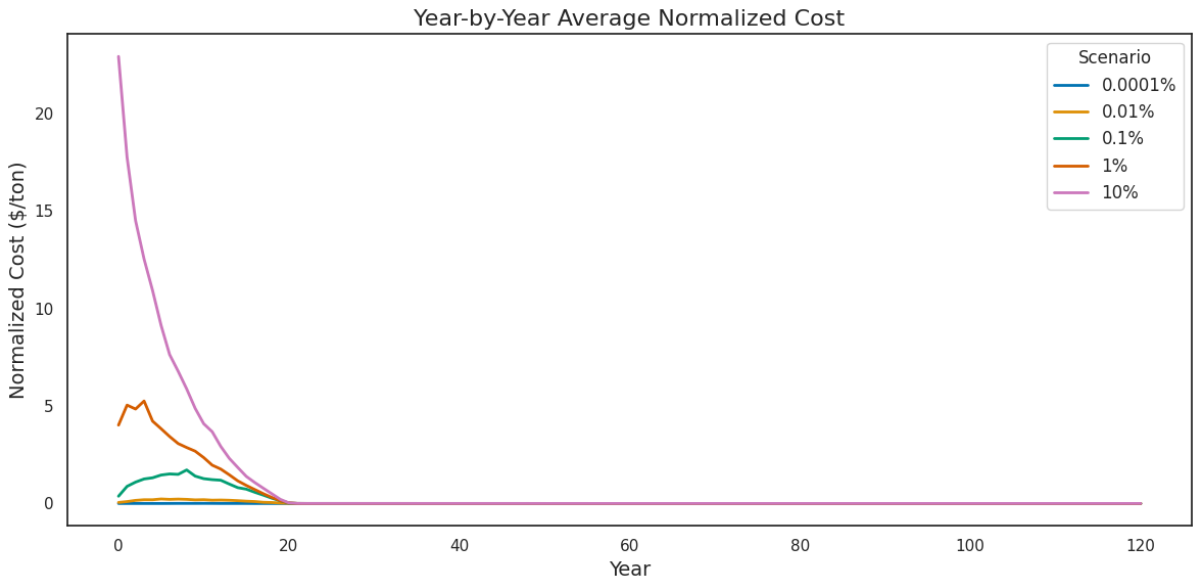

Figure 30. Year-by-Year Average Normalized Cost under Bayesian Updating Framework.

Average % CO_2 Leaked (Figure 31):

This figure shows the projected percentage of CO_2 leaked over time. For example, under a 0.1% annual well failure probability, which is the highest probability of failure according to historical data, the cumulative leakage from year 10 to year 120 is approximately 0.65%, and from year 20 to year 120, it increases slightly to about 0.8%. These results provide insight into the evolving environmental risk over the project lifecycle and demonstrate that, even under this worst-case failure rate (0.1%), the cumulative percentage of CO_2 leaked remains below 1% at all stages—meeting typical performance thresholds for long-term containment. Here some observations:

- Early project years show the highest average percentages of CO_2 leaked, especially for higher well failure probabilities.
- The 1% threshold for total CO_2 leakage is only exceeded in scenarios with annual failure probabilities of 1% or higher, underscoring the critical importance of this parameter. This

finding can support the EPA's requirement to assess well integrity and zonal isolation for all wells within the AoR.

- After the injection period ends, the CO_2 leakage percentage continues to decrease for all scenarios. While the leakage does not drop to zero, it steadily trends downward and approaches zero by year 120.
- The reason leakage does not fully vanish is the presence of a non-zero detection threshold, which prevents the detection and remediation of minor leaks. These undetected leaks continue post-injection but at very low rates, contributing minimally to overall leakage volume.

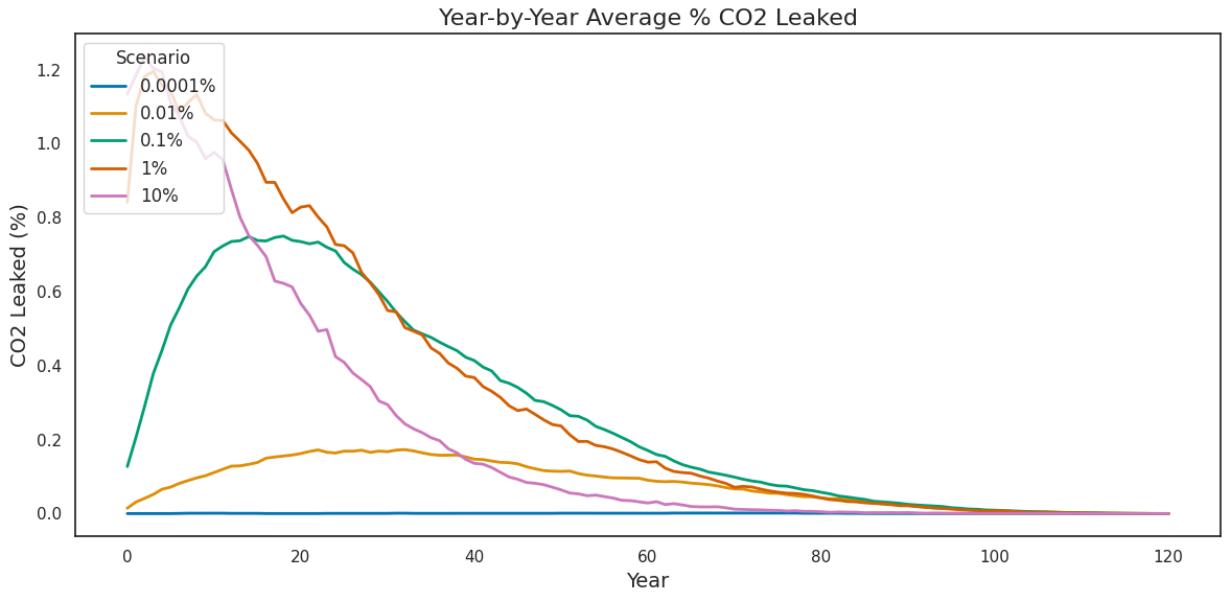

Figure 31. Year-by-Year Average Percentage of CO_2 Leaked under Bayesian Updating Framework

3.9. Monitoring & Remediation Analysis

In this analysis, simulations are used to estimate the value of monitoring by quantifying financial damages under a worst-case scenario—assuming all 240 wells fail—and evaluating how different detection thresholds influence compliance with permanence criteria. While regulatory requirements under Class VI permits assume zero tolerance for leakage and mandate site shutdown upon detection, using permanence standards—such as the IPCC (2005) guideline of 99%

containment over 100 years and the LCFS requirement that 90% of modeled scenarios remain below 1% cumulative leakage (CARB, 2018)—provides a practical and risk-informed benchmark for cost-effective monitoring investment.

Although tighter detection thresholds improve early leak identification and permanence compliance, they also increase remediation costs, requiring a careful trade-off analysis. Framing monitoring design around permanence criteria provides a smart, flexible strategy for investment planning, especially when facing uncertainty and limited resources.

Main Observations:

- Very low detection thresholds catch small leaks early but often result in high remediation costs. Conversely, high thresholds may delay detection, allowing significant leakage. A threshold around 20 tons per day (TPD) strikes an effective balance between early response and cost control.
- At ~20 TPD, 90% of modeled outcomes show less than 1% leakage over 100 years, aligning with the IPCC (2005) and CARB (2018) permanence standards. Under this condition, monitoring investments up to $8 per ton of CO_2 injected are financially justifiable—spending beyond this level offers diminishing returns in ensuring permanence compliance.

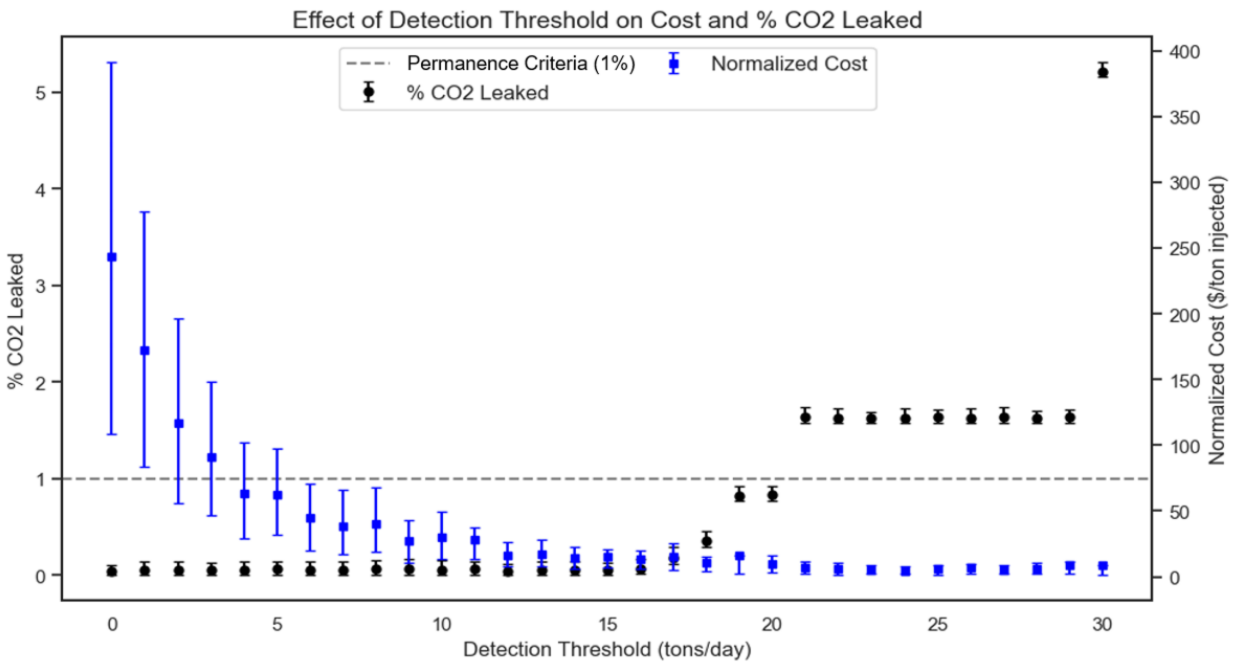

Figure 32. Effect of detection threshold on cost and cumulative % of CO_2 leaked. The bars correspond to the p10 and p90 values.

CHAPTER IV: DISCUSSION

4.1. PHYSICAL MECHANISMS AND RESERVOIR CONDITIONS THAT DRIVE CO_2 AND BRINE LEAKAGE

Predicting CO_2 and brine leakage through an open wellbore remains a significant challenge due to the complex interplay of multiphase flow, buoyancy effects, and pressure propagation. Given the uncertainty in leakage behavior, CMG-GEM results were compared against NRAP-OPEN-IAM simulations (see Appendix A.2) under same reservoir assumptions. The results differed by up to an order of magnitude—an outcome attributed to fundamental differences in the numerical frameworks: CMG-GEM uses a fully coupled, isothermal formulation that omits thermodynamic effects like Joule-Thomson cooling and temperature-dependent density variations in the wellbore, while NRAP-OPEN-IAM includes non-isothermal drift-flux modeling but lacks feedback from reservoir pressure and saturation changes, as it treats the wellbore and reservoir as decoupled systems.

Numerous studies have attempted to replicate historical CO_2 or gas blowouts and field test results (e.g., Adams et al. (2021); Freifeld et al. (2016); Lindeberg et al. (2017); Pan et al. (2018)), yet accurately capturing the coupled dynamics of CO_2 and brine leakage remains elusive. Nonetheless, this study is designed around worst-case scenarios, assuming the presence of open wellbores fully connected from the injection zone to the surface. As a result, it intends to capture within the full range of leakage behaviors and complexities observed in historical CO_2 or gas blowouts and field tests. This approach enables the estimation of upper bounds for potential CO_2 and brine leakage rates in the event of well failure, along with their associated environmental and financial impacts. It also provides insight into how different subsurface settings and trapping mechanisms influence overall leakage risk.

The dynamic interplay between reservoir pressure, CO_2 saturation, and leakage behavior fundamentally governs both risk and cost. When the pressure front reaches an open wellbore, brine leakage increases sharply, with leakage rates closely tied to the magnitude of reservoir overpressure. In cases where the CO_2 plume does not reach the wellbore, brine leakage typically ceases within 10 years after injection ends, as the pressure gradient dissipates.

However, if the CO_2-rich phase plume reaches the well and CO_2 saturation is sufficient, leakage transitions from brine-dominated to CO_2-dominated. In this phase, brine is largely displaced by CO_2, and further leakage is driven primarily by CO_2 saturation and the pressure differential between the reservoir and the atmosphere.

It is important to note that field and experimental data have shown that accumulation of a denser fluid (e.g., water) within the open wellbore can occur. This accumulation may eventually suppress or "kill" flow, as observed in controlled testing scenarios, thereby reducing or halting leakage rates despite the pressure differential (Adams et al., 2021).

After injection stops, pressure within the CO_2 plume declines quickly but does not return to hydrostatic levels, due to the buoyancy of the CO_2. At this stage, mobile CO_2 saturation drives leakage, which gradually declines as CO_2 becomes residually trapped. There are no field studies that characterize leakage dynamics months or years after injection. The Aliso Canyon gas storage field well blowout showed a steady-state leakage phase from day 80 to 110, but no long-term data were collected afterward (Lindeberg et al., 2017). Thus, projections of post-injection leakage behavior remain entirely dependent on numerical simulations.

However, these findings have clear implications for monitoring strategy: while brine leakage risk largely vanishes within 10 years post-injection, wells located within the CO_2 plume

may continue to leak CO_2 if mobile-phase saturation remains high. Rapid residual trapping significantly reduces long-term CO_2 leakage risk.

Another important finding is the timing of peak leakage rates. In this study, peak CO_2 and brine leakage rates occurred just before injection ceased, when both pressure and CO_2 saturation were at their maximum. This contrasts with findings by (Pan & Oldenburg, 2020), who used T2Well simulations to model short-term leakage behavior (~1 month). In their work, peak CO_2 leakage occurred early, once brine was fully displaced, and then plateaued at a relatively constant rate.

The simulations also highlighted the rapid propagation of the pressure front, which reached wells 2 km from the injector almost immediately after injection began. This supports prior findings by (Nordbotten & Celia, 2006), who emphasized that pressure waves travel faster than CO_2 plumes, thereby enabling early brine displacement well before CO_2 arrival.

Another important observation was that, in all CMG-GEM cases, once CO_2 reached the open wellbore, it significantly displaced the brine. This created a gas-dominated flow regime with minimal two-phase interaction, which implies an efficient gas lift mechanism. In reality, during gas lift complex interactions happen as brine would likely continue to interact with and impede CO_2 flow. The expected competition between phases, intermittent flow regimes, and more complex gas-brine dynamics were not modeled, highlighting a potential limitation in the simulation's physical realism.

Another critical factor influencing leakage behavior is near-wellbore phenomena. Studies by Abdel Azim (2016), Bahrami et al. (2004) and Pérez-Martinez et al. (2012) have shown that strong pressure gradients near the well can create vacuum-like conditions that draw water into the conduit. This process may trigger brine breakthrough and, in some cases, suppress or completely

halt gas flow. This phenomenon, known as the upconing effect—where brine migrates upward into the wellbore due to localized pressure depletion and a rapid decline in CO_2 saturation—was not observed in this study. In fact, the opposite trend was seen: as the grid was refined around the open wellbore, CO_2 saturation increased while pressure decreased (see Figure A4).

Despite these limitations, the scenarios modeled here are intentionally constructed as worst-case cases, representing the upper bound of leakage and financial risk. This approach aligns with the study's goal: to provide a conservative framework for understanding the consequences of open-wellbore leakage in geologic carbon storage projects.

4.2. Site-Specific Variables Most Strongly Influence the Environmental and Financial Impacts

Sensitivity analyses using NRAP-OPEN-IAM and CMG-GEM revealed that several site-specific variables—including permeability, depth, vertical-to-horizontal permeability ratio (kv/kh), pore size distribution (λ), salinity, thickness, and capillary entry pressure—affect CO_2 and brine leakage behavior. However, their impact on financial outcomes is substantially reduced when detection and remediation strategies are in place.

Environmental Impacts

Permeability, thickness kv/kh, and λ most strongly influence CO_2 leakage rates (Figure 25). These parameters govern plume mobility and interaction with leakage pathways. Higher permeability and kv/kh promote CO_2 migration but reduce pressure buildup, lowering brine leakage. Although these variables affect leakage volume, their financial significance diminishes when leaks are detected and remediated promptly.

Financial Impact

Well density is the most influential factor for both environmental and financial outcomes (Figure 24). In high-density cases (e.g., 4.8 wells/km²), pressure is more dissipated (more open wellbores), leading to higher CO_2 leakage but lower brine leakage. In low-density scenarios (e.g., 0.27 wells/km²), CO_2 leakage is negligible, but brine leakage is higher due to less pressure dissipation (i.e., less open wellbores cause less pressure dissipation), resulting in higher well and water remediation costs.

In the base case—240 open wells at 2.4 wells/km²—the median financial impact is approximately \$0.24 per ton of CO_2 injected per open wellbore. This worst-case assumption demonstrates how well count and placement strongly affect financial exposure. Estimating the number of wells intersecting the CO_2 plume and those within the area of review (AoR) can be a practical proxy for assessing site-specific financial impact. Moreover, wells affected by reservoir pressure—even without plume contact—can significantly contribute to costs. In the low-density case, brine leakage from pressure changes drove financial impact despite inexistent CO_2 leakage. This corroborates EPA's focus on performing corrective actions and enhancing monitoring on wells within the AoR (U.S. EPA, 2013).

As an analog to well integrity, different annual well failure probabilities were also analyzed to reflect realistic scenarios of leakage through compromised wellbores (Figure 29). Historical data suggests that a 0.1% annual failure rate is among the highest observed in practice (Jordan & Benson, 2009; Porse et al., 2014; Trabucchi et al., 2012). Under this scenario, the 90th-percentile CO_2 leakage remains well below 1%, and the normalized financial cost is modest, around \$1.40 per ton of CO_2 injected. These results indicate that rare well failures ($\leq$0.1%) pose limited risk to project permanence and cost-effectiveness.

Cost Breakdown

Brine leakage is the dominant cost driver due to early pressure propagation during injection. Most costs are incurred upfront, with injection interruption and water remediation comprising the bulk. CO_2-related climate compensation is negligible, accounting for just 0.2% of total expenses (Figure 22).

Although the model assumes leakage to the surface, the framework is applicable to groundwater scenarios. The remediation approach—brine extraction, treatment, and reinjection—mirrors strategies for managing contamination of Underground Sources of Drinking Water (USDWs).

This analysis also informs carbon credit certification. Even under conservative assumptions (e.g., 240 open wells in the AoR), the p90 CO_2 leakage rate remains below 2%. This low figure suggests that sites with effective monitoring and remediation could justify lower credit buffer requirements.

4.3. Evolving Environmental and Financial Impacts Throughout the Project Lifecycle

This analysis focuses on the base case scenario—a flat-lying reservoir with 240 open wellbores—and applies a range of annual well failure probabilities to simulate leakage risk over time. Using Bayes' theorem, the model updates the probability of future leakage based on continued non-leakage observations, reflecting how real-world operational experience can reduce perceived risk. In this scenario, wells are remediated upon detection, and the results—shown in Figures 30 and 31—illustrate how both environmental and financial impacts evolve over the lifetime of a project.

Unlike previous studies that primarily emphasized detection thresholds, this approach offers a time-resolved risk framework that dynamically adjusts expected leakage rates and financial liabilities as site performance data accumulates. It demonstrates how early non-leakage observations can lower projected risks, thereby reducing long-term liability.

Understanding how financial and environmental impacts evolve over time is critical for the success of geologic carbon storage (GCS) projects. To our knowledge, this is the first study to jointly quantify these impacts across both the injection and post-injection periods. These insights are highly relevant for insurers evaluating fair risk premiums, for project developers designing adaptive monitoring strategies, and for building public trust in the long-term safety of CO_2 storage.

Normalized Cost Over Time

Simulation results show that the vast majority of financial risk is concentrated during the injection phase (Figure 30). For the highest historically observed annual well failure probability (0.1%), the normalized cost peaks at approximately $2 per ton of CO_2 injected, then drops to zero immediately after injection stops. This trend is consistent across all failure probability scenarios and reflects a key insight: under well-managed conditions, the net present cost of future damages is effectively zero once injection ends.

This is primarily because, after injection stops, reservoir pressure declines sharply, reducing the driving force required for CO_2 and brine to migrate to the surface. As a result, any post-injection leakage that does occur is extremely limited—below the assumed detection threshold of monitoring systems, and therefore not financially consequential.

Bayesian updating reinforces this finding by continually lowering the estimated probability of future leakage in the absence of observed incidents. Together, these results support the scaling

down of financial safeguards post-injection and highlight the importance of focusing mitigation efforts during the active injection period, when both pressure and leakage risk are highest.

CO_2 Leakage Percent Over Time

The projected percentage of CO_2 leaked over time follows a similar trend (Figure 31). Under a 0.1% annual failure probability, the cumulative percentage of CO_2 leaked reaches its maximum—approximately 0.8% of the total injected volume—around the end of the injection period. After that point, leakage tapers off significantly. Even 50 years post-injection, the projected additional leakage remains under 0.2%, and by 100 years, no further leakage is expected.

These results underscore the long-term integrity of well-managed storage sites and demonstrate alignment with permanence thresholds such as those predicted by IPCC and LCFS protocols. They suggest that most climate risk associated with leakage is front-loaded and manageable with appropriate monitoring and response strategies.

Overall, this time-dependent framework enables risk management strategies—such as credit buffers and insurance premiums—to be aligned with actual project behavior. It provides operators and insurers with a basis for adjusting safeguards dynamically, concentrating resources during higher-risk periods and reducing over-coverage as uncertainty decreases. This supports capital efficiency, regulatory compliance, and stakeholder confidence across the lifecycle of a CO_2 storage project.

4.4. Optimization of Monitoring Investments Based on Site-Specific Leakage Impacts

Effective monitoring is essential not only for regulatory compliance but also for reducing financial liabilities and reinforcing public confidence in CO_2 storage projects. This section

evaluates how different detection thresholds influence the cost-effectiveness of monitoring strategies and their ability to satisfy long-term containment goals.

The results show that a detection threshold of approximately 20 tons per day (TPD) provides the most balanced outcome (Figure 32). At this threshold, 90% of modeled outcomes remain below 1% cumulative leakage over 100 years, satisfying both (IPCC, 2005) recommendations for 99% CO_2 containment and the LCFS requirement that 90% of modeled scenarios stay under 1% leakage (CARB, 2018).

Monitoring investments up to $8 per ton of CO_2 injected are justified under this optimized threshold, beyond which diminishing returns become apparent. While this $8 estimate is conservative—particularly under the assumption that all 240 wells in the model domain fail with 100% probability—it offers a valuable upper bound for planning purposes. But again, this assumes that all 240 wells fail. If we instead assume an annual failure probability of 0.1%, the cost can decrease to $0.008 per ton of CO_2 injected. According to Ogland-Hand et al. (2023), monitoring costs typically range around $2 per ton of CO_2, and IEAGHG reports estimates between $0.80 and $2 per ton, depending on site complexity and monitoring strategy. Even though the $8 figure exceeds typical costs, having early insight into financial implications enables operators to conduct cost-benefit analyses and optimize monitoring investments, such as frontloading monitoring investment to time of highest risk early in the project, while being in line with both permanence requirements and budgetary constraints.

Moreover, the detection threshold itself can be refined based on site-specific monitoring results and historical performance. This would allow operators to establish a tailored threshold that reflects actual leakage behavior and monitoring resolution, improving the efficiency and accuracy of the response strategy.

It is important to note that in this analysis, we assume the monitoring system detects leakage with 100% certainty once the threshold is exceeded. In practice, detection probability depends on the capabilities of the monitoring technology and site-specific factors. If detection likelihoods are available—for example, as probabilities associated with particular monitoring observations—these can be incorporated into the Bayesian framework to update the estimated probability of leakage more accurately.

Additionally, one emerging challenge in the field is defining an overall detection threshold for a given monitoring system. While the complexity of monitoring network design makes this difficult—due to dependencies on spatial resolution, sensor type, leakage pathway geometry, and noise levels—developing reasonable approximations will help clarify how detection thresholds reduce leakage risk, improve system performance, and provide a framework for tailoring monitoring intensity to actual project conditions. This helps project developers and regulators identify financially efficient approaches that still meet permanence and safety criteria.

CHAPTER V: CONCLUSIONS AND RECOMMENDATIONS

5.1. CONCLUSIONS

This thesis set out to investigate how subsurface conditions influence the material and financial impacts of CO_2 and brine leakage in geologic carbon storage (GCS) systems, with the goal of estimating upper-bound environmental and economic consequences from potential leakage events. The motivation stems from the urgent need to de-risk carbon storage investments, optimize monitoring investments, and comply with regulatory requirements—particularly the financial responsibility mandates of the U.S. EPA's Class VI permitting framework. Due to limited operational track records and the absence of standardized risk quantification methodologies, current insurance and financial assurance practices often rely on conservative assumptions. This can lead to inefficiencies in project planning and inflated premiums.

To address these challenges, a methodology was developed that integrates multiphase flow simulations, wellbore leakage modeling, and environmental and financial cost analysis. A portfolio of dynamic simulations was constructed to represent a broad range of plausible subsurface and project conditions, including variations in reservoir geometry (flat, dipping, and anticlinal), permeability, thickness, depth, porosity, well density, and extension of the injection zone. All models were grounded in real-world data from the U.S. Gulf Coast, ensuring regional relevance and enhancing the robustness of the simulation outcomes.

CO_2 and brine can migrate through various pathways such as fractures, faults, and spill points; however, legacy plugged and abandoned (P&A) wells are recognized as the most significant risk pathway. This analysis focused on a worst-case scenario in which all P&A wells intersecting the storage formation were assumed to be fully open and vertically connected to the surface—lacking plugs and wellheads. These open wells served as simplified analogs for vertical

conduits and could also represent worst case analogs for damaged caprock, fractures, or faults that allow upward fluid migration through simple aperture. These hypothetical conduits were distributed at varying locations and distances from the injection well to capture a range of leakage possibilities. This conservative framing enabled rigorous estimation of maximum potential environmental and financial impact.

To quantify the financial consequences of leakage, a simplified cost model was developed. Unlike other frameworks that may attempt to account for third-party damages—such as impacts on water wells, oil and gas operations, or public health—this study focused on the most probable, direct, and quantifiable cost drivers: brine remediation, leaky well repair, loss of tax credits, and contractual penalties. Only two stakeholders were considered in the model: the CO_2 emitter and the injection operator.

Environmental damages were limited to brine leakage reaching the surface, which is more likely to produce observable and traceable impacts. In contrast, CO_2 leakage was excluded from environmental cost calculations because evidence suggests that when CO_2 reaches the atmosphere, it rapidly disperses and poses minimal risk to human health or ecosystems. Similarly, damages to underground sources of drinking water (USDWs) were not included, given the limited evidence of widespread harm and the difficulty in quantifying such impacts in a generalized cost model. However, the financial remediation methods modeled for surface brine leakage (e.g., pumping, treatment, reinjection) would also apply in cases where USDW contamination occurs—assuming that the leakage is detectable and measurable.

To account for evolving site conditions, Bayesian updating was incorporated into the framework to dynamically adjust risk and cost estimates over time, based on actual site performance and the absence of observed leakage events.

This modeling framework is designed to scale with larger projects and higher injection rates. While the base simulations assume CO_2 injection into a single sand body or reservoir layer, the findings can be reasonably extrapolated to scenarios involving multiple stacked injection zones—an approach commonly used in real-world applications. In such cases, the modeled layer can serve as a proxy for the uppermost portion of a thicker storage complex.

Importantly, reservoir thickness and permeability—key parameters that control the maximum achievable injection rate—were found to have limited influence on overall financial and environmental impacts, particularly when robust monitoring and remediation strategies are implemented. As injection volumes increase, operators are expected to distribute CO_2 across multiple layers to manage pressure buildup and meet project capacity requirements.

For conservative planning, it can be assumed that legacy plugged-and-abandoned (P&A) wells intersect all active injection layers. This assumption enables the proportional extension of the risk and cost estimates presented in this study to larger, more complex storage architectures, while preserving the core risk assessment principles.

In conclusion, this thesis demonstrates that even under conservative, worst-case assumptions, the environmental and financial risks associated with geologic CO_2 storage are low and manageable. For an annual well failure probability of 0.1%—the highest rate documented in historical records—the average projected cost is approximately $1.4 per ton of CO_2 injected. Although this cost may seem modest, a 0.1% failure rate implies that more than 1 in 10 wells would fail through the entire casing over the course of the project, making this a highly conservative and extreme scenario. In reality, most documented leakage incidents occur through smaller apertures or more complex pathways, such as degraded plugs or poor bonding between rock, casing, and cement. By adopting these worst-case conditions, this study establishes an upper

bound for evaluating long-term risk and financial liability, providing a valuable reference point for project developers, regulators, and insurers.

This cost reflects the expected financial liability over the lifetime of the project, including both environmental remediation and regulatory penalties. At this same failure probability, the 90th-percentile cumulative CO_2 leakage is just 0.4% of the total injected volume—well below the 1% IPCC threshold and comfortably within LCFS permanence criteria. These findings affirm the permanence effectiveness of well-sited CO_2 storage systems, even under pessimistic assumptions.

When evaluating how leakage and costs evolve over time using the Bayesian framework, the results remain reassuring. From year 10 to 120, projected cumulative CO_2 leakage reaches only 0.65%. Extending the period to start at year 20 increases this slightly to 0.8%, but it decreases to 0% at year 120. This means that no CO_2 leaks 100 years after injection stops under this worst-case scenario. Financial impacts follow a similar pattern: under the 0.1% scenario, the projected cost between years 10 and 120 is approximately $2 per ton of CO_2 injected. Once injection ceases at year 20, leakage and costs decline sharply. From year 20 onward, no further detectable CO_2 or brine leakage is projected, and financial impacts fall to zero. This outcome has significant implications for long-term liability planning, suggesting that post-injection site care and monitoring requirements can reasonably be relaxed after injection ends, especially if supported by monitoring data.

A breakdown of the total financial impact shows that 35% is attributed to environmental remediation—including brine cleanup and well repair—while the remaining 65% stems from the loss of tax credits and contractual penalties. The analysis assumed a conservative well repair time of 430 days, which significantly contributes to these financial losses. However, in real-world GCS projects, strong financial and regulatory incentives exist to reduce downtime. As a result, actual repair times—and consequently, overall financial impacts—are likely to be significantly lower.

Also, this study assessed how varying detection thresholds affect monitoring effectiveness and cost-efficiency. A threshold of 20 tons per day (TPD) was found to be optimal from an economic perspective, ensuring that 90% of modeled outcomes stay under 1% cumulative leakage over 100 years, satisfying both IPCC and LCFS requirements. At this threshold, monitoring investments up to $8 per ton are justified under the assumption that all 240 wells in the project area will fail. When assuming a more realistic 0.1% failure probability, this cost can drop to just $0.008 per ton. The analysis also supports front-loading monitoring efforts during high-risk periods and adapting intensity as site-specific performance data becomes available.

Also, the simulations clearly show that subsurface conditions—such as reservoir geometry, lateral extent of the injection zone, and petrophysical variability—have only a minor influence on total leakage volumes and financial consequences when effective detection and remediation systems are in place. Instead, the most critical factors are well density and the annual probability of failure, which act as proxies for legacy well integrity and well type. These two parameters primarily determine the scale of leakage events, making them the dominant drivers of both environmental and financial risk over the project lifecycle. Focusing on these key variables—and how their impacts change over time—can lead to more targeted and cost-effective risk assessments, monitoring strategies, and policy frameworks that enhance the long-term safety, credibility, and financial sustainability of carbon storage operations. Together, these findings support a more rational and evidence-based approach to financing, insuring, and managing the long-term liability of CO_2 storage projects.

5.2. Recommendations and Future Work

Building on the findings of this study, several recommendations are proposed to guide future research, improve simulation practices, and inform regulatory and policy development.

First, current simulations do not fully account for near-wellbore effects, which field tests have shown can significantly influence leakage behavior. Specifically, water intrusion and upconing phenomena can suppress or entirely halt CO_2 flow due to pressure depletion and brine displacement near the well. These effects—observed in field experiments but not captured in the current modeling framework—could materially reduce leakage rates and thus affect environmental and financial risk estimates. Future modeling should integrate these localized physical processes to improve the realism and accuracy of leakage predictions.

Second, open wellbores in this study act as an upper boundary condition, influencing reservoir pressure and CO_2 saturation throughout the model domain. Even when only a subset of wells is assumed to fail probabilistically, the input conditions used for analysis reflect the cumulative impact of all open wellbores, possibly leading to overestimation of leakage rates. Additionally, lateral boundary conditions were found to significantly influence pressure buildup, brine displacement, and long-term risk projections. Future work should prioritize scalable, physically representative methods for modeling aquifer size and boundary behavior.

Third, more work is needed to quantitatively link well construction characteristics—such as completion type, casing material, and construction year—to failure probability. By identifying correlations between these variables and observed leakage or failure events, practitioners can develop more refined, evidence-based failure probability estimates. These values can then be integrated into risk assessments and monitoring plans at the individual well level. This could also support site-specific prioritization of monitoring investments based on well risk profile and proximity to the plume.

Fourth, the financial and leakage results derived in this study should not be interpreted as forecasts but rather as conservative upper bounds on potential outcomes. For insurance purposes and financial responsibility planning, the outputs of this research are best used as caps or maximum

expected damages. Different assumptions about annual failure probability (e.g., less than 0.1%) can be used to assess lower-risk scenarios and evaluate trade-offs in monitoring and remediation costs.

Fifth, the financial model developed in this study is intentionally conservative and designed for flexibility. While results represent upper-bound estimates, users can easily adjust key variables such as well failure rates, CO_2 tax credit value, or well repair time to reflect site-specific conditions. Additionally, some insurers now offer coverage for lost revenue—such as tax credit loss during injection interruptions—which can be directly incorporated into the framework. Expanding the model to support real-time updates and site-specific parameterization would further strengthen its applicability for dynamic risk management, insurance underwriting, and investment planning.

Sixth, simulation results show that after injection ceases, CO_2 and brine leakage rates decline rapidly to levels that are often undetectable with existing monitoring technologies. This finding suggests that monitoring efforts should be focused during the injection period, when risks are highest and intervention can mitigate significant damage. Post-injection regulatory requirements should be revisited to reflect the reduced risk profile, potentially enabling more efficient resource allocation and reducing long-term liability management burdens for operators.

Lastly, future research should improve the characterization of sensor detection thresholds, spatial and temporal resolution, and detection reliability under varying site conditions. These attributes directly affect the probability of early leakage detection and must be integrated into adaptive risk modeling frameworks. Enhanced understanding will support optimization of monitoring system design, justify expenditures, and ensure alignment with regulatory and project performance standards.

APPENDIX

A.1. AREA OF REVIEW (AOR) CALCULATION

To determine the Area of Review (AoR), the critical pressure had to be calculated. The critical pressure was used to calculate the CO_2 and brine leakage rates when using NRAP-OPEN-IAM and when determining the AoR for the CMG-GEM open wellbore simulations. According to (Nicot et al., 2009) critical pressure is defined as the minimum value of pressure increase sufficient to lift denser brine up an open wellbore to the base of the freshwater aquifer. The equation to calculate the critical pressure in a reservoir is as follows:

$$\Delta P = g \times \frac{\varepsilon}{2} \times (Z_u - Z_i)^2$$

Where:

ΔP = Critical pressure

g = gravity

ε = density gradient, a linear coefficient depending on the salinity increase with depth, and also geothermal gradient:

$$\varepsilon = \frac{\rho_u - \rho_i}{Z_u - Z_i}$$

ρ_u = Fluid density at USDW

ρ_i = Fluid density at the injection zone

Z_u = Depth of the top of the injection formation

Z_i = Depth of the base of the USDWs.

For the case at hand and in order to determine the pressure it takes to lift the brine up to the atmosphere, it was assumed Z_i of 0 meters. Based on this equation, different critical pressure values were calculated for the different cases in the sensitivity analysis.

A.2. SENSITIVITY ANALYSIS USING NRAP-OPEN-IAM

For the leaky well simulation, NRAP-OPEN-IAM software was used (https://edx.netl.doe.gov/sites/nrap/nrap-open-iam/). NRAP-OPEN-IAM comprises a set of reduced-order and analytical models of various components of the Geologic Carbon Storage System, potential leakage pathways, including impact to groundwater resources and the atmosphere.

The open wellbore model used to calculate CO_2 and brine leakage rates into the atmosphere (Pan et al., 2011) implements the drift-flux approach to simulate CO_2 and brine flow through an open conduit. This model treats the leakage of CO_2 up an open wellbore or up an open (i.e., uncemented) casing/tubing. This model treats the non-isothermal flow of CO_2 and brine up an open wellbore, allows for the phase transition of CO_2 from supercritical to gaseous, with Joule-Thompson cooling, and considers exsolution of CO_2 from brine phase.

The NRAP-OPEN-IAM is designed to determine the leakage from a point in the reservoir to the atmosphere. Therefore, results (i.e., calculated pressure and CO_2 saturation) for a single layer must be extracted from the numerical model results. For this analysis, pressure and CO_2 saturation from the uppermost model layer were extracted from the reservoir model (CMG-GEM). The extracted model layer has the largest CO_2 plume extent and the highest CO_2 concentration.

For these simulations, 0.2 MT of CO_2 was injected per year for 20 years (4MT of CO_2 in total), and a 100-year post-injection period was analyzed. As for the critical pressure, since leakage

rates to the surface are being calculated, it was assumed that the fluid salinity at the USDW is 0 ppm, effectively representing fresh water. For the sensitivity analysis, the reservoir model corresponds to the base case scenario: 240 open wellbores located at different locations on the project area, and flat-lying reservoir.

For the sensitivity analysis, 24 simulations were done. For these 24 simulations, the cumulative CO_2 and brine leakage (kg) were calculated to understand the most important variables that influence CO_2 and brine leakage out of the atmosphere and hence, risk. To normalize the results, the cumulative volume of CO_2 injected in the reservoir (ft^3) per case was calculated. Then, the CO_2 and brine leakage were divided by the cumulative volume of CO_2 injected.

Variables	Normalized Cumulative CO_2 Leakage			Normalized Cumulative Brine Leakage		
	Low	**Base**	**High**	**Low**	**Base**	**High**
Depth	0.313 (0.77)	0.17	0.14 (-0.16)	13.58 (1.73)	4.97	6.36 (0.28)
Thickness	0.18 (0.05)	0.17	0.1 (-0.38)	5.44 (0.09)	4.97	5.19 (0.04)
Porosity	0.16 (-0.03)	0.17	0.16 (-0.05)	5.28 (0.06)	4.97	4.81 (-0.03)
Permeability	1.69 (8.57)	0.17	0.01 (-0.93)	10.99 (1.21)	4.97	8.92 (0.79)
Kv/Kh	0.37 (1.09)	0.17	0.13 (-0.22)	4.62 (-0.06)	4.97	5 (0)
Salinity	0.21 (0.23)	0.17	0.06 (-0.62)	5.08 (0.02)	4.97	8.47 (0.7)
Critical Water Saturation	0.16 (-0.06)	0.17	0.21 (0.24)	5.01 (0)	4.97	4.91 (-0.01)
Critical Gas Saturation	0.19 (0.08)	0.17	0.14 (-0.17)	4.99 (0)	4.97	5.02 (0.01)
Capillary Entry Pressure	0.13 (-0.26)	0.17	0.36 (1.06)	5.53 (0.11)	4.97	4.4 (-0.11)
λ	0.52 (1.97)	0.17	0.12 (-0.3)	4.43 (-0.1)	4.97	5.25 (0.05)
Aquifer Size	1.28 (6.27)	0.17	0.17 (0)	8.41 (0.69)	4.97	5.02 (0)

Table A1: CO_2 and brine leakage rates for different variables using NRAP-OPEN-IAM. The values in the parenthesis show the change in percentage as a decimal value with respect to the base case.

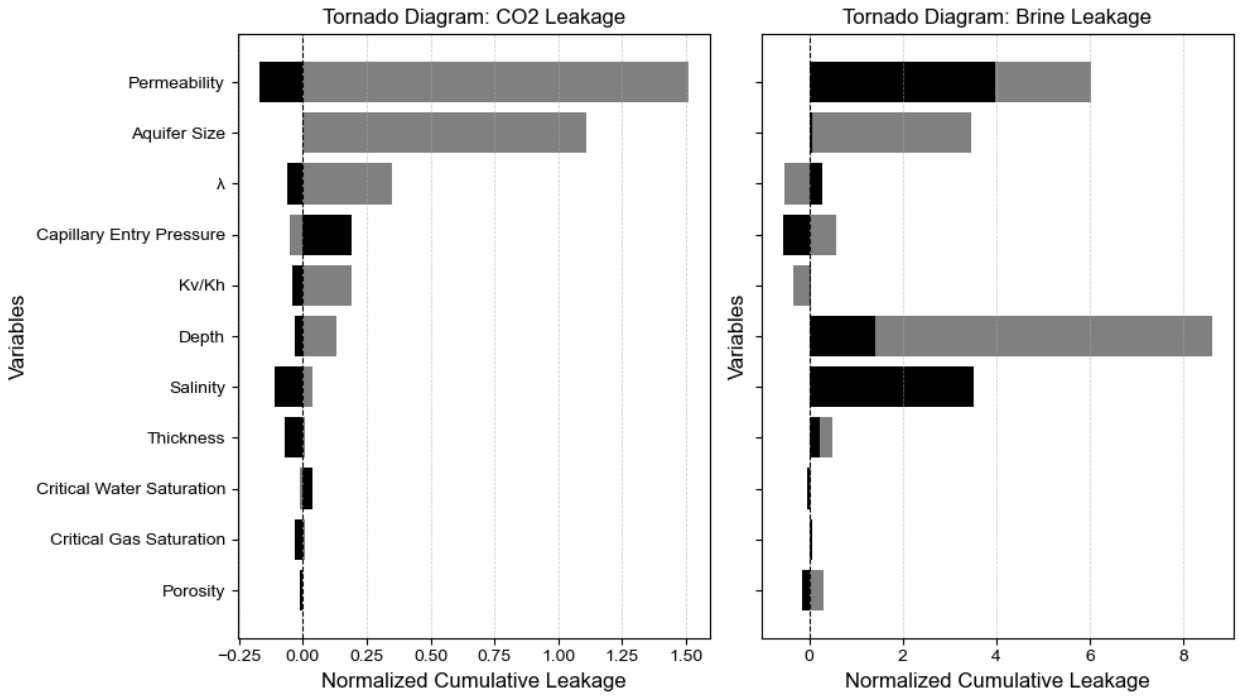

Figure A1. Sensitivity of CO_2 and Brine Leakage to Subsurface Parameters: Tornado Diagrams. Black and gray bars represent the high and low case, respectively. These simulations were done using NRAP-OPEN-IAM.

To understand how leakage rates vary with distance, three open wellbores were placed at different distances from the injection well: 100 m, 500 m, and 1,000 m. For this analysis, the base case reservoir model was used—a flat-lying reservoir with 0.2 MT of CO_2 injected per year for 20 years, followed by a 100-year post-injection period.

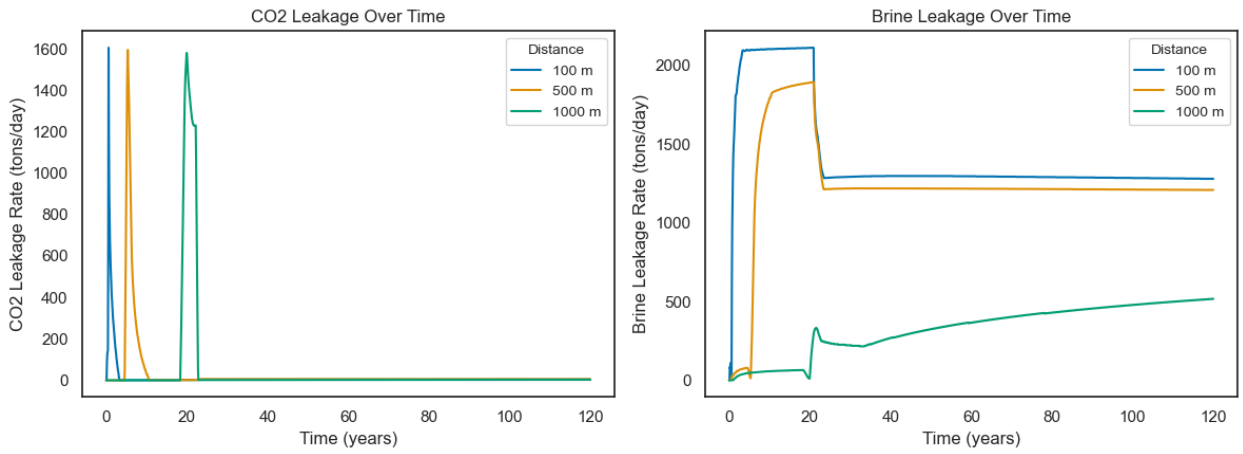

Figure A2. CO_2 and Brine Leakage Rates at different distances: 100 m, 500 m, and 1,000 m. The software used was NRAP-OPEN-IAM.

A.3. Effects of Grid Discretization Around an Open Wellbore

To analyze near-wellbore effects, the simulation grid was discretized around the open wellbore. Two grid resolutions were evaluated: one with 10×10×1 meter cells and another with finer 1×1×1 meter cells, both applied at the injection well and open wellbore locations.

The model domain spans 10 km × 10 km, and base reservoir properties—such as thickness, permeability, depth, and salinity—were used. The model was run as a closed boundary system, with 0.1 MT of CO_2 injected annually for 20 years (totaling 2 MT), followed by a 50-year post-injection monitoring period. The open wellbore was positioned 500 meters from the injection well, as shown in Figure A3.

Main Observations:

- Larger grid cells around the open wellbore lead to higher simulated pressure. This occurs because pressure is distributed across a greater volume, reducing the model's ability to capture

sharp pressure drops near the wellbore. Finer grid cells more accurately capture the localized pressure drawdown associated with leakage, leading to more realistic pressure gradients.

- Coarser grid cells result in higher pressure buildup near the open wellbore, which in turn drives more CO_2 leakage. As more CO_2 escapes the system, the local CO_2 saturation decreases. Thus, simulations with larger grid cells show lower CO_2 saturation near the wellbore due to increased leakage rates.

Because pressure differentials are the main driver of CO_2 and brine leakage, the grid resolution significantly affects the accuracy of leakage estimates. Coarser grid cells smooth the pressure field, leading to inflated leakage rates. In this study, the full-scale simulations used grid cells coarser than 10 meters (approximately 75 × 75 × 3 meters), suggesting that the reported CO_2 and brine leakage values are conservative upper bounds. In real-world applications, near-wellbore effects—such as localized pressure drawdown around open wellbores—would likely reduce leakage rates compared to those estimated in this study. As a result, actual environmental and financial impacts may be lower than the conservative estimates produced using coarser grid cells.

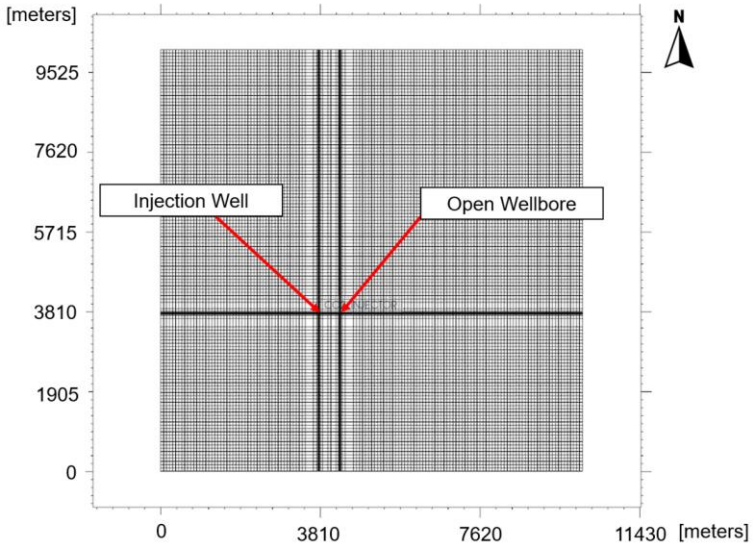

Figure A3**.** Model domain used for grid size sensitivity analysis, measuring 10 km by 10 km. The open wellbore is positioned 500 meters from the injection well.

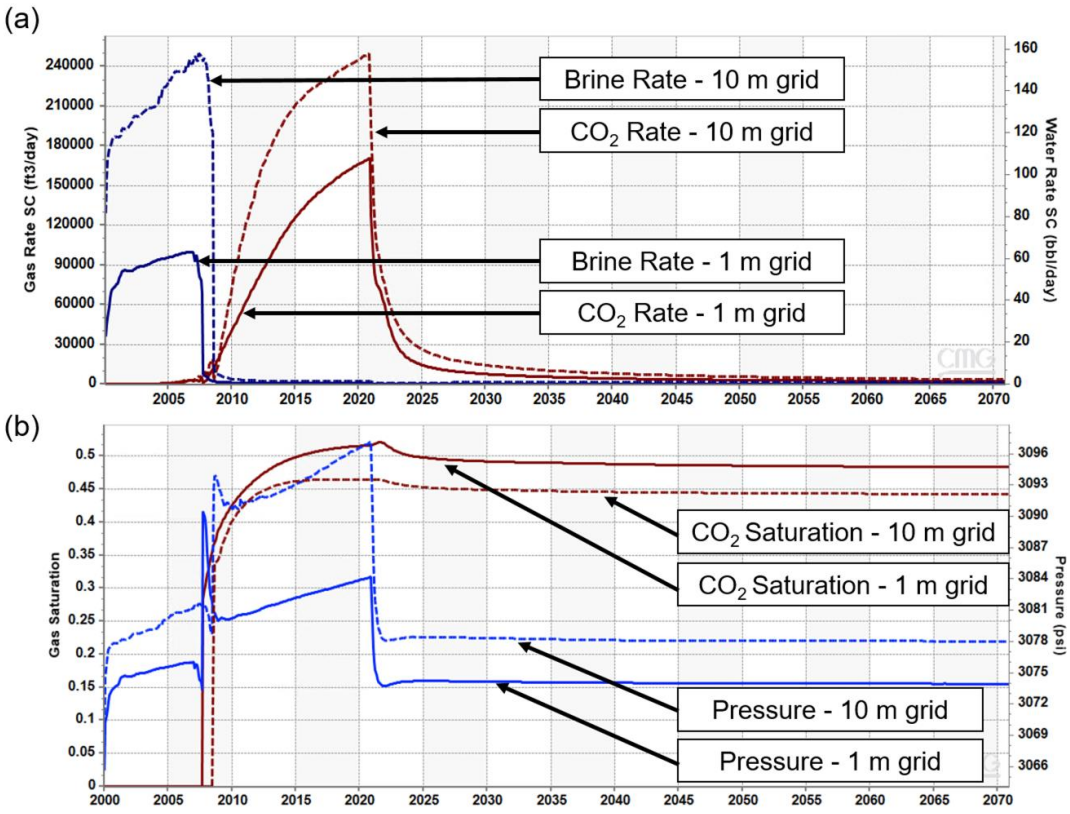

Figure A4**.** Results from the grid size sensitivity analysis. Plot (a) displays the CO_2 and brine leakage rates over time, while plot (b) shows the CO_2 saturation and pressure at the grid cell containing the open wellbore. The "1 m grid" corresponds to the 1 x 1 x 1 meter cells, whereas the "10 m grid" corresponds to the 10 x 10 x 1 meter cells.

A.4. Effects of Different Aquifer Lateral Extensions on Leakage Rates

To assess the effect of saline aquifer lateral extent on CO_2 and brine leakage rates, three scenarios were analyzed based on varying boundary conditions that simulate different aquifer sizes:

- Low case: 25.2 × 25.2 km
- Base case: 770 × 770 km
- High case: 7610 × 7610 km

Although the physical model domain remains 10 × 10 km, boundary conditions were adjusted to represent these lateral extents using the geometric progression method described in Section 2.3. All scenarios used base reservoir properties, with a CO_2 injection rate of 0.2 million tonnes (MT) per year for 20 years (4 MT total), followed by a 100-year post-injection monitoring period. One open wellbore was placed 500 meters from the injection well, and the grid resolution was set at 132 × 132 × 5.

Main Observations:

- Base and High Cases: Both scenarios behave similarly and reflect an open-boundary system. While minor differences in pressure, CO_2 saturation, and leakage rates exist, they remain small. Due to the buoyant nature of CO_2, reservoir pressure does not return to hydrostatic levels (3067 psi) after injection ceases in either case.
- Low Case: The low-capacity aquifer acts as a closed system, resulting in sustained overpressure throughout the simulation. This elevated pressure drives increased CO_2 leakage and results in lower CO_2 saturation near the leakage pathway.
- Pressure Behavior: Regardless of boundary configuration, pressure propagates rapidly across the model domain, initiating brine leakage in the first year of the project. The effects of

boundary conditions become more evident during the post-injection period, particularly in the high-capacity case, where pressure continues to decline further than in the base or low scenarios.

The lateral extent of the saline aquifer plays a critical role in influencing CO_2 and brine leakage rates. Larger saline aquifers tend to behave as open-boundary systems, dissipating pressure more effectively and reducing leakage risk, while smaller aquifers exhibit closed-system behavior, leading to sustained overpressure and increased leakage. However, accurately defining boundary conditions to simulate realistic large-scale reservoirs remains a key area for further research. Notably, pressure does not return to hydrostatic conditions within the 100-year simulation window in any scenario in the entire model domain. This raises important questions about whether this behavior reflects true reservoir dynamics or is an artifact of how boundary conditions were modeled. One possible explanation is that brine displacement and redistribution may occur more slowly than expected, leading to more localized pressure buildup and extended pressure dissipation timescales. Additional studies are warranted to determine whether prolonged overpressure is a realistic outcome or a result of model simplifications.

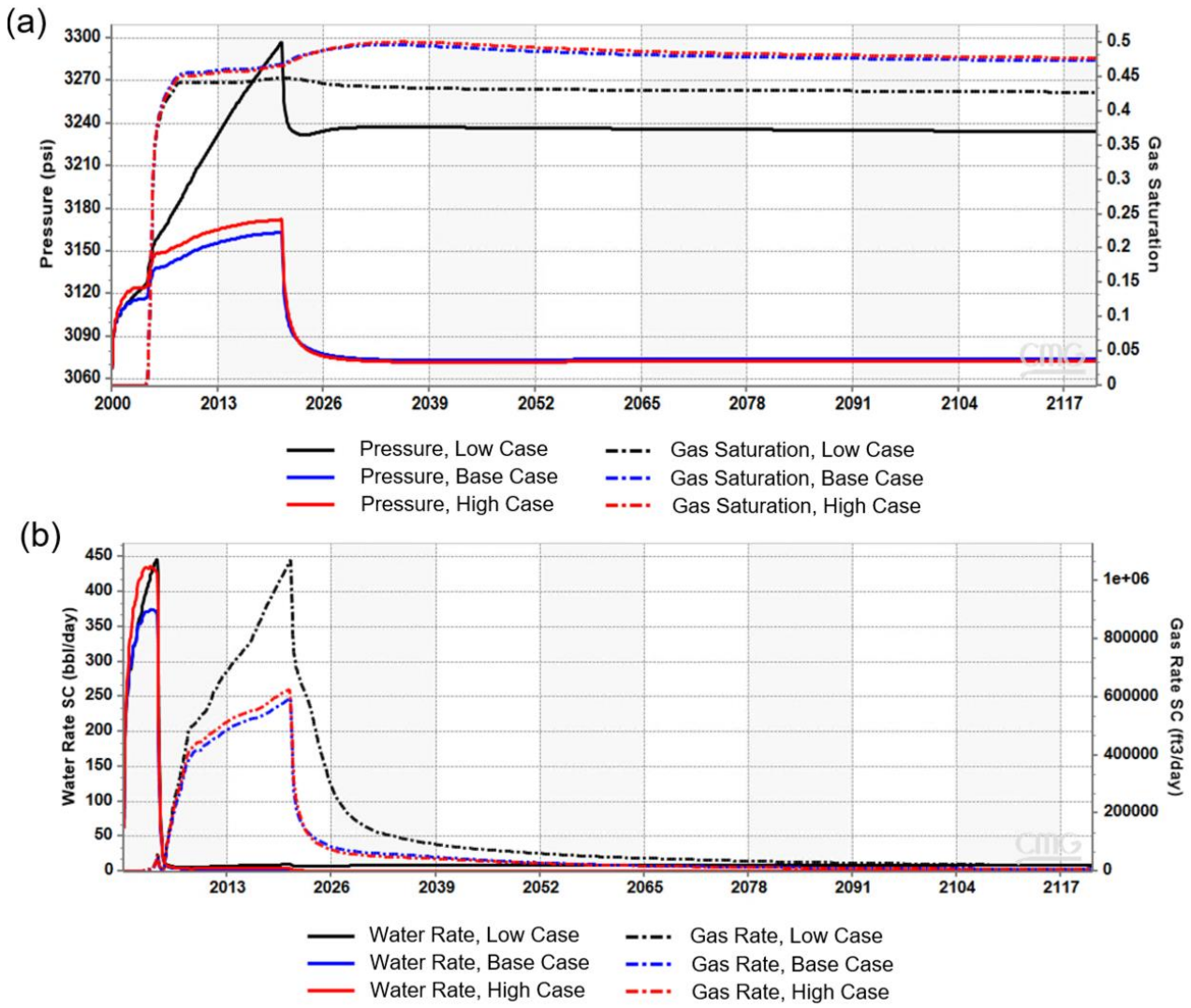

Figure A5. Results from the saline aquifer lateral extension sensitivity analysis. Plot (a) shows pressure and CO_2 saturation at the grid cell containing the open wellbore. Plot (b) displays the brine and CO_2 leakage rates through the open wellbore from the reservoir to the surface.

A.5. CMG-GEM AoR Analysis

Figure A6 shows the pressure front at year 20, simulated using CMG-GEM, for two scenarios: one without open wellbores and one with four open wellbores. The Area of Review (AoR) was determined using the critical pressure equation presented in Section A.1.

In this analysis, the open wellbores are modeled as cased conduits connecting the injection zone directly to the surface, without any intermediate connection to thief zones or aquifers. As a result, the fluid salinity within the well is assumed to match that of the injection zone. Under these conditions, the critical pressure buildup for defining the AoR becomes zero—meaning that the critical pressure for AoR definitions is the hydrostatic pressure, so even minimal pressure increases would initiate fluid migration from the injection zone.

Due to the limited size of the model domain, the calculated AoR exceeds the model boundaries and therefore cannot be visualized within the simulation extent. Nonetheless, the comparison between the two scenarios clearly demonstrates how the number of open wellbores influences the pressure front. Open wellbores act as vertical pressure sinks, effectively serving as upper boundary conditions that dissipate pressure and limit pressure buildup within the reservoir.

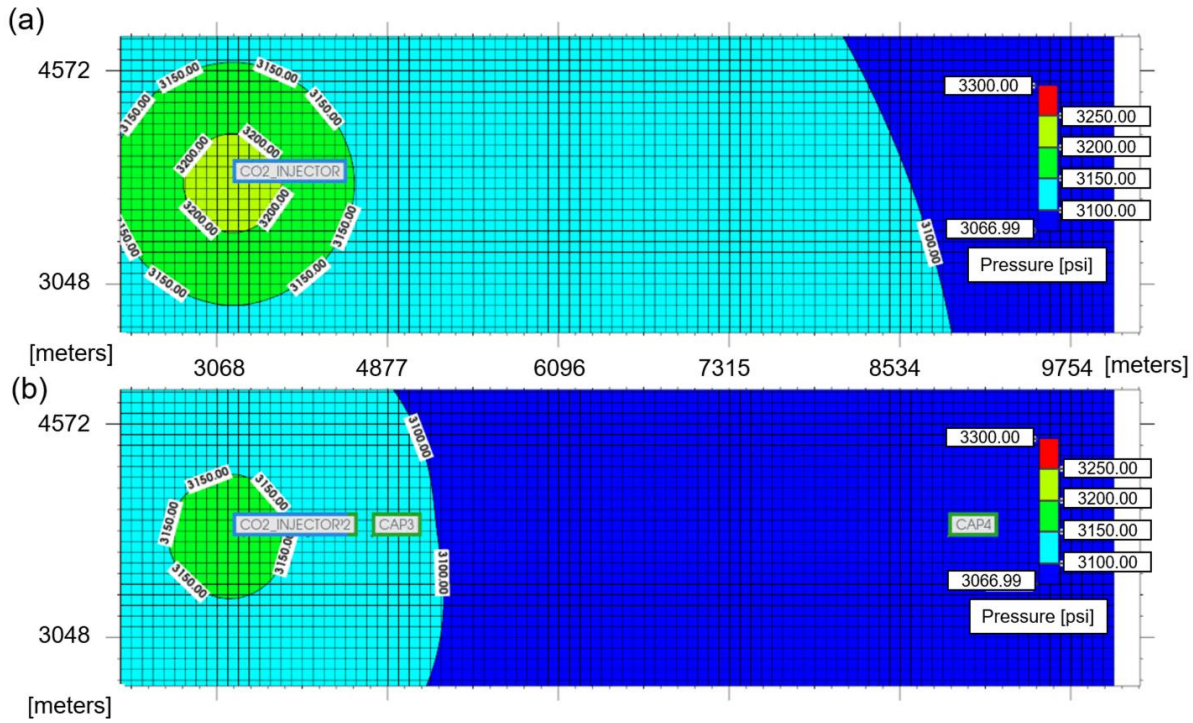

Figure A6. This model is a sample of the model domain. Pressure contour for (a) case with no open wellbores and for (b) case with four open wellbores. Open wellbores CAP1, CAP2, CAP3, and CAP4 are located 100 m, 500 m, 1,000 m, and 5,000 m from the injection well, respectively.

A.6. BAYESIAN UPDATING ADJUSTMENT SENSITIVITY ANALYSIS

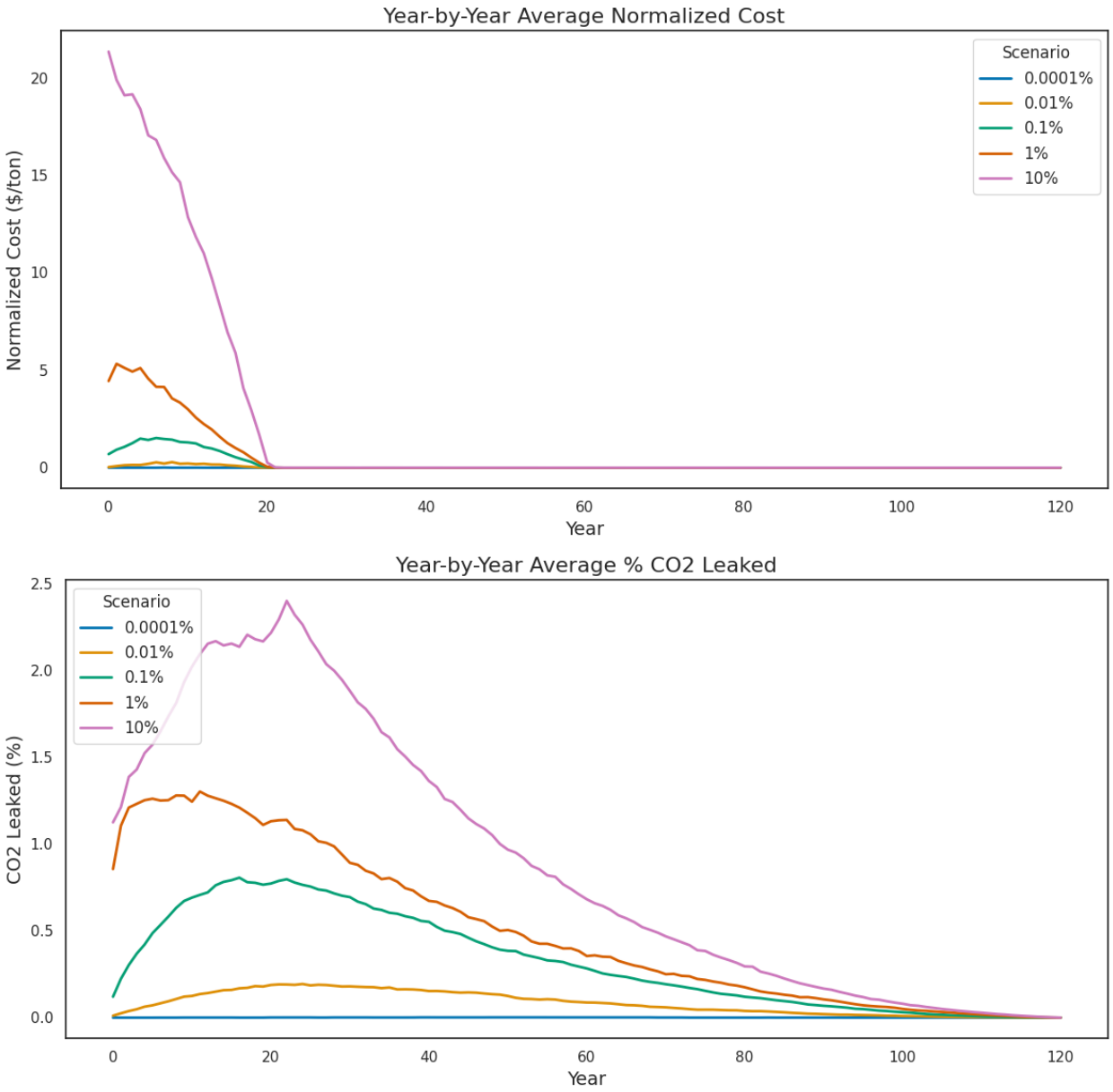

Figure A7. Year-by-Year Average Normalized Cost and % of CO_2 Leaked under the Constant Probability Framework. In this scenario, the annual probability of well failure remains constant over time and is not updated using Bayesian learning based on observed (non-) leakage events. That is, the model does not incorporate feedback from the absence of leakage to reduce perceived risk. Additionally, wells can fail in multiple years throughout the simulation—they are not permanently fixed after a failure in a given iteration. Instead, failures are reassigned independently each year, allowing repeated failures over the project lifetime.

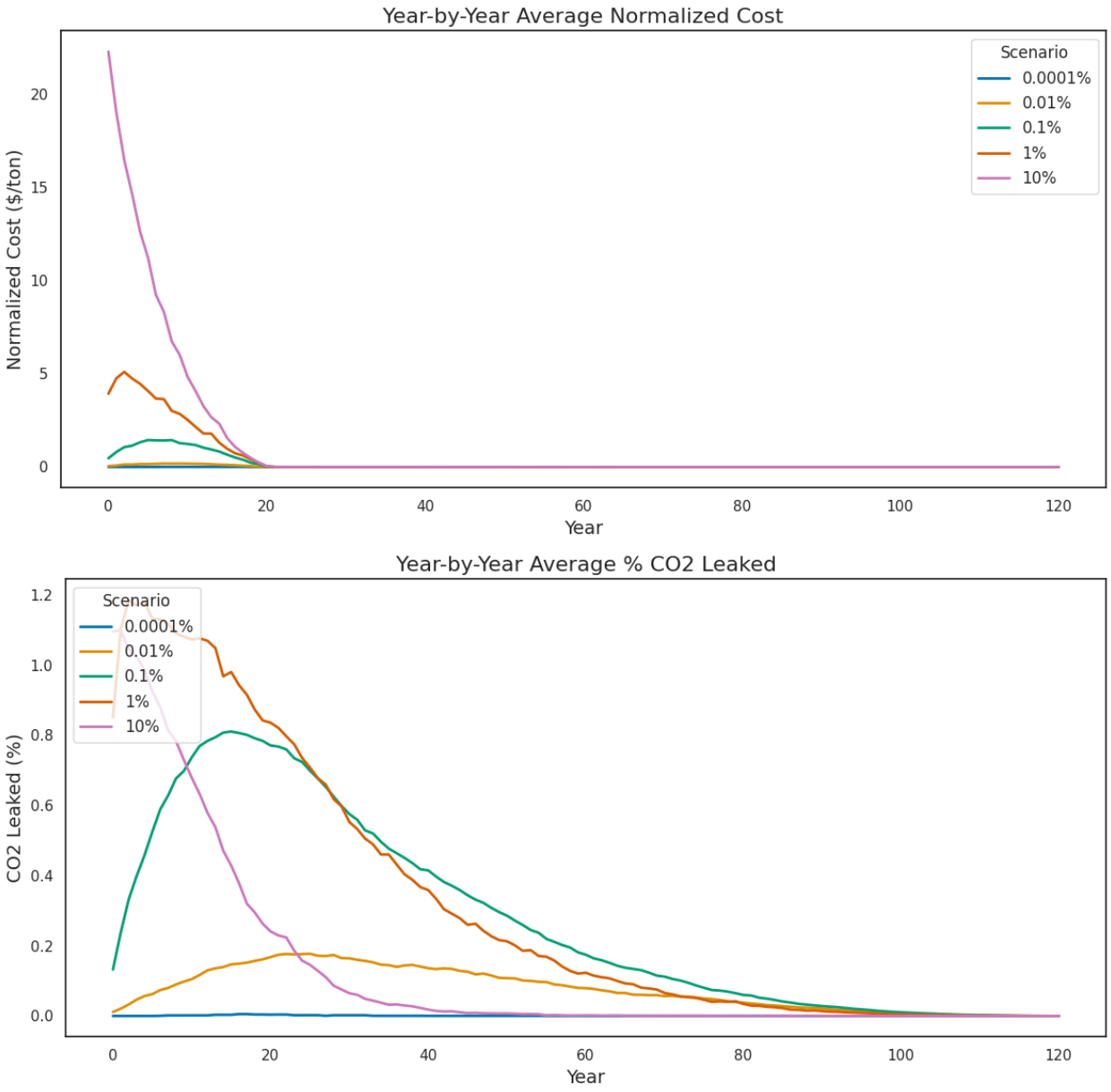

Figure A8. Year-by-Year Average Normalized Cost and % of CO_2 Leaked under Static Failure Probability Scenario. In this case, the annual probability of failure remains constant throughout the project, as it is not updated based on non-leakage observations (i.e., Bayesian updating is not applied). Wells that fail are permanently repaired within each simulation iteration following their failure.

A.7. Detection and Remediation Adjustment – Python Code

This Python code estimates the environmental and financial consequences of CO_2 and brine leakage from a geologic storage site. It simulates leakage detection and remediation using probabilistic inputs and provides cost distributions per ton of injected CO_2.

This script models leakage from one storage scenario (single CSV file) by:

- Reading gas and water rate outputs from reservoir simulations (e.g., CMG).
- Simulating detection and repair delays.
- Calculating leakage volumes and associated financial penalties.
- Running 1,000 Monte Carlo iterations with uncertainty in detection thresholds, remediation delays, and cost parameters.

The script produces:

- CDF of normalized cost with vertical lines at P10, P50, and P90.
- CDF of final % CO_2 leaked with the same statistical markers.
- Printed summary statistics for decision-making or thesis discussion.

```
import pandas as pd
import numpy as np
import matplotlib.pyplot as plt
import seaborn as sns
from scipy.interpolate import interp1d
import math
import random

# ============================
# USER SETTINGS
# ============================
#Insert your simulation results file name or file path
filename = insert here

n_iter = 1000
TOTAL_INJECTED_TONS = 4e6
PROJECT_DURATION_DAYS = 120 * 365.0
```

```
# Triangular detection threshold (tons/day)
th_left, th_mode, th_right = 0.55, 10, 30

# Normal fix time distribution (days), truncated≥0
fix_mean, fix_std = 433, 154

# FOAK penalty distribution: uniform(5..20) $/ton (base year=2014)
FOAK_min, FOAK_max = 5.0, 20.0

# Economic & discount parameters
inflation_annual = 0.029
discount_annual  = 0.029
carbon_price_2025 = 85.0       # $/ton, base year=2025
remediation_2010  = 56100.0    # lumpsum $/well, base year=2010
base_year = 2025

# Injection rate => 0.2 Mt/yr => ~200,000 t/yr => ~547.945 t/day
injection_tpd = 200000.0 / 365.0

# CO₂ conversion ft³/day => tons/day
co2_ft3_to_tons   = 5.61e-5
# Water conversion bbl/day => tons/day, ~0.159 if density=1
brine_bbl_to_tons = 0.159

# Water cost is lognormal:
# we want "annual capital cost" and "annual operating cost" each with known p25, p50, p75 =>
base=1999
# We'll sum them to get $/(1000 gallons). Then lumpsum at fix time for total water 0..fix_time
# Using 1 ton water ~264.4 gallons => we can scale from $/(1000 gal) to $/ton.

# We'll define function to solve mu,sigma for lognormal from p25, median, p75
z25, z75 = -0.67449, 0.67449
def solve_lognormal_params(p25, median, p75):
    """
    Returns (mu, sigma) for lognormal s.t.
    - p25 => x_25 => log(x_25) = mu + sigma*z25
    - p50 => median => exp(mu)= median
    - p75 => x_75 => log(x_75) = mu + sigma*z75
    """
    mu  = math.log(median)
    ln25= math.log(p25)
    ln75= math.log(p75)
    sigma = (ln75 - ln25)/(z75 - z25)
    return mu, sigma

# Suppose for the "unit annual capital cost" => p25=23, median=78, p75=350 => base=1999
```

```
capex_p25, capex_med, capex_p75 = 23.0, 78.0, 350.0
capex_mu, capex_sigma = solve_lognormal_params(capex_p25, capex_med, capex_p75)

# Suppose for the "unit annual operating cost" => p25=5, median=16, p75=41 => base=1999
opex_p25, opex_med, opex_p75 = 5.0, 16.0, 41.0
opex_mu,  opex_sigma  = solve_lognormal_params(opex_p25, opex_med, opex_p75)

def sample_detection_threshold():
    """One threshold for entire iteration."""
    return np.random.triangular(th_left, th_mode, th_right)

def sample_fix_time():
    """One fix-delay for entire iteration."""
    val = np.random.normal(fix_mean, fix_std)
    return max(val, 0.0)

def sample_foak():
    """One FOAK penalty (base 2014) for entire iteration, uniform(5..20)."""
    return random.uniform(FOAK_min, FOAK_max)

def discount_factor(fix_yr):
    """Discount lumpsum from fix_yr => base_year(2025)."""
    return 1/((1+discount_annual)**(fix_yr- base_year))

def sample_water_costs_lognormal():
    """
    For each well, we draw a LN for capital, LN for operating => sum => $/(1000 gal) base=1999
    We'll do it inside the loop for each well.
    """
    ln_c = random.gauss(capex_mu, capex_sigma)
    ln_o = random.gauss(opex_mu, opex_sigma)
    return math.exp(ln_c) + math.exp(ln_o)  # base=1999 => $/(1000gal)

# ============================
# 1) READ & BUILD
# ============================
df = pd.read_csv(filename)
df["Time (day)"] = pd.to_numeric(df["Time (day)"], errors="coerce")
df.sort_values("Time (day)", inplace=True)

time_days = df["Time (day)"].to_numpy()
dt_array  = np.diff(time_days, prepend=time_days[0])

# Gas columns
gas_cols = [c for c in df.columns if ("Gas Rate" in c) and ("ft3/day" in c) and ("Water" not in c)]
# Water columns
```

```
water_cols = [c for c in df.columns if ("Water Rate" in c) and ("bbl/day" in c)]

wells_data= {}

# Build gas interpolation
for gcol in gas_cols:
    wname = gcol.split("-Gas")[0].strip()
    rate_ft3 = df[gcol].fillna(0.0).values
    gas_rate_tpd = rate_ft3* co2_ft3_to_tons
    incr_g= gas_rate_tpd* dt_array
    cum_g= np.cumsum(incr_g)
    f_gas= interp1d(time_days, cum_g, bounds_error=False, fill_value=(cum_g[0], cum_g[-1]))
    wells_data[wname] = {
        "gas_rate_tpd": gas_rate_tpd,
        "gas_interp":   f_gas
    }

# Build water interpolation
for wcol in water_cols:
    wname= wcol.split("-Water")[0].strip()
    if wname not in wells_data:
        wells_data[wname] = {}
    wrate_bbl= df[wcol].fillna(0.0).values
    wrate_tpd= wrate_bbl* brine_bbl_to_tons
    incr_w= wrate_tpd* dt_array
    cum_w= np.cumsum(incr_w)
    f_w= interp1d(time_days, cum_w, bounds_error=False, fill_value=(cum_w[0], cum_w[-1]))
    wells_data[wname]["water_rate_tpd"]= wrate_tpd
    wells_data[wname]["water_interp"]  = f_w

# If a well missing water => zero
for wnm in wells_data:
    if "water_rate_tpd" not in wells_data[wnm]:
        z= np.zeros_like(time_days)
        wells_data[wnm]["water_rate_tpd"]= z
        fz= interp1d(time_days, z, bounds_error=False, fill_value=(0,0))
        wells_data[wnm]["water_interp"]= fz

def sum_rate_tpd(wdict):
    #return wdict["gas_rate_tpd"] + wdict["water_rate_tpd"]
    return wdict["gas_rate_tpd"] + wdict["water_rate_tpd"]

def detection_time(wdict, threshold):
    sr = sum_rate_tpd(wdict)
    idx= np.where(sr >= threshold)[0]
    if len(idx)>0:
```

```
        return time_days[idx[0]]
    return None

def leaked_co2_tons(wdict, day):
    return float(wdict["gas_interp"](min(day, PROJECT_DURATION_DAYS)))

def leaked_water_tons(wdict, day):
    return float(wdict["water_interp"](min(day, PROJECT_DURATION_DAYS)))

def lumpsum_co2_cost(co2_leaked, fix_yr, foak_base):
    """
    co2_leaked => 0..fix_time
    lumpsum => co2_leaked*(foak_base + carbon) + remediation => all inflated => discount
    foak_base => random from [5..20], base year=2014
    carbon => 85 $/ton base 2025
    remediation => 56100 base 2010
    """
    # inflation
    foak_infl = (1+inflation_annual)**(fix_yr- 2014)
    carb_infl = (1+inflation_annual)**(fix_yr- 2025)
    rem_infl  = (1+inflation_annual)**(fix_yr- 2010)

    cost_infl= co2_leaked*(carbon_price_2025* carb_infl) + remediation_2010* rem_infl
    dfac= discount_factor(fix_yr)
    return cost_infl* dfac

def lumpsum_water_cost(water_leaked, fix_yr, unit_annual_1000gal):
    """
    water_leaked => tons => convert to gallons => thousands => multiply unit_annual_1000gal(
base=1999).
    Then inflate => discount.
    """
    gallons= water_leaked* 264.4
    thou_gal= gallons/1000.0
    cost_1999= thou_gal* unit_annual_1000gal
    inf_fac= (1+inflation_annual)**(fix_yr- 1999)
    cost_infl= cost_1999* inf_fac
    dfac= discount_factor(fix_yr)
    return cost_infl* dfac

def lumpsum_foak_penalty(d_time, fix_time, foak_base):
    """
    FOAK_base => random draw in [5..20], base=2014
    mass not injected from detection-> fix_time up to year20
    inflate => discount
    """
```

```
    d_yr= d_time/365.0
    f_yr= fix_time/365.0
    if d_yr>=20:
        return 0.0
    no_inject_yr= max(0, min(f_yr,20.0)- d_yr)
    no_inject_days= no_inject_yr*365.0
    mass_not_injected= no_inject_days* injection_tpd

    fix_year= base_year+ f_yr
    foak_infl= (1+inflation_annual)**(fix_year- 2014)
    cost_2014= mass_not_injected* foak_base
    cost_infl= cost_2014* foak_infl
    disc_fac= 1/((1+discount_annual)**(fix_year- base_year))
    return cost_infl* disc_fac

# ============================
# 2) MONTE CARLO
# ============================
norm_costs= []
perc_leaked= []

for _ in range(n_iter):
    # One detection threshold, fix_delay, FOAK penalty for entire iteration
    iteration_threshold= sample_detection_threshold()
    iteration_fix_delay= sample_fix_time()
    iteration_foak_base= sample_foak()  # uniform(5..20)

    total_cost= 0.0
    total_co2_leaked= 0.0

    # Now we process each well
    for wnm, wdat in wells_data.items():
        # For each well, we sample lognormal for water cost
        # => unit_annual_1000gal in base=1999 => capital+operating
        ln_cap = random.gauss(capex_mu, capex_sigma)
        ln_ope = random.gauss(opex_mu, opex_sigma)
        water_unit_1999= math.exp(ln_cap) + math.exp(ln_ope)  # $/(1000 gallons) base=1999

        d_time= detection_time(wdat, iteration_threshold)
        if d_time is None:
            # never detect => leak 0..120 => no lumpsum
            co2_120= leaked_co2_tons(wdat, PROJECT_DURATION_DAYS)
            total_co2_leaked+= co2_120
        else:
            fix_time= d_time+ iteration_fix_delay
            if fix_time> PROJECT_DURATION_DAYS:
```

```
            # not fixed => leak 0..120 => no lumpsum
            co2_120= leaked_co2_tons(wdat, PROJECT_DURATION_DAYS)
            total_co2_leaked+= co2_120
        else:
            # lumpsum => co2+ water => 0..fix_time
            co2_leak= leaked_co2_tons(wdat, fix_time)
            water_leak= leaked_water_tons(wdat, fix_time)
            total_co2_leaked+= co2_leak

            fix_yr= base_year+ (fix_time/365.0)
            cost_co2= lumpsum_co2_cost(co2_leak, fix_yr, iteration_foak_base)
            cost_h2o= lumpsum_water_cost(water_leak, fix_yr, water_unit_1999)
            cost_foak= lumpsum_foak_penalty(d_time, fix_time, iteration_foak_base)

            total_cost+= (cost_co2+ cost_h2o+ cost_foak)

    norm_c= total_cost/ TOTAL_INJECTED_TONS
    perc_l= (total_co2_leaked/ TOTAL_INJECTED_TONS)*100.0
    norm_costs.append(norm_c)
    perc_leaked.append(perc_l)

norm_costs= np.array(norm_costs)
perc_leaked= np.array(perc_leaked)

def stats_dict(arr):
    return {
        "p10":  np.percentile(arr,10),
        "p50":  np.percentile(arr,50),
        "p90":  np.percentile(arr,90),
        "mean": np.mean(arr)
    }

cstats= stats_dict(norm_costs)
pstats= stats_dict(perc_leaked)
print("Normalized Cost Stats ($/ton):", cstats)
print("Final % CO₂ Leaked Stats:", pstats)

# plotting
sns.set_theme(style="white", palette="colorblind")
plt.rcParams["font.family"]= "Arial"
plt.rcParams["font.size"]  = 12

fig, (ax1,ax2)= plt.subplots(1,2, figsize=(10,4))

# cost cdf
sorted_c= np.sort(norm_costs)
```

```
cdf_c= np.arange(1,len(sorted_c)+1)/len(sorted_c)
ax1.step(sorted_c, cdf_c, where="post", label="Norm Cost")
ax1.set_xlabel("Normalized Cost ($/ton)")
ax1.set_ylabel("Cumulative Probability")
ax1.set_title("CDF of Normalized Cost")
ax1.axvline(cstats["p10"], color="r", ls="--", label=f"p10={cstats['p10']:.2f}")
ax1.axvline(cstats["p50"], color="g", ls="--", label=f"p50={cstats['p50']:.2f}")
ax1.axvline(cstats["p90"], color="orange", ls="--", label=f"p90={cstats['p90']:.2f}")
ax1.legend()

# final % leaked cdf
sorted_p= np.sort(perc_leaked)
cdf_p= np.arange(1,len(sorted_p)+1)/len(sorted_p)
ax2.step(sorted_p, cdf_p, where="post", color="g", label="Final % Leaked")
ax2.set_xlabel("Final % of CO2 Leaked (%)")
ax2.set_ylabel("Cumulative Probability")
ax2.set_title("CDF of Final % Leaked")
ax2.axvline(pstats["p10"], color="r", ls="--", label=f"p10={pstats['p10']:.2f}")
ax2.axvline(pstats["p50"], color="g", ls="--", label=f"p50={pstats['p50']:.2f}")
ax2.axvline(pstats["p90"], color="orange", ls="--", label=f"p90={pstats['p90']:.2f}")
ax2.legend()

plt.tight_layout()
plt.show()
```

A.8. ANNUAL PROBABILITIES OF WELL FAILURE ADJUSTMENT – PYTHON CODE

This code estimates the financial and environmental impacts of CO_2 and brine leakage from geologic carbon storage (GCS) sites. It uses leakage rates derived from dynamic multiphase simulations and calculates associated costs using a probabilistic Monte Carlo approach. The model assumes open wellbores as leakage pathways and evaluates the influence of failure probabilities, detection thresholds, fix times, and cost factors.

The script performs the following tasks:

- Reads leakage rate data from a CMG simulation CSV file.
- Computes CO_2 and brine leakage volumes over time for each leaky well.
- Simulates detection and remediation events.
- Calculates associated costs using economic assumptions and leakage impact valuation.

- Repeats this process under various annual well failure probabilities using Monte Carlo simulation.

The code generates:

- Box plots of:
    - Normalized remediation cost per ton of injected CO_2.
    - Final percentage of CO_2 leaked.
- Cumulative Distribution Functions (CDFs) of cost and leakage across scenarios.
- A summary table with p10, mean, and p90 statistics of costs and leakage for each probability scenario.

```
import pandas as pd
import numpy as np
import matplotlib.pyplot as plt
import seaborn as sns
from scipy.interpolate import interp1d
import random
import math

# ========================================
# USER SETTINGS
# ========================================
#Insert file path
filename = insert file path

n_iter = 1000  # Monte Carlo iterations per probability

# Single failure probability scenario
p_values = [1e-6, 1e-4, 1e-3, 0.01, 0.1]
p_labels = ["0.0001%", "0.01%", "0.1%", "1%", "10%"]

TOTAL_INJECTED_TONS = 4e6
PROJECT_DURATION_DAYS = 120 * 365.0
PROJECT_YEARS = 120
PROJECT_DAYS  = PROJECT_YEARS * 365

# Detection threshold: Triangular distribution (tons/day)
th_left, th_mode, th_right = 0.55, 10, 30
```

```
# Fix time: Normal distribution (days), truncated≥0
fix_mean, fix_std = 433, 154

# STP conversion for CO₂: 1 ft³/day => ~5.61e-5 tons/day
ft3_to_tons = 5.61e-5

# Economic & discount parameters
inflation = 0.029
discount = 0.029
FOAK_penalty_base = 20    # $/ton, base year=2014
carbon_price_base = 85    # $/ton, base year=2025
remediation_base = 56100  # $/well, base year=2010
base_year = 2025

# Water conversion
gallons_per_ton = 264.4    # 1 ton water ~264.4 gallons

# --------------------------------
# Water Lognormal Distribution (base 1999)
# --------------------------------
def solve_lognormal_params(p25, median, p75):
    z25, z75 = -0.67449, 0.67449
    mu = math.log(median)
    sigma = (math.log(p75) - math.log(p25)) / (z75 - z25)
    return mu, sigma

capex_mu, capex_sigma = solve_lognormal_params(23.0, 78.0, 350.0)
opex_mu, opex_sigma   = solve_lognormal_params(5.0, 16.0, 41.0)

def sample_water_unit_cost():
    """Sample water treatment unit cost in $/(1000 gallons), base=1999."""
    ln_cap = random.gauss(capex_mu, capex_sigma)
    ln_ope = random.gauss(opex_mu, opex_sigma)
    return math.exp(ln_cap) + math.exp(ln_ope)

# FOAK penalty: Uniform distribution from $5 to $20 (base=2014)
FOAK_min, FOAK_max = 5.0, 20.0

def sample_foak():
    return random.uniform(FOAK_min, FOAK_max)

# ----------------------------
# Cost Calculation Helpers
# ----------------------------
def discount_factor(fix_yr):
```

```
    return 1 / ((1 + discount) ** (fix_yr - base_year))

def lumpsum_co2_cost(co2_leaked, fix_yr, foak_val):
    """
    In this code snippet, we ignore the FOAK_val per-ton cost for CO2,
    and only inflate the carbon_price_base + remediation for demonstration.
    """
    foak_infl = (1 + inflation) ** (fix_yr - 2014)
    carb_infl = (1 + inflation) ** (fix_yr - 2025)
    rem_infl  = (1 + inflation) ** (fix_yr - 2010)
    cost_infl = co2_leaked * (carbon_price_base * carb_infl) + remediation_base * rem_infl
    return cost_infl * discount_factor(fix_yr)

def lumpsum_water_cost(water_leaked, fix_yr, water_unit_1999):
    gallons = water_leaked * gallons_per_ton
    thou_gal = gallons / 1000.0
    cost_1999 = thou_gal * water_unit_1999
    inf_fac = (1 + inflation) ** (fix_yr - 1999)
    return cost_1999 * inf_fac * discount_factor(fix_yr)

def lumpsum_foak_penalty(d_time, fix_time, foak_val):
    d_yr = d_time / 365.0
    f_yr = fix_time / 365.0
    if d_yr >= 20:
        return 0.0
    no_inject_yr = max(0.0, min(f_yr, 20.0) - d_yr)
    no_inject_days = no_inject_yr * 365.0
    mass_not_injected = no_inject_days * (200000.0 / 365.0)  # injection_tpd
    fix_year = base_year + f_yr
    foak_infl = (1 + inflation) ** (fix_year - 2014)
    cost_2014 = mass_not_injected * foak_val
    return cost_2014 * foak_infl * discount_factor(fix_year)

# ----------------------------
# Data Reading & Interpolation
# ----------------------------
df = pd.read_csv(filename)
df["Time (day)"] = pd.to_numeric(df["Time (day)"], errors="coerce")
df.sort_values("Time (day)", inplace=True)

time_days = df["Time (day)"].values
dt_array  = np.diff(time_days, prepend=time_days[0])

gas_cols = [c for c in df.columns if "Gas Rate" in c and "ft3/day" in c and "Water" not in c]
water_cols = [c for c in df.columns if "Water Rate" in c and "bbl/day" in c]
```

```
well_data = {}

# Build gas interpolation
for col in gas_cols:
    well_name = col.split("-Gas")[0].strip()
    rate_ft3 = df[col].fillna(0.0).values
    gas_rate_tpd = rate_ft3 * ft3_to_tons
    incr_tons = gas_rate_tpd * dt_array
    cum_tons = np.cumsum(incr_tons)
    f_interp = interp1d(time_days, cum_tons, bounds_error=False,
                        fill_value=(cum_tons[0], cum_tons[-1]))
    well_data[well_name] = {
        "gas_rate_tpd": gas_rate_tpd,
        "cum_interp":   f_interp
    }

# Build water interpolation
for col in water_cols:
    well_name = col.split("-Water")[0].strip()
    if well_name not in well_data:
        well_data[well_name] = {}
    rate_bbl = df[col].fillna(0.0).values
    water_rate_tpd = rate_bbl * 0.159
    incr_tons = water_rate_tpd * dt_array
    cum_tons = np.cumsum(incr_tons)
    f_interp = interp1d(time_days, cum_tons, bounds_error=False,
                        fill_value=(cum_tons[0], cum_tons[-1]))
    well_data[well_name]["water_rate_tpd"] = water_rate_tpd
    well_data[well_name]["water_interp"] = f_interp

# If missing water data => assign zero
for wnm in well_data:
    if "water_rate_tpd" not in well_data[wnm]:
        zarr = np.zeros_like(time_days)
        well_data[wnm]["water_rate_tpd"] = zarr
        fz = interp1d(time_days, zarr, bounds_error=False, fill_value=(0, 0))
        well_data[wnm]["water_interp"] = fz

def sum_rate_tpd(wdict):
    gas = wdict["gas_rate_tpd"]
    water = wdict.get("water_rate_tpd", 0.0)
    return gas + water

def detection_time_instantaneous(wdict, threshold, failure_time):
    sr = sum_rate_tpd(wdict)
    mask = time_days >= failure_time
```

```
    sr_after = sr[mask]
    time_after = time_days[mask]
    idx = np.where(sr_after >= threshold)[0]
    if len(idx) > 0:
        return time_after[idx[0]]
    return None

def leaked_co2_tons(wdict, day):
    return float(wdict["cum_interp"](min(day, PROJECT_DURATION_DAYS)))

# ----------------------------
# Main Simulation Function
# ----------------------------
def run_one_iteration(p_fail):
    iteration_threshold = np.random.triangular(th_left, th_mode, th_right)
    iteration_fix_delay = max(np.random.normal(fix_mean, fix_std), 0.0)
    iteration_foak_base = sample_foak()

    total_cost = 0.0
    total_leaked = 0.0

    for wname, wdat in well_data.items():
        # Year-by-year failure check
        failure_year = None
        for y in range(int(PROJECT_DAYS/365.0)):
            if random.random() <= p_fail:
                failure_year = y
                break

        if failure_year is None:
            continue

        failure_time = failure_year * 365.0
        d_time = detection_time_instantaneous(wdat, iteration_threshold, failure_time)
        if d_time is None:
            # Not detected => leak from failure_time to end
            total_leaked += (leaked_co2_tons(wdat, PROJECT_DURATION_DAYS)
                             - leaked_co2_tons(wdat, failure_time))
            continue

        f_time = d_time + iteration_fix_delay
        if f_time > PROJECT_DURATION_DAYS:
            # Not fixed => leak from failure_time to end
            total_leaked += (leaked_co2_tons(wdat, PROJECT_DURATION_DAYS)
                             - leaked_co2_tons(wdat, failure_time))
            continue
```

```
        # If fixed at f_time
        co2_leak = leaked_co2_tons(wdat, f_time) - leaked_co2_tons(wdat, failure_time)
        water_leak = (float(wdat["water_interp"](min(f_time, PROJECT_DURATION_DAYS)))
                      - float(wdat["water_interp"](failure_time)))
        total_leaked += co2_leak

        fix_yr = base_year + (f_time / 365.0)
        water_unit_1999 = sample_water_unit_cost()

        cost_co2 = lumpsum_co2_cost(co2_leak, fix_yr, iteration_foak_base)
        cost_h2o = lumpsum_water_cost(water_leak, fix_yr, water_unit_1999)
        cost_foak = lumpsum_foak_penalty(d_time, f_time, iteration_foak_base)

        total_cost += (cost_co2 + cost_h2o + cost_foak)

    norm_cost = total_cost / TOTAL_INJECTED_TONS
    perc_leaked = (total_leaked / TOTAL_INJECTED_TONS) * 100.0
    return norm_cost, perc_leaked

def run_monte_carlo(p_fail, n_iter=1000):
    cost_arr = []
    perc_arr = []
    for _ in range(n_iter):
        c, p = run_one_iteration(p_fail)
        cost_arr.append(c)
        perc_arr.append(p)
    return np.array(cost_arr), np.array(perc_arr)

# ----------------------------
# Run for Each Probability & Collect Results
# ----------------------------
scenario_results = {}
for pval, label in zip(p_values, p_labels):
    cost_vals, perc_vals = run_monte_carlo(pval, n_iter)
    scenario_results[label] = (cost_vals, perc_vals)

# ----------------------------
# Create DataFrames for Box Plots
# ----------------------------
box_data_cost = []
box_data_perc = []
for label in scenario_results:
    cost_arr = scenario_results[label][0]
    perc_arr = scenario_results[label][1]
    for cval in cost_arr:
```

```
        box_data_cost.append({"Scenario": label, "Normalized Cost": cval})
    for pval in perc_arr:
        box_data_perc.append({"Scenario": label, "Final % Leaked": pval})

df_cost = pd.DataFrame(box_data_cost)
df_perc = pd.DataFrame(box_data_perc)

# ----------------------------
# Box Plots
# ----------------------------
sns.set_theme(style="white", palette="colorblind")
plt.rcParams["font.family"] = "Arial"
plt.rcParams["font.size"] = 12

fig, axes = plt.subplots(1, 2, figsize=(10,4))
sns.boxplot(x="Scenario", y="Normalized Cost", data=df_cost, ax=axes[0])
axes[0].set_title("Box Plot of Normalized Cost by Scenario")
axes[0].tick_params(axis='x', rotation=45)
axes[0].set_ylim([0,100])

sns.boxplot(x="Scenario", y="Final % Leaked", data=df_perc, ax=axes[1])
axes[1].set_title("Box Plot of Final % Leaked by Scenario")
axes[1].tick_params(axis='x', rotation=45)

plt.tight_layout()
plt.show()

# ----------------------------
# Overlaid CDF Plots
# ----------------------------
fig2, (ax1, ax2) = plt.subplots(1, 2, figsize=(10,4))

# CDF of Normalized Cost
for label in scenario_results:
    sorted_vals = np.sort(scenario_results[label][0])
    cdf = np.arange(1, len(sorted_vals)+1) / len(sorted_vals)
    ax1.step(sorted_vals, cdf, where="post", label=label)
ax1.set_title("CDF of Normalized Cost ($/ton injected)")
ax1.set_xlabel("Normalized Cost ($/ton)")
ax1.set_ylabel("Cumulative Probability")
ax1.legend()

# CDF of Final % Leaked
for label in scenario_results:
    sorted_vals = np.sort(scenario_results[label][1])
    cdf = np.arange(1, len(sorted_vals)+1) / len(sorted_vals)
```

```
    ax2.step(sorted_vals, cdf, where="post", label=label)
ax2.set_title("CDF of Final % Leaked")
ax2.set_xlabel("Final % Leaked (%)")
ax2.set_ylabel("Cumulative Probability")
ax2.legend()

plt.tight_layout()
plt.show()

# ----------------------------
# Generate Table of Statistics (p10, mean, p90) for Each Scenario
# ----------------------------
stats_dict = {}
def compute_p10_mean_p90(arr):
    return np.percentile(arr, 10), np.mean(arr), np.percentile(arr, 90)

print("\n===== Summary Table: Normalized Cost and % Leaked (p10, mean, p90) =====\n")
print(f"{'Scenario':<12}{'Cost_p10':>12}{'Cost_mean':>12}{'Cost_p90':>12}"
      f"{'Leak_p10':>12}{'Leak_mean':>12}{'Leak_p90':>12}")

for label in scenario_results:
    cost_arr = scenario_results[label][0]
    perc_arr = scenario_results[label][1]
    cost_p10, cost_mean, cost_p90 = compute_p10_mean_p90(cost_arr)
    leak_p10, leak_mean, leak_p90 = compute_p10_mean_p90(perc_arr)
    print(f"{label:<12}"
          f"{cost_p10:12.3f}{cost_mean:12.3f}{cost_p90:12.3f}"
          f"{leak_p10:12.3f}{leak_mean:12.3f}{leak_p90:12.3f}")
```

A.9. BAYESIAN UPDATING ADJUSTMENT – PYTHON CODE

This Python script simulates the evolution of CO_2 leakage risk, detection, and financial impact over a 120-year geologic carbon storage (GCS) project using Bayesian updating. It supports multiple well failure probability scenarios and tracks year-by-year risk and costs via a parallelized Monte Carlo simulation.

This script is designed to:

- Simulate well failures under different prior failure probability distributions.

- Implement Bayesian learning to update leakage risk based on whether leakage is observed.
- Quantify annual CO_2 leakage and associated financial costs using stochastic modeling.
- Output year-by-year trends in leakage, normalized cost, and failure probabilities for policy and risk assessment.

This script outputs:

- Three line plots:
  - Normalized Cost vs Year
  - % CO_2 Leaked vs Year
  - Failure Probability vs Year
- All plots differentiate the scenarios using distinct colorblind-friendly color schemes.
- Console output shows progress of iterations and number of wells processed.

```
import math
import random
import numpy as np
import pandas as pd
import matplotlib.pyplot as plt
import seaborn as sns
from scipy.interpolate import interp1d
import concurrent.futures

# ============================================
# USER SETTINGS
# ============================================
#Insert simulation results file name or file path
filename = insert here

n_iter = 1000          # Monte Carlo iterations per scenario
```

```
PROJECT_YEARS = 120      # Project duration in years
PROJECT_DAYS  = PROJECT_YEARS * 365
TOTAL_INJECTED_TONS = 4e6

# Scenarios: Each tuple is (label, alpha0, beta0)
scenarios = [
    ("0.0001%", 0.0001, 99.9999),
    ("0.01%",   0.01, 99.99),
    ("0.1%",    0.1, 99.9),
    ("1%",      1, 99),
    ("10%",     10, 90)
 ]

# Distributions for detection threshold, fix time, FOAK penalty (iteration-level)
th_left, th_mode, th_right = 0.55, 10, 30   # Triangular detection threshold (tons/day)
fix_mean, fix_std = 433, 154                # Normal fix time (days)
FOAK_min, FOAK_max = 5.0, 20.0              # Uniform FOAK penalty (base year=2014)

# Economic & discount parameters
inflation_annual  = 0.029
discount_annual   = 0.029
carbon_price_2025 = 85.0
remediation_2010  = 56100.0
base_year         = 2025

# Injection rate (~200,000 t/yr => ~548 t/day)
injection_tpd = 200000.0 / 365.0

# Conversions
co2_ft3_to_tons   = 5.61e-5
brine_bbl_to_tons = 0.159
gallons_per_ton   = 264.4

# Lognormal water cost parameters (base=1999)
def solve_lognormal_params(p25, median, p75):
   z25, z75 = -0.67449, 0.67449
   mu = math.log(median)
   sigma = (math.log(p75) - math.log(p25)) / (z75 - z25)
   return mu, sigma

capex_mu, capex_sigma = solve_lognormal_params(23.0, 78.0, 350.0)
opex_mu, opex_sigma   = solve_lognormal_params(5.0, 16.0, 41.0)

# ============================================
# 1) READ & BUILD WELL DATA (CUMULATIVE ARRAYS)
# ============================================
```

```
def build_well_data(csv_file):
    print("Loading well data from file...")
    df = pd.read_csv(csv_file)
    df["Time (day)"] = pd.to_numeric(df["Time (day)"], errors="coerce")
    df.sort_values("Time (day)", inplace=True)
    time_arr = df["Time (day)"].values
    dt_array  = np.diff(time_arr, prepend=time_arr[0])
    gas_cols   = [c for c in df.columns if ("Gas Rate" in c) and ("ft3/day" in c) and ("Water" not in
c)]
    water_cols = [c for c in df.columns if ("Water Rate" in c) and ("bbl/day" in c)]
    well_data = {}

    # For each well, store time array and cumulative gas and water (in tons)
    for col in gas_cols:
        wname = col.split("-Gas")[0].strip()
        rate_ft3 = df[col].fillna(0.0).values
        gas_rate_tpd = rate_ft3 * co2_ft3_to_tons
        gas_cum = np.cumsum(gas_rate_tpd * dt_array)
        well_data.setdefault(wname, {})["time_arr"] = time_arr
        well_data[wname]["gas_cum"] = gas_cum

    for col in water_cols:
        wname = col.split("-Water")[0].strip()
        rate_bbl = df[col].fillna(0.0).values
        water_rate_tpd = rate_bbl * brine_bbl_to_tons
        water_cum = np.cumsum(water_rate_tpd * dt_array)
        well_data.setdefault(wname, {})["time_arr"] = time_arr
        well_data[wname]["water_cum"] = water_cum

    # For wells without water data, fill with zero array.
    for w in well_data:
        if "water_cum" not in well_data[w]:
            well_data[w]["water_cum"] = np.zeros_like(time_arr)
    print("Well data loaded for", len(well_data), "wells.")
    return well_data

# ============================================
# 2) COST FUNCTIONS
# ============================================
def discount_factor(fix_yr):
    return 1.0 / ((1.0 + discount_annual) ** (fix_yr - base_year))

def lumpsum_co2_cost(co2_leaked, fix_yr, foak_val):
    foak_infl = (1 + inflation_annual) ** (fix_yr - 2014)
    carb_infl = (1 + inflation_annual) ** (fix_yr - 2025)
    rem_infl  = (1 + inflation_annual) ** (fix_yr - 2010)
```

```
    cost_infl = co2_leaked * (carbon_price_2025 * carb_infl) + remediation_2010 * rem_infl
    return cost_infl * discount_factor(fix_yr)

def lumpsum_water_cost(water_leaked, fix_yr, water_unit_1999):
    gallons  = water_leaked * gallons_per_ton
    thou_gal = gallons / 1000.0
    cost_1999 = thou_gal * water_unit_1999
    inf_fac = (1 + inflation_annual) ** (fix_yr - 1999)
    return cost_1999 * inf_fac * discount_factor(fix_yr)

def lumpsum_foak_penalty(d_time, fix_time, foak_val):
    d_yr = d_time / 365.0
    f_yr = fix_time / 365.0
    if d_yr >= 20:
        return 0.0
    no_inject_yr = max(0.0, min(f_yr, 20.0) - d_yr)
    no_inject_days = no_inject_yr * 365.0
    mass_not_injected = no_inject_days * injection_tpd
    fix_year = base_year + (f_yr)
    foak_infl = (1 + inflation_annual) ** (fix_year - 2014)
    cost_2014 = mass_not_injected * foak_val
    return cost_2014 * foak_infl * discount_factor(fix_year)

def sample_water_unit_cost():
    ln_cap = random.gauss(capex_mu, capex_sigma)
    ln_ope = random.gauss(opex_mu, opex_sigma)
    return math.exp(ln_cap) + math.exp(ln_ope)

# ==========================================
# 3) OPTIMIZED DETECTION/ FIX LOGIC
# ==========================================
def detection_time_after_fail_opt(wdat, threshold, fail_time):
    """
    Vectorized detection time using precomputed cumulative arrays.
    Computes instantaneous rates for gas and water (from the cumulative arrays)
    and returns the first time at which their sum exceeds the threshold.
    """
    time_arr = wdat["time_arr"]
    gas = wdat["gas_cum"]
    water = wdat["water_cum"]
    # Compute instantaneous rates for each interval:
    dt = np.diff(time_arr)
    # Avoid division by zero:
    dt[dt == 0] = 1.0
    gas_rate = np.diff(gas) / dt
    water_rate = np.diff(water) / dt
```

```
    rates = gas_rate + water_rate
    start_idx = np.searchsorted(time_arr, fail_time)
    if start_idx >= len(time_arr) - 1:
        return None
    condition = rates[start_idx:] >= threshold
    if np.any(condition):
        idx = start_idx + int(np.argmax(condition))
        return time_arr[idx]
    return None

# ==========================================
# 4) VECTORIZED COST & LEAK CALCULATION
# ==========================================
def compute_cost_leak_from_t_onward_vectorized(well_data, fail_year, t, iter_threshold,
iter_fix_delay, iter_foak_val, well_keys):
    total_cost = 0.0
    total_leak = 0.0
    day_t   = t * 365.0
    day_end = PROJECT_YEARS * 365.0
    for i, wname in enumerate(well_keys):
        fy = fail_year[i]
        if fy >= PROJECT_YEARS or fy < t:
            continue
        day_fail = fy * 365.0
        if day_fail > day_end:
            continue
        wdat = well_data[wname]
        # Vectorized detection:
        d_time = detection_time_after_fail_opt(wdat, iter_threshold, day_fail)
        if d_time is None or d_time > day_end:
            leak_co2 = np.interp(day_end, wdat["time_arr"], wdat["gas_cum"]) - np.interp(day_fail,
wdat["time_arr"], wdat["gas_cum"])
            total_leak += leak_co2
            continue
        fix_time = d_time + iter_fix_delay
        if fix_time > day_end:
            leak_co2 = np.interp(day_end, wdat["time_arr"], wdat["gas_cum"]) - np.interp(day_fail,
wdat["time_arr"], wdat["gas_cum"])
            total_leak += leak_co2
            continue
        co2_leak = np.interp(fix_time, wdat["time_arr"], wdat["gas_cum"]) - np.interp(day_fail,
wdat["time_arr"], wdat["gas_cum"])
        total_leak += co2_leak
        water_leak = np.interp(fix_time, wdat["time_arr"], wdat["water_cum"]) -
np.interp(day_fail, wdat["time_arr"], wdat["water_cum"])
        fix_yr = base_year + (fix_time / 365.0)
```

```
        cost_co2 = lumpsum_co2_cost(co2_leak, fix_yr, iter_foak_val)
        cost_h2o = lumpsum_water_cost(water_leak, fix_yr, sample_water_unit_cost())
        cost_foak = lumpsum_foak_penalty(day_fail, fix_time, iter_foak_val)
        total_cost += (cost_h2o + cost_co2 + cost_foak)
    return total_cost, total_leak

# ==========================================
# 5) VECTORIZED YEAR-BY-YEAR FAIL LOGIC WITH BETA UPDATE
# ==========================================
def run_one_iteration_new_logic_fast_opt(well_data, alpha_0, beta_0, well_keys):
    num_wells = len(well_keys)
    # Represent "no failure" as PROJECT_YEARS
    fail_year = np.full(num_wells, PROJECT_YEARS, dtype=float)
    cost_year = np.zeros(PROJECT_YEARS + 1)
    leak_year = np.zeros(PROJECT_YEARS + 1)
    prob_year = np.zeros(PROJECT_YEARS + 1)
    # Sample iteration-level parameters once:
    iter_threshold = random.triangular(th_left, th_mode, th_right)
    iter_fix_delay = max(random.gauss(fix_mean, fix_std), 0.0)
    iter_foak_val = random.uniform(FOAK_min, FOAK_max)
    alpha = alpha_0
    beta = beta_0
    p_f = alpha / (alpha + beta)
    alpha_lgivenf = 100
    beta_lgivenf = 0

    for t in range(PROJECT_YEARS):
        p_l = p_f * alpha_lgivenf / (alpha_lgivenf + beta_lgivenf)
        prob_year[t] = p_l

        # Candidate wells: fail_year is None OR fail_year >= t
        # meaning they haven't failed before year t
        candidates = []
        for widx in range(len(fail_year)):
            if fail_year[widx] is None or fail_year[widx] >= t:
                candidates.append(widx)

        fails_at_t = 0
        # Nested loop to assign a fail year in [t..PROJECT_YEARS)
        for widx in candidates:
            fail_assigned = False
            for yr in range(t, PROJECT_YEARS):
                if random.random() < p_l:
                    fail_year[widx] = yr
                    if yr == t:
                        fails_at_t += 1
```

```
                fail_assigned = True
                break

        # If fail_assigned remains False, the well's fail_year stays None
        # meaning it never fails within the project horizon.

    # Bayesian update: treat any well assigned fail_year == t
    # as a "predicted fail" that didn't truly occur, so we add that count to beta
    beta_lgivenf += fails_at_t

    c_t, l_t = compute_cost_leak_from_t_onward_vectorized(well_data, fail_year, t,
iter_threshold, iter_fix_delay, iter_foak_val, well_keys)
    cost_year[t] = c_t / TOTAL_INJECTED_TONS
    leak_year[t] = (l_t / TOTAL_INJECTED_TONS) * 100.0

  prob_year[PROJECT_YEARS] = p_l
  cost_year[PROJECT_YEARS] = 0.0
  leak_year[PROJECT_YEARS] = 0.0
  return cost_year, leak_year, prob_year, fail_year

# ==========================================
# 6) PARALLELIZED MONTE CARLO WRAPPER FOR MULTIPLE SCENARIOS
# ==========================================
def run_monte_carlo_new_logic_fast_opt(well_data, n_iter, alpha0, beta0):
  well_keys = list(well_data.keys())
  cost_arrays = []
  leak_arrays = []
  prob_arrays = []

  # Use ProcessPoolExecutor for parallel Monte Carlo iterations.
  with concurrent.futures.ProcessPoolExecutor() as executor:
    futures = [executor.submit(run_one_iteration_new_logic_fast_opt, well_data, alpha0, beta0,
well_keys)
           for _ in range(n_iter)]
    for i, fut in enumerate(concurrent.futures.as_completed(futures)):
      if i % 10 == 0:
        print(f"Completed Monte Carlo iteration {i+1}/{n_iter}")
      costY, leakY, probY, _ = fut.result()
      cost_arrays.append(costY)
      leak_arrays.append(leakY)
      prob_arrays.append(probY)

  mean_cost = np.mean(cost_arrays, axis=0)
  mean_leak = np.mean(leak_arrays, axis=0)
  mean_prob = np.mean(prob_arrays, axis=0)
  return mean_cost, mean_leak, mean_prob
```

```
# ============================================
# 7) PLOTTING FUNCTION WITH IMPROVED STYLE
# ============================================
def plot_results(years, results_cost, results_leak, results_prob):
    sns.set(style="white")
    plt.rcParams.update({
        "figure.figsize": (12, 6),
        "figure.dpi": 100,
        "font.size": 14,
        "axes.titlesize": 16,
        "axes.labelsize": 14,
        "legend.fontsize": 12
    })

    palette = sns.color_palette("colorblind", n_colors=len(results_cost))

    # Plot Average Normalized Cost vs. Year
    plt.figure()
    for (label, cost), color in zip(results_cost.items(), palette):
        plt.plot(years, cost, label=label, color=color, linewidth=2)
    plt.xlabel("Year")
    plt.ylabel("Normalized Cost ($/ton)")
    plt.title("Year-by-Year Average Normalized Cost")
    plt.legend(title="Scenario", loc="upper right")
    plt.tight_layout()
    plt.show()

    # Plot Average % CO2 Leaked vs. Year
    plt.figure()
    for (label, leak), color in zip(results_leak.items(), palette):
        plt.plot(years, leak, label=label, color=color, linewidth=2)
    plt.xlabel("Year")
    plt.ylabel("CO2 Leaked (%)")
    plt.title("Year-by-Year Average % CO2 Leaked")
    plt.legend(title="Scenario", loc="upper left")
    plt.tight_layout()
    plt.show()

    # Plot Average Failure Probability p(t) vs. Year
    plt.figure()
    for (label, prob), color in zip(results_prob.items(), palette):
        plt.plot(years, prob, label=label, color=color, linewidth=2)
    plt.xlabel("Year")
    plt.ylabel("Failure Probability p(l)")
    plt.title("Year-by-Year Average Failure Probability")
```

```
    plt.legend(title="Scenario", loc="best")
    plt.tight_layout()
    plt.show()

# ==========================================
# 8) MAIN FUNCTION
# ==========================================
def main():
    print("Setting up simulation and plotting...")
    sns.set_theme(style="white", palette="colorblind")
    plt.rcParams["font.family"] = "Arial"
    plt.rcParams["font.size"] = 14

    well_data = build_well_data(filename)
    years = np.arange(PROJECT_YEARS + 1)
    results_cost = {}
    results_leak = {}
    results_prob = {}

    # Run simulation for each scenario
    for label, alpha0, beta0 in scenarios:
        print(f"\nRunning scenario {label} with initial alpha0={alpha0} and beta0={beta0}")

        mean_cost, mean_leak, mean_prob = run_monte_carlo_new_logic_fast_opt(well_data,
n_iter, alpha0, beta0)
        results_cost[label] = mean_cost
        results_leak[label] = mean_leak
        results_prob[label] = mean_prob

    plot_results(years, results_cost, results_leak, results_prob)

if __name__ == "__main__":
    main()
```

REFERENCES

Abdel Azim, R. (2016). Evaluation of water coning phenomenon in naturally fractured oil reservoirs. *Journal of Petroleum Exploration and Production Technology*, *6*(2), 279–291. https://doi.org/10.1007/s13202-015-0185-7

Adams, B., Fleming, M. R., Bielicki, J., Garapati, N., & Saar, M. O. (2021). *An Analysis of the Demonstration of a CO_2-based Thermosiphon at the SECARB Cranfield Site* [Application/pdf]. 9 p. https://doi.org/10.3929/ETHZ-B-000467171

Application of Red Trail Energy, LLC Requesting Consideration for the Geologic Storage of Carbon Dioxide in the Broom Creek Formation from the Red Trail, LLC Ethanol Facility (Industrial Commission of the State of North Dakota 2021). https://www.dmr.nd.gov/dmr/sites/www/files/documents/Oil%20and%20Gas/Class%20VI/Red%20Trail/C28848.pdf

Bahrami, H., Shadizadeh, S. R., & Goodarzniya, I. (2004). *Numerical Simulation of Coning Phenomena in Naturally Fractured Reservoirs*.

Baker, R. O., Yarranton, H. W., & Jensen, J. (2015). *Practical Reservoir Engineering and Characterization*. Elsevier Science.

Bielicki, J. M., Pollak, M. F., Deng, H., Wilson, E. J., Fitts, J. P., & Peters, C. A. (2016). The Leakage Risk Monetization Model for Geologic CO_2 Storage. *Environmental Science & Technology*, *50*(10), 4923–4931. https://doi.org/10.1021/acs.est.5b05329

Bielicki, J. M., Pollak, M. F., Fitts, J. P., Peters, C. A., & Wilson, E. J. (2014a). Causes and financial consequences of geologic CO2 storage reservoir leakage and interference with other subsurface resources. *International Journal of Greenhouse Gas Control*, *20*, 272–284. https://doi.org/10.1016/j.ijggc.2013.10.024

Bielicki, J. M., Pollak, M. F., Fitts, J. P., Peters, C. A., & Wilson, E. J. (2014b). Causes and financial consequences of geologic CO2 storage reservoir leakage and interference with other subsurface resources. *International Journal of Greenhouse Gas Control*, *20*, 272–284. https://doi.org/10.1016/j.ijggc.2013.10.024

Bielicki, J. M., Pollak, M. F., Wilson, E. J., Fitts, J. P., & Peters, C. A. (2013a). A Methodology for Monetizing Basin-Scale Leakage Risk and Stakeholder Impacts. *Energy Procedia*, *37*, 4665–4672. https://doi.org/10.1016/j.egypro.2013.06.375

Bielicki, J. M., Pollak, M. F., Wilson, E. J., Fitts, J. P., & Peters, C. A. (2013b). A Methodology for Monetizing Basin-Scale Leakage Risk and Stakeholder Impacts. *Energy Procedia*, *37*, 4665–4672. https://doi.org/10.1016/j.egypro.2013.06.375

Borazjani, S., Hemmati, N., Behr, A., Genolet, L., Mahani, H., Zeinijahromi, A., & Bedrikovetsky, P. (2021). Simultaneous determination of gas–water relative permeability and capillary pressure from steady-state corefloods. *Journal of Hydrology*, *598*, 126355. https://doi.org/10.1016/j.jhydrol.2021.126355

Bump, A. P., Hovorka, S. D., & Meckel, T. A. (2021). Common risk segment mapping: Streamlining exploration for carbon storage sites, with application to coastal Texas and Louisiana. *International Journal of Greenhouse Gas Control*, *111*, 103457. https://doi.org/10.1016/j.ijggc.2021.103457

Callas, C., Saltzer, S. D., Steve Davis, J., Hashemi, S. S., Kovscek, A. R., Okoroafor, E. R., Wen, G., Zoback, M. D., & Benson, S. M. (2022). Criteria and workflow for selecting depleted hydrocarbon reservoirs for carbon storage. *Applied Energy*, *324*, 119668. https://doi.org/10.1016/j.apenergy.2022.119668

CARB. (2018). *Carbon Capture and Sequestration Protocol under the Low Carbon Fuel Standard*. https://ww2.arb.ca.gov/sites/default/files/2020-03/CCS_Protocol_Under_LCFS_8-13-18_ada.pdf

Carroll, S. A., Keating, E., Mansoor, K., Dai, Z., Sun, Y., Trainor-Guitton, W., Brown, C., & Bacon, D. (2014). Key factors for determining groundwater impacts due to leakage from geologic carbon sequestration reservoirs. *International Journal of Greenhouse Gas Control*, *29*, 153–168. https://doi.org/10.1016/j.ijggc.2014.07.007

Celia, M. A., & Bachu, S. (2003). Geological Sequestration of CO2: Is Leakage Unavoidable and Acceptable? *International Conference on Greenhouse Gas Control Technologies Kyoto, Japan, 6th*. https://doi.org/10.1016/B978-008044276-1/50076-3

Celia, M. A., Nordbotten, J. M., Court, B., Dobossy, M., & Bachu, S. (2011). Field-scale application of a semi-analytical model for estimation of CO2 and brine leakage along old wells. *International Journal of Greenhouse Gas Control*, *5*(2), 257–269. https://doi.org/10.1016/j.ijggc.2010.10.005

Corey, A. T. (1954). The Interrelation between Gas and Oil Relative Permeabilities. *Prod. Month*, *19*, 38–41.

Damen, K., Faaij, A., & Turkenburg, W. (2006). Health, Safety and Environmental Risks of Underground Co2 Storage – Overview of Mechanisms and Current Knowledge. *Climatic Change*, *74*(1–3), 289–318. https://doi.org/10.1007/s10584-005-0425-9

Deel, D., & Mahajan, K. (n.d.). *Risk Assessment and Management for Long-Term Storage of CO2 in Geologic Formations—United States Department of Energy R&D*. *5*(1).

Deng, H., Bielicki, J. M., Oppenheimer, M., Fitts, J. P., & Peters, C. A. (2014). Policy implications of Monetized Leakage Risk from Geologic CO2 Storage Reservoirs. *Energy Procedia*, *63*, 6852–6863. https://doi.org/10.1016/j.egypro.2014.11.719

Esposito, A., & Benson, S. M. (2011). Remediation of possible leakage from geologic CO2 storage reservoirs into groundwater aquifers. *Energy Procedia*, *4*, 3216–3223. https://doi.org/10.1016/j.egypro.2011.02.238

Foroozesh, J., Dier, M. A., & Rezk, M. G. (2018). A simulation study on CO_2 sequestration in saline aquifers: Trapping mechanisms and risk of CO_2 leakage. *MATEC Web of Conferences*, *225*, 03004. https://doi.org/10.1051/matecconf/201822503004

Freifeld, B. M., Pan, L., Doughty, C., Zakem, S., Hart, K., & Hostler, S. (2016). *Demonstration of Geothermal Energy Production Using Carbon Dioxide as a Working Fluid at the SECARB Cranfield Site, Cranfield, Mississippi*.

Frontier Carbon Solutions, Inc., & Schlumberger Technology Corporation. (2022). *Underground Injection Control Carbon Sequestration Class VI Permit Application for Sweetwater Carbon Storage Hub*.

Gasda, S. E., Bachu, S., & Celia, M. A. (2004). Spatial characterization of the location of potentially leaky wells penetrating a deep saline aquifer in a mature sedimentary basin. *Environmental Geology*, *46*(6–7), 707–720. https://doi.org/10.1007/s00254-004-1073-5

Geological survey (Ed.). (2008). *Best practice for the storage of CO2 in saline aquifers: Observations and guidelines from the SACS and CO2STORE projects*. British Geological Survey.

Ghomian, Y., Bennett, M., Skrivanos, C., Marchiano, I., & Haynes, A. K. (2024). Applying Boundary Conditions for Large Aquifer Models in Geological CO2 Storage Projects;

Why and How? *SPE Annual Technical Conference and Exhibition*, D011S001R002. https://doi.org/10.2118/220913-MS

Gianni, E., Tyrologou, P., Behnous, D., Farkas, M. P., Álvarez, P. F.-C., Crespo, J. G., Ramirez, R. C., Koukouzas, N., & Carneiro, J. (2025). *Fields – A geochemical approach*.

Gupta, P. K., & Yadav, B. (2020). Leakage of CO2 from geological storage and its impacts on fresh soil–water systems: A review. *Environmental Science and Pollution Research*, *27*(12), 12995–13018. https://doi.org/10.1007/s11356-020-08203-7

Holtz, M. H. (2022). *Residual Gas Saturation to Aquifer Influx: A Calculation Method for 3-D Computer Reservoir Model Construction*.

Hosseini, S. A., Ershadnia, R., Lun, L., Morgan, S., Bennett, M., Skrivanos, C., Li, B., Soltanian, M. R., Pawar, R., & Hovorka, S. D. (2024). Dynamic modeling of geological carbon storage in aquifers – workflows and practices. *International Journal of Greenhouse Gas Control*, *138*, 104235. https://doi.org/10.1016/j.ijggc.2024.104235

Hovorka, S. D., Smye, K. M., Hennings, P. H., Bump, A. P., Okezie, C. C., & Luciano, A. K. (2024). *A Tale of Two Geologic Systems – Comparing the Impacts of Injection into the Permian Basin to the Gulf of Mexico*. GHGT-17. https://papers.ssrn.com/sol3/papers.cfm?abstract_id=5064850

Humphries Choptiany, J. M., & Pelot, R. (2014). A Multicriteria Decision Analysis Model and Risk Assessment Framework for Carbon Capture and Storage. *Risk Analysis*, *34*(9), 1720–1737. https://doi.org/10.1111/risa.12211

IEA. (2020). *Special Report on Carbon Capture Utilisation and Storage: CCUS in clean energy transitions*.

IEAGHG. (2024). *'Insurance Coverage for CO2 Storage Projects*. https://doi.org/doi.org/10.62849/2024-TR04

IPCC. (2005). *IPCC Special Report on Carbon Dioxide Capture and Storage*.

IPCC. (2018). *Global Warming of 1.5°C.* https://www.ipcc.ch/site/assets/uploads/sites/2/2019/06/SR15_Full_Report_High_Res.pdf

IPCC. (2023). *IPCC, 2023: Climate Change 2023: Synthesis Report.* (First). Intergovernmental Panel on Climate Change (IPCC). https://doi.org/10.59327/IPCC/AR6-9789291691647

IRS, Department of the Treasury. (2023). *26 CFR § 1.45Q-5 – Recapture of credit. In Code of Federal Regulations*. https://www.govinfo.gov/content/pkg/CFR-2023-title26-vol1/pdf/CFR-2023-title26-vol1-sec1-45Q-5.pdf

Jenkins, C., Chadwick, A., & Hovorka, S. D. (2015). The state of the art in monitoring and verification—Ten years on. *International Journal of Greenhouse Gas Control*, *40*, 312–349. https://doi.org/10.1016/j.ijggc.2015.05.009

Jones, D. G., Beaubien, S. E., Blackford, J. C., Foekema, E. M., Lions, J., De Vittor, C., West, J. M., Widdicombe, S., Hauton, C., & Queirós, A. M. (2015). Developments since 2005 in understanding potential environmental impacts of CO2 leakage from geological storage. *International Journal of Greenhouse Gas Control*, *40*, 350–377. https://doi.org/10.1016/j.ijggc.2015.05.032

Jordan, P. D., & Benson, S. M. (2009). Well blowout rates and consequences in California Oil and Gas District 4 from 1991 to 2005: Implications for geological storage of carbon dioxide. *Environmental Geology*, *57*(5), 1103–1123. https://doi.org/10.1007/s00254-008-1403-0

Juanes, R., Spiteri, E. J., Orr, F. M., & Blunt, M. J. (2006). Impact of relative permeability hysteresis on geological CO_2 storage. *Water Resources Research*, *42*(12), 2005WR004806. https://doi.org/10.1029/2005WR004806

Keating, E., Dai, Z., Dempsey, D., & Pawar, R. (2014). Effective detection of CO2 leakage: A comparison of groundwater sampling and pressure monitoring. *Energy Procedia*, *63*, 4163–4171. https://doi.org/10.1016/j.egypro.2014.11.448

Kestin, J., Khalifa, H., & Correia, R. (1981). Tables of the dynamic and kinematic viscosity of aqueous KCl solutions in the temperature range 25–150 °C and the pressure range 0.1–35 MPa. *Journal of Physical and Chemical Reference Data - J PHYS CHEM REF DATA*, *10*, 71–88. https://doi.org/10.1063/1.555641

Khan, C., Ge, L., & Rudolph, V. (2015). *Reservoir Simulation Study for CO2 Sequestration in Saline Aquifers*. *5*(4).

Kreitler, C. W., & Richter, B. C. (1986). *Hydrochemical Characterization of Saline Aquifers of the Texas Gulf Coast Used for Disposal of Industrial Waste*.

Kumar, A., Ozah, R., Noh, M., Pope, G. A., Bryant, S., Sepehrnoori, K., & Lake, L. W. (2005). Reservoir Simulation of CO2 Storage in Deep Saline Aquifers. *SPE Journal*.

Land, C. S. (1968). Calculation of Imbibition Relative Permeability for Two- and Three-Phase Flow From Rock Properties. *Society of Petroleum Engineers Journal*, *8*(02), 149–156. https://doi.org/10.2118/1942-PA

Lewicki, J. L., Birkholzer, J., & Tsang, C.-F. (2007). Natural and industrial analogues for leakage of CO2 from storage reservoirs: Identification of features, events, and processes and lessons learned. *Environmental Geology*, *52*(3), 457–467. https://doi.org/10.1007/s00254-006-0479-7

Lindeberg, E., Bergmo, P., Torsæter, M., & Grimstad, A.-A. (2017). Aliso Canyon Leakage as an Analogue for Worst Case CO2 Leakage and Quantification of Acceptable Storage Loss. *Energy Procedia*, *114*, 4279–4286. https://doi.org/10.1016/j.egypro.2017.03.1914

Little, M. G., & Jackson, R. B. (2010). Potential Impacts of Leakage from Deep CO_2 Geosequestration on Overlying Freshwater Aquifers. *Environmental Science & Technology*, *44*(23), 9225–9232. https://doi.org/10.1021/es102235w

Lyu, Y., Fang, X., Li, H., & Wang, G. (2024). Long-distance migration assisted structural trapping during CO2 storage in offshore basin. *Research Square*. https://doi.org/10.21203/rs.3.rs-4780259/v1

Meyer, V., Houdu, E., Poupard, O., & Le Gouevec, J. (2009). Quantitative risk evaluation related to long term CO2 gas leakage along wells. *Energy Procedia*, *1*(1), 3595–3602. https://doi.org/10.1016/j.egypro.2009.02.154

Nghiem, L. X., & Li, Y. K. (1986). Effect of phase behavior on CO2 displacement efficiency at low temperatures: Model studies with an equation of state. *Society of Petroleum Engineers Journal*, *1:4*.

Ni, H., Boon, M., Garing, C., & Benson, S. M. (2019). Predicting CO2 residual trapping ability based on experimental petrophysical properties for different sandstone types. *International Journal of Greenhouse Gas Control*, *86*, 158–176. https://doi.org/10.1016/j.ijggc.2019.04.024

Nicot, J.-P. (2009). A survey of oil and gas wells in the Texas Gulf Coast, USA, and implications for geological sequestration of CO2. *Environmental Geology*, *57*(7), 1625–1638. https://doi.org/10.1007/s00254-008-1444-4

Nicot, J.-P., Oldenburg, C. M., Bryant, S. L., & Hovorka, S. D. (2009). Pressure perturbations from geologic carbon sequestration: Area-of-review boundaries and borehole leakage driving forces. *Energy Procedia*, *1*(1), 47–54. https://doi.org/10.1016/j.egypro.2009.01.009

Nogues, J. P., Court, B., Dobossy, M., Nordbotten, J. M., & Celia, M. A. (2012). A methodology to estimate maximum probable leakage along old wells in a geological sequestration operation. *International Journal of Greenhouse Gas Control*, *7*, 39–47. https://doi.org/10.1016/j.ijggc.2011.12.003

Nordbotten, J. M., & Celia, M. A. (2006). An improved analytical solution for interface upconing around a well. *Water Resources Research*, *42*(8), 2005WR004738. https://doi.org/10.1029/2005WR004738

Nordbotten, J. M., Kavetski, D., Celia, M. A., & Bachu, S. (2009). Model for CO_2 Leakage Including Multiple Geological Layers and Multiple Leaky Wells. *Environmental Science & Technology*, *43*(3), 743–749. https://doi.org/10.1021/es801135v

Oak, M. J., Baker, L. E., & Thomas, D. C. (1990). *Three-Phase Relative Permeability*.

Ogland-Hand, J., Cox, K. J., Adams, B. M., Bennett, J. A., Johnson, P. J., Middleton, E. J., Talsma, C. J., & Middleton, R. S. (2023). *How to Net-Zero America: Nationwide Cost and Capacity Estimates for Geologic CO2 Storage*. https://doi.org/10.31224/3293

Oldenburg, C. M., Bryant, S. L., & Nicot, J.-P. (2009). Certification framework based on effective trapping for geologic carbon sequestration. *International Journal of Greenhouse Gas Control*, *3*(4), 444–457. https://doi.org/10.1016/j.ijggc.2009.02.009

Pan, L., & Oldenburg, C. M. (2020). Mechanistic modeling of CO2 well leakage in a generic abandoned well through a bridge plug cement-casing gap. *International Journal of Greenhouse Gas Control*, *97*, 103025. https://doi.org/10.1016/j.ijggc.2020.103025

Pan, L., Oldenburg, C. M., Freifeld, B. M., & Jordan, P. D. (2018). Modeling the Aliso Canyon underground gas storage well blowout and kill operations using the coupled well-reservoir simulator T2Well. *Journal of Petroleum Science and Engineering*, *161*, 158–174. https://doi.org/10.1016/j.petrol.2017.11.066

Pan, L., Webb, S. W., & Oldenburg, C. M. (2011). Analytical solution for two-phase flow in a wellbore using the drift-flux model. *Advances in Water Resources*, *34*(12), 1656–1665. https://doi.org/10.1016/j.advwatres.2011.08.009

Pawar, R. J., Bromhal, G. S., Carey, J. W., Foxall, W., Korre, A., Ringrose, P. S., Tucker, O., Watson, M. N., & White, J. A. (2015). Recent advances in risk assessment and risk management of geologic CO2 storage. *International Journal of Greenhouse Gas Control*, *40*, 292–311. https://doi.org/10.1016/j.ijggc.2015.06.014

Peng, D.-Y., & Robinson, D. B. (1976). A New Two-Constant Equation of State. *Industrial & Engineering Chemistry Fundamentals*, *15*(1), 59–64. https://doi.org/10.1021/i160057a011

Pérez-Martinez, E., Rodriguez-de La Garza, F., & Samaniego-Verduzco, F. (2012). Water Coning in Naturally Fractured Carbonate Heavy Oil Reservoir – A Simulation Study. *SPE Latin America and Caribbean Petroleum Engineering Conference*, SPE-152545-MS. https://doi.org/10.2118/152545-MS

Pollak, M. F., Bielicki, J. M., Dammel, J. A., Wilson, E. J., Fitts, J. P., & Peters, C. A. (2013). The Leakage Impact Valuation (LIV) Method for Leakage from Geologic CO2 Storage

Reservoirs. *Energy Procedia*, *37*, 2819–2827. https://doi.org/10.1016/j.egypro.2013.06.167

Porse, S. L., Wade, S., & Hovorka, S. D. (2014). Can We Treat CO2 Well Blowouts like Routine Plumbing Problems? A Study of the Incidence, Impact, and Perception of Loss of Well Control. *Energy Procedia*, *63*, 7149–7161. https://doi.org/10.1016/j.egypro.2014.11.751

Ramírez, A., Hagedoorn, S., Kramers, L., Wildenborg, T., & Hendriks, C. (2010). Screening CO2 storage options in The Netherlands. *International Journal of Greenhouse Gas Control*, *4*(2), 367–380. https://doi.org/10.1016/j.ijggc.2009.10.015

Raza, A., Gholami, R., Sarmadivaleh, M., Tarom, N., Rezaee, R., Bing, C. H., Nagarajan, R., Hamid, M. A., & Elochukwu, H. (2016). Integrity analysis of CO 2 storage sites concerning geochemical-geomechanical interactions in saline aquifers. *Journal of Natural Gas Science and Engineering*, *36*, 224–240. https://doi.org/10.1016/j.jngse.2016.10.016

Rowe, A. M. Jr., & Chou, J. C. S. (1970). Pressure-volume-temperature-concentration relation of aqueous sodium chloride solutions. *Journal of Chemical & Engineering Data*, *15*(1), 61–66. https://doi.org/10.1021/je60044a016

Seni, S. J., Hentz, T. F., Kaiser, W. R., & E.G., W., Jr. (1997). *Atlas of Northern Gulf of Mexico Gas and Oil Reservoirs: Vol. Miocene and Older Reservoir*.

Skalle, P., & Podia, A. L. (1998). Trends extracted from 800 Gulf Coast blowouts during 1960-1996. *IADC/SPE Drilling Conference*.

Tallgrass High Plains Storage, LLC, & Numeric Solutions, LLC. (2023, December). *Underground Injection Control Carbon Sequestration Class VI Permit Application for Eastern Wyoming Sequestration Hub*.

The Application of Blue Flint Sequester Company, LLC Requesting Consideration for the Geologic Storage of Carbon Dioxide in the Broom Creek Formation from the Blue Flint Ethanol Facility (Industrial Commission of the State of North Dakota May 25, 2023).

The Application of Dakota Gasification Company Requesting Consideration for the Geologic Storage of Carbon Dioxide from the Great Plains Synfuels Plant (Industrial Commission of the State of North Dakota January 24, 2023).

The Application of DCC West Project LLC Requesting Consideration for the Geologic Storage of Carbon Dioxide in the Broom Creek Formation from the Milton R. Young Station (Industrial Commission of the State of North Dajota October 4, 2023). https://www.dmr.nd.gov/dmr/sites/www/files/documents/Oil%20and%20Gas/Class%20VI/DCC%20West/C30122.pdf

The Application of Minnkota Power Cooperative, INC. Requesting Consideration for the Geologic Storage of Carbon Dioxide in the Deadwood Formation from the Milton R. Young Station (Industrial Commission of the State of North Dakota January 21, 2022).

Thibeau, S., & Mucha, V. (2011). Have We Overestimated Saline Aquifer CO_2 Storage Capacities? *Oil & Gas Science and Technology – Revue d'IFP Energies Nouvelles*, *66*(1), 81–92. https://doi.org/10.2516/ogst/2011004

Trabucchi, C., Donlan, M., Huguenin, M., Konopka, M., & Bolthrunis, S. (2012). *Valuation of Potential Risks Arising from a Model, Commercial-Scale CCS Project Site*. Industrial Economics, Incorporated.

Trabucchi, C., Donlan, M., Spirt, V., Friedman, S., & Esposito, R. (2014). Application of a Risk-Based Probabilistic Model (CCSvt Model) to Value Potential Risks Arising from Carbon

Capture and Storage. *Energy Procedia*, *63*, 7608–7618. https://doi.org/10.1016/j.egypro.2014.11.795

Trabucchi, C., Donlan, M., & Wade, S. (2010). A multi-disciplinary framework to monetize financial consequences arising from CCS projects and motivate effective financial responsibility. *International Journal of Greenhouse Gas Control*, *4*(2), 388–395. https://doi.org/10.1016/j.ijggc.2009.10.001

Ulfah, M., Hovorka, S. D., Spence, D. B., Bump, A. P., & Hosseini, S. A. (2021). *Plume Migration and Pressure Evolution Analyses for Recommendations in Offshore CO2 Storage Acreage Leasing Policy*.

UNFCCC. (2023). *2023 Synthesis report on GST elements*. https://unfccc.int/sites/default/files/resource/SYR_Views%20on%20%20Elements%20for%20CoO.pdf

U.S. DOE. (2017). *Best Practices: Monitoring, Verification, and Accounting (MVA) for Geologic Storage Projects*. National Energy Technology Laboratory.

U.S. EPA. (2001). *Remediation Technology Cost Compendium—Year 2000*.

U.S. EPA. (2008). *Vulnerability Evaluation Framework for Geologic Sequestration of Carbon Dioxide*. https://nepis.epa.gov/Exe/ZyNET.exe/P1002TH7.TXT?ZyActionD=ZyDocument&Client=EPA&Index=2006+Thru+2010&Docs=&Query=&Time=&EndTime=&SearchMethod=1&TocRestrict=n&Toc=&TocEntry=&QField=&QFieldYear=&QFieldMonth=&QFieldDay=&IntQFieldOp=0&ExtQFieldOp=0&XmlQuery=&File=D%3A%5Czyfiles%5CIndex%20Data%5C06thru10%5CTxt%5C00000006%5CP1002TH7.txt&User=ANONYMOUS&Password=anonymous&SortMethod=h%7C-

&MaximumDocuments=1&FuzzyDegree=0&ImageQuality=r75g8/r75g8/x150y150g16/i425&Display=hpfr&DefSeekPage=x&SearchBack=ZyActionL&Back=ZyActionS&BackDesc=Results%20page&MaximumPages=1&ZyEntry=1&SeekPage=x&ZyPURL

U.S. EPA. (2010a). *Federal Requirements Under the Underground Injection Control (UIC) Program for Carbon Dioxide (CO2) Geologic Sequestration (GS) Wells*. https://www.govinfo.gov/content/pkg/FR-2010-12-10/pdf/2010-29954.pdf

U.S. EPA. (2010b). *Geologic CO2 Sequestration Technology and Cost Analysis*. Office of Water (4606-M).

U.S. EPA. (2011). *Underground Injection Control (UIC) Program Class VI Financial Responsibility Guidance* (EPA 816-R-11-005). U.S. EPA. https://www.epa.gov/system/files/documents/2022-11/uicfinancialresponsibilityguidancefinal072011v_0.pdf

U.S. EPA. (2013a). *Underground Injection Control (UIC) Program Class VI Well Area of Review Evaluation and Corrective Action Guidance*. https://www.epa.gov/sites/default/files/2015-07/documents/epa816r13005.pdf

U.S. EPA. (2013b). *Underground Injection Control (UIC) Program Class VI Well Site Characterization Guidance*. https://www.epa.gov/sites/default/files/2015-07/documents/epa816r13004.pdf

Wabash Carbon Services, LLC. "Underground Injection Control Permit: Class VI." (January 19, 2024). https://www.epa.gov/system/files/documents/2024-01/in-165-6a-0001_wabash_final_permit.pdf

Wang, Z., Dilmore, R. M., Bacon, D. H., & Harbert, W. (2021). Evaluating probability of containment effectiveness at a GCS site using integrated assessment modeling approach

with Bayesian decision network. *Greenhouse Gases: Science and Technology*, *11*(2), 360–376. https://doi.org/10.1002/ghg.2056

Wang, Z., & Small, M. J. (2014). A Bayesian approach to CO2 leakage detection at saline sequestration sites using pressure measurements. *International Journal of Greenhouse Gas Control*, *30*, 188–196. https://doi.org/10.1016/j.ijggc.2014.09.011

Watson, T. L., & Bachu, S. (2008). Identification of Wells with High CO2-Leakage Potential in Mature Oil Fields Developed for CO2-Enhanced Oil Recovery. *SPE Symposium on Improved Oil Recovery*, SPE-112924-MS. https://doi.org/10.2118/112924-MS

Xiao, T., McPherson, B., Esser, R., Jia, W., Dai, Z., Chu, S., Pan, F., & Viswanathan, H. (2020). Chemical Impacts of Potential CO2 and Brine Leakage on Groundwater Quality with Quantitative Risk Assessment: A Case Study of the Farnsworth Unit. *Energies*, *13*(24), 6574. https://doi.org/10.3390/en13246574

Yang, C., Hovorka, S. D., Treviño, R. H., & Delgado-Alonso, J. (2015). Integrated Framework for Assessing Impacts of CO_2 Leakage on Groundwater Quality and Monitoring-Network Efficiency: Case Study at a CO_2 Enhanced Oil Recovery Site. *Environmental Science & Technology*, *49*(14), 8887–8898. https://doi.org/10.1021/acs.est.5b01574

Yang, Y., Small, M. J., Ogretim, E. O., Gray, D. D., Wells, A. W., Bromhal, G. S., & Strazisar, B. R. (2012). A Bayesian belief network (BBN) for combining evidence from multiple CO_2 leak detection technologies. *Greenhouse Gases: Science and Technology*, *2*(3), 185–199. https://doi.org/10.1002/ghg.1284

Zhang, M., & Bachu, S. (2011). Review of integrity of existing wells in relation to CO2 geological storage: What do we know? *International Journal of Greenhouse Gas Control*, *5*(4), 826–840. https://doi.org/10.1016/j.ijggc.2010.11.006

Zheng, L., Nico, P., Spycher, N., Domen, J., & Credoz, A. (2021). Potential impacts of CO_2 leakage on groundwater quality of overlying aquifer at geological carbon sequestration sites: A review and a proposed assessment procedure. *Greenhouse Gases: Science and Technology*, *11*(5), 1134–1166. https://doi.org/10.1002/ghg.2104

Zhou, Y., Hatzignatiou, D. G., & Helland, J. O. (2017). On the estimation of CO 2 capillary entry pressure: Implications on geological CO 2 storage. *International Journal of Greenhouse Gas Control*, *63*, 26–36. https://doi.org/10.1016/j.ijggc.2017.04.013